SHOCK WAVES
IN A
HIGH TEMPERATURE PLASMA

by

IAN GRANT CAMERON, B.Sc., A.R.C.S.
Imperial College, London.

Thesis submitted for the Degree
of Doctor of Philosophy in the
University of London,
November, 1961.

ACKNOWLEDGEMENT

The author wishes to express his thanks to his supervisor, Professor H. Jones, for his advice and guidance throughout the course of this work.

ABSTRACT

Two problems arising from a discharge at low pressure in a T-tube apparatus are considered. In the first, a calculation of the motion is made which arises when a high temperature plasma, crossed by a uniform magnetic field, expands into a cold gas at low pressure. The expansion produces a shock wave in the gas and a rarefaction wave travelling in the opposite direction in the plasma. This rarefaction wave is reflected from the wall which contains the plasma and returns in the direction of the shock wave. The motion is considered up to the point at which the rarefaction wave reaches the shock front, thereby weakening it and reducing its speed. Several cases are examined: some in which the densities of the plasma and the gas are different, and some in which a magnetic field crosses the cold gas as well as the hot plasma. From the calculations, conditions favourable to a slow rate of attenuation of the shock wave are determined.

The second problem considered is the nature of the structure of a hydromagnetic shock wave which is advancing into a cold gas. The relevant equations are derived and their solution obtained by numerical

integration. Reasonable assumptions are made relating to the temperature dependence of the electrical conductivity and the viscosity. Shock profiles are drawn and it is found that there is a sharp rise in the initial stages of the shock front, followed by an extended region in which all the variables change slowly. In the region where the density rises rapidly the temperature rises to about a quarter of its final steady state value.

CONTENTS

CHAPTER I

Introduction

The object of this work is to discuss the nature of shock waves generated in a gas at low pressure. There are many ways of generating such shock waves in the laboratory, but here particular attention is given to those produced by electromagnetic driving in a T-tube apparatus, similar to that used by Kolb[2,3] and others.

In a T-tube apparatus, which is shown diagramatically in figure 1, a low inductance condenser bank is discharged between the electrodes in the discharge tube, whilst the return current lead is placed close to the back of this tube, so as to induce a transverse magnetic field. As a result of the interaction between this field and the discharge, there is a Lorentz force $\underline{j} \wedge \underline{H}$, where $\underline{j}$ denotes the electric current and $\underline{H}$ the magnetic field vector, which drives a shock wave up the side arm.

The apparatus is basically very similar to an ordinary shock tube; it consists of a long tube together with a diaphragm separating two gases, the one at a high pressure and the other at a low pressure. By piercing

2, 3 : these numbers refer to the references at the end.

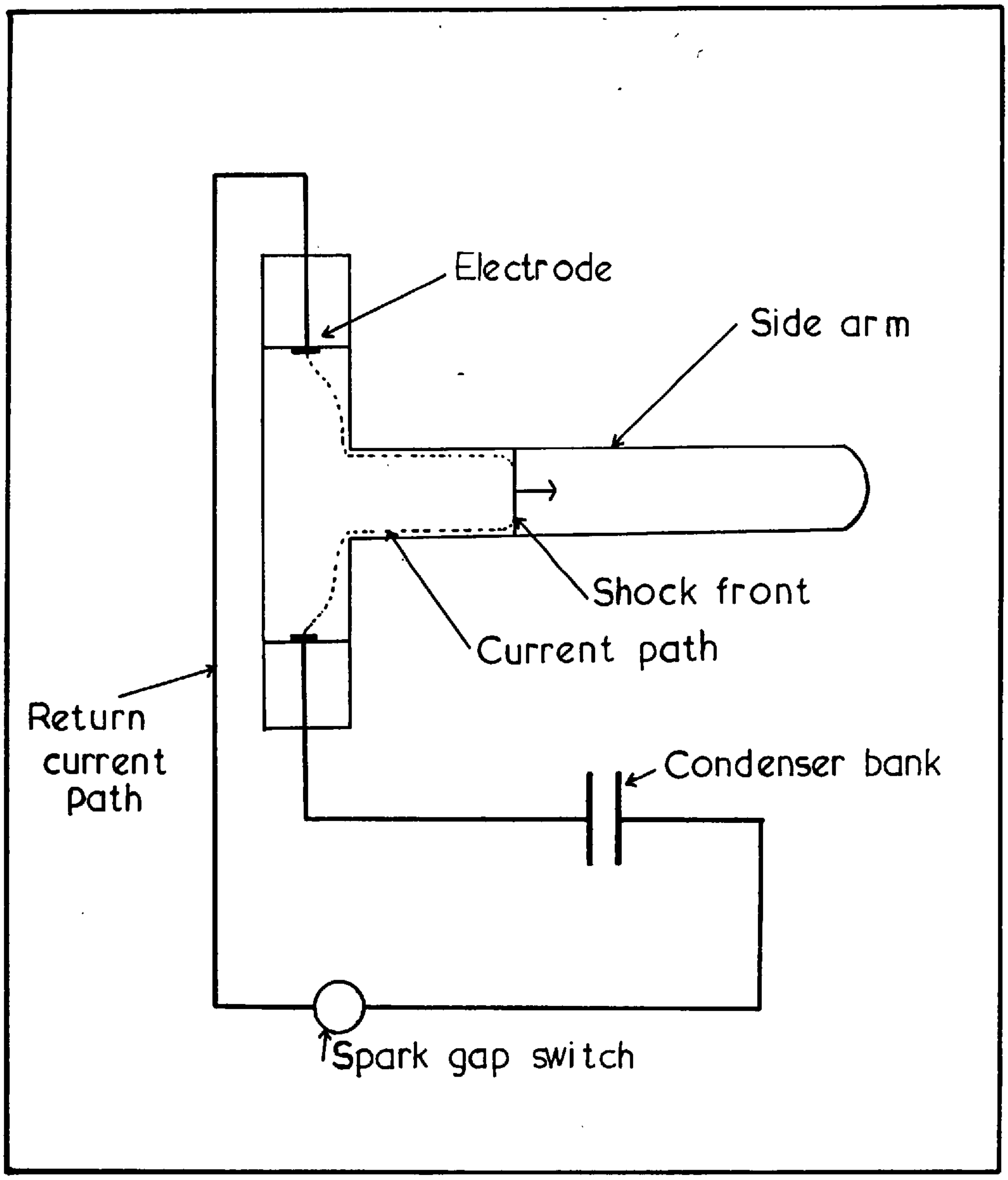

FIG.1. KOLB'S APPARATUS

it suddenly the diaphragm may be burst and the compression wave which advances into the low pressure gas, steepens rapidly to form a shock wave. The greater the pressure difference the stronger is the shock, though there is a limit to the pressure difference which the diaphragm can withstand without bursting naturally. It is this limit which determines the maximum strength of the shocks that may be produced by this method. The greatest Mach numbers that may be reached are of the order 30, but by using a T-tube, Mach numbers of the order hundreds may be attained, leading to plasmas with temperatures in the million degree range.

The discharge tubes used by Kolb were made of quartz and were about 2 cm. in diameter and 12 cm. in length. Typical values of the voltage V, capacitance C and inductance L were as follows $V = 15$ kV, $C = 5\mu f$ and $L = 0.25\ \mu h$. The ringing frequency, f, of the condenser bank is given by $f = 1/\sqrt{LC}$ which, for the numerical values given above, is of magnitude 900 k.c. As a result of the ringing of the condenser bank a whole series of shock waves will be produced. Experiments were carried out using hydrogen, deuterium and helium at initial pressures of the order of 1 mm. of mercury. Shock fronts with velocities in the range $10^6 - 10^7$ cm/sec.

were obtained and the temperatures of the plasmas behind the shock fronts were in the range $10^6 - 10^7$ °K.

A deatiled dependence of the shock velocity and temperature of the plasma behind the shock front on the ambient pressure, discharge voltage, inductance, capacitance and the distance from the discharge were found by a series of experiments. By utilizing extra coils the magnetic field driving the shock, and thus the shock velocity, could be increased but, above a certain value, an increase in the shock velocity did not result in a very large increase in the temperature of the plasma. An important parameter for producing strong shocks was found to be the initial rate of rise of the current; the quicker the rise, the stronger was the shock. Not very reproducible results were obtained by attempting to strike a discharge with a slow rise time in a transverse magnetic field. There was a tendency for the external field to blow out the gas, before an appreciable electron density could be produced.

The preferential driving of the plasma in the direction determined by $\left| \underline{j}_{int} \wedge \underline{H}_{ext} \right|$, $\underline{j}_{int}$ denoting the internal current and $\underline{H}_{ext}$ the total external magnetic field, was demonstrated by placing the electrodes 4 cm. from the bottom of the tube and inside a solonoid. It was arranged that the transverse external field and the primary discharge were out of phase, so that the Lorentz force changed directions after a certain time. As a result, the first two shock waves were directed up the tube and the next two down. This experiment showed that the acceleration of the plasma was due principally to the existence of an external field, rather than to the ohmic heating of a cold gas with a subsequent expansion of the hot plasma.

A diagram showing the behaviour of the shock velocity as a function of the distance from the electrodes is shown in figure 2. It is seen that the velocity

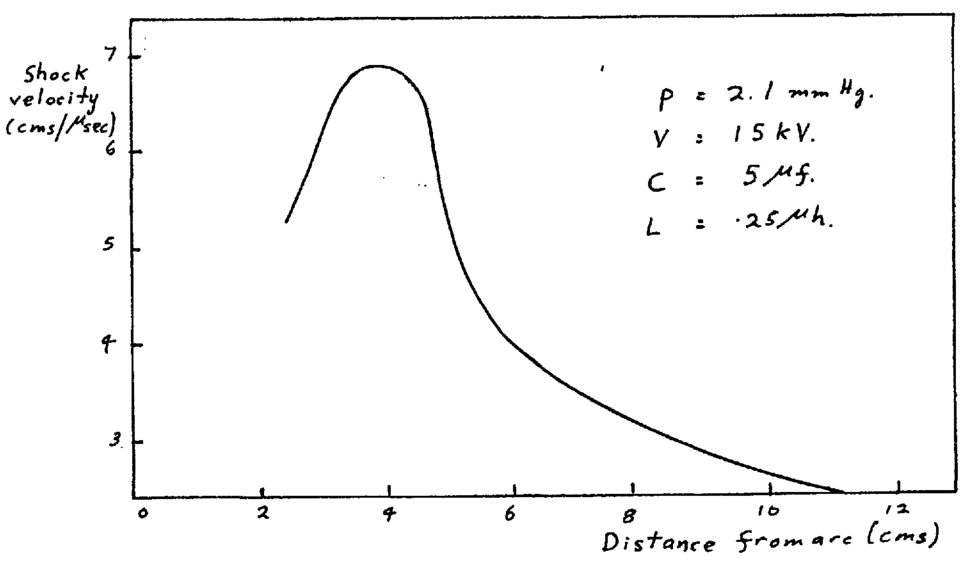

Figure 2. Dependence of the shock velocity on the distance from the discharge.

quickly falls off from its maximum value. One of the reasons for this decay is that heat is lost to the walls of the shock tube, and as the temperature behind the shock front is increased the effect of wall cooling becomes increasingly important. This loss to the walls was reduced in some of Kolb's later experiments by the introduction of a rising axial magnetic field. In these experiments, provided the temperature of the plasma is sufficiently high, the magnetic field can be assumed to change slowly compared to the transit time of a sound wave across the tube, and this compression will, therefore, be essentially adiabatic. Thus this field will heat the plasma adiabatically and compress it into the centre of the tube, thereby reducing wall cooling effects.

Shock heating of plasmas by electromagnetically driven shock waves has been used in many other experiments to produce high temperature plasmas. Much work has been done using the so-called "fast linear pinch" device. In this apparatus an axial discharge starts in a current sheet near the wall of the discharge tube, and the resulting magnetic field drives the current carrying gas towards the axis with such violence that an intense shock wave is produced. Although the geometry of this apparatus is vastly different from the T-tube geometry, in the initial stages of the discharge, when cylindrical convergence is negligible, the two are equivalent, though the succeeding motion is, of course, vastly different.

An alternative way of shock heating a plasma was utilized by Elmore, Little and Quinn in a device called Scylla. In such a device the gas is heated as a result of the interaction between an azimuthal current and the axial magnetic field which this current induces. An annular shock tube device, similar to the T-tube, was used by R.M. Patrick[4] for a series of experiments. The container for the gas in this apparatus is formed by the annulus between two concentric glass cylinders. Radial currents are created by discharging a capacitor bank connected to the inner and outer cylinders which form the electrodes. The azimuthal magnetic field induced by these radial currents furnishes the driving force for the shock wave, which advances down the tube in a similar manner to those in T-tubes.

Returning again to the T-tube apparatus, at the same time as the shock wave forms a rarefaction wave develops which travels back into the region where the discharge took place. This rarefaction wave is reflected from the wall of the discharge tube up the side arm where it overtakes and weakens the shock wave. As the distance which the rarefaction wave has to travel to the back wall is quite short, the weakening of the shock may occur before the steady state conditions in the shock front itself have been established. ~~Again~~ If the rarefaction wave returned very quickly this would furnish another reason for the attenuation of the shock wave ~~as~~ shown in figure 2.

In chapters III and IV the distance travelled by the shock wave before the rarefaction wave begins to weaken it is investigated for various initial conditions. It is found that this distance is not much greater than the width of the shock tube in typical cases, but by differentially cooling the gas in the discharge tube, and thereby increasing its density relative to that in the side arm, this distance may be somewhat increased.

The effect of placing a constant magnetic field of about 10^4 gauss across the side arm is also considered, and it is found that this does not have any significant effect on the flow.

The shock waves generated in T-tube experiments can lead to very high temperature plasmas, and the width of the shock front in these cases may be quite large. Thus there is an interest in the structure of the shock fronts of such waves, as the steady state of the gas behind the front will not be established unless the overall width of the shock front is less than the dimensions of the apparatus being used to produce the shock. In chapter VI the structure of the shock front is considered with particular reference to that of a shock wave advancing into a cold gas, as is relevant to T-tube experiments. Because the gas ahead of the shock front is not preionized, the value of the viscosity and electrical conductivity for a fully ionized gas may only be used when the gas has reached a sufficiently high temperature. Below this temperature their values for an ordinary gas must be taken. These values of the transport coefficients are discussed in chapter V. The shock profiles are compared with those obtained for a shock wave advancing into a preionized gas; it is found that the shock front is much sharper in the initial stages where the compression is due solely to viscous and heat conduction effects.

CHAPTER II

Hydromagnetic Shock Waves and Waves of Finite Amplitude

1. Basic equations

The mathematical theory of the problems to be discussed comes from a fairly new branch of physics called magnetohydrodynamics. This branch of physics came about as a result of the union of two sections of science, the one dealing with fluid flow and the other with magnetic fields. It is thus the study of the motion of an electrically conducting fluid in the presence of a magnetic field. Electric currents induced in the field as a result of its motion modify the field; at the same time their flow in the magnetic field produces mechanical forces which modify the motion. Applications of magnetohydrodynamics are many: there are the cosmical aspects dealing with problems concerning the earth's interior, the sun, the stars or interstellar space; there are also the laboratory applications and, as has already been indicated, it is with these that we are concerned here.

Maxwell's equations, together with an extended form of Ohm's law, are the basic electromagnetic equations of the theory. In electromagnetic units these equations may be written

$$\mathrm{curl}\,\underline{H} = 4\pi(\underline{j} + q\underline{v}) + \frac{1}{c^2}\frac{\partial \underline{E}}{\partial t}, \tag{1.1}$$

$$\mathrm{div}\,\underline{H} = 0, \tag{1.2}$$

$$\mathrm{curl}\,\underline{E} = -\frac{\partial H}{\partial t}, \tag{1.3}$$

$$\mathrm{div}\,\underline{E} = 4\pi c^2 q, \tag{1.4}$$

$$\underline{j} = \sigma(\underline{E} + \underline{v}\wedge\underline{H}), \tag{1.5}$$

where $\underline{H}$ = magnetic field,

$\underline{j}$ = current density,

q = electric charge density,

$\underline{v}$ = velocity vector,

$\underline{E}$ = electric field.

c = velocity of light.

Throughout this work the permeability will be taken as unity, and thus no distinction will be made between the magnetic field and the magnetic induction.

The hydrodynamic equations are those expressing the conservation of mass, momentum and energy and neglecting dissipative effects, these may be written

$$\frac{D}{Dt}(\rho\underline{v}) = 0, \tag{1.6}$$

$$\frac{D\underline{v}}{Dt} = -\frac{1}{\rho}\nabla p + \frac{1}{\rho}\underline{F}, \tag{1.7}$$

$$\frac{\partial}{\partial t}\left[\frac{1}{2}\rho v^2 + \rho\mathcal{E} + \frac{H^2}{8\pi}\right] + \mathrm{div}\left[\rho\underline{v}\left(\frac{1}{2}v^2 + i\right) + \frac{\underline{E}\wedge\underline{H}}{4\pi}\right] = 0, \tag{1.8}$$

where p = pressure,
ρ = density,
ε = internal energy/unit mass,
i = $\varepsilon + p/\rho$ = enthalpy/unit mass.

$\frac{D}{Dt}$ is the usual hydrodynamical time derivative following the motion, i.e.

$$\frac{D}{Dt} = \frac{\partial}{\partial t} + \underline{v} \cdot \text{grad} \tag{1.9}$$

In the first bracket of equation (1.8) $\frac{H^2}{8\pi}$ is the magnetic pressure and in the second bracket of the same equation $\frac{\underline{E} \wedge \underline{H}}{4\pi}$ is the Poynting energy vector. $\underline{F}$ in equation (1.7) represents the force due to electrodynamical effects and is given by

$$\underline{F} = q\left(\underline{E} + \underline{v} \wedge \underline{H}\right) + \underline{j} \wedge \underline{H} \tag{1.10}$$

In the presence of conductors the electromagnetic equations may be simplified by what is known as the hydromagnetic approximation. This approximation assumes that the electrostatic forces are negligible compared with the electromagnetic forces. Mathematically the approximation states that

$$\frac{1}{c^2}\frac{\partial \underline{E}}{\partial t} \ll \underline{j}, \tag{1.11}$$

and

$$q\underline{v} \ll \underline{j}. \tag{1.12}$$

whence the equations (1.1) to (1.4) and (1.10) may be written

$$\operatorname{curl} \underline{H} = 4\pi \underline{j} , \tag{1.13}$$

$$\operatorname{div} \underline{H} = 0 , \tag{1.14}$$

$$\operatorname{curl} \underline{E} = -\frac{\partial \underline{H}}{\partial t} , \tag{1.15}$$

$$\underline{F} = \underline{j} \wedge \underline{H} \tag{1.16}$$

Equation (1.4) is no longer needed as charge density has been neglected.

That condition (1.11) is satisfied in the presence of conductors can be seen by putting $\underline{j} = \sigma \underline{E}$, its value for a stationary conductor, when the condition is equivalent to stating that $\underline{E}$ does not change much in a time of the order $1/c^2\sigma$. Thus provided σ is not $\ll 1/c^2$ this condition will be satisfied quite earily.

Consider now condition (1.12) which is equivalent to

$$\frac{v \operatorname{div} E}{4\pi c^2} \ll \frac{1}{4\pi} \operatorname{curl} H , \tag{1.17}$$

i.e. $$v \operatorname{div} E \ll c^2 \operatorname{curl} H . \tag{1.18}$$

If we assume that $O(\operatorname{div} E) \simeq O(\operatorname{curl} E)$ then (1.18) may be written

$$v \operatorname{curl} E \ll c^2 \operatorname{curl} H , \tag{1.19}$$

i.e. $$\frac{v\,(\text{length scale})}{(\text{time scale})} \ll c^2 \qquad (1.20)$$

Again this is a condition which is easily satisfied for the applications which are relevant here.

$\underline{E}$ and $\underline{j}$ may be eliminated from the basic equations to give a single equation for $\underline{H}$. Equations (1.15) and (1.5) give

$$\frac{\partial \underline{H}}{\partial t} = -\operatorname{curl}\underline{E} = \operatorname{curl}\left(\underline{j}/\sigma - \underline{v}\wedge\underline{H}\right),$$

$$= \operatorname{curl}(\underline{v}\wedge\underline{H}) - \frac{1}{4\pi\sigma}\operatorname{curl}\underline{j}, \qquad (1.21)$$

assuming that σ is constant in space. Substituting for $\underline{j}$ from equation (1.13) gives

$$\frac{\partial \underline{H}}{\partial t} = \operatorname{curl}(\underline{v}\wedge\underline{H}) - \frac{1}{4\pi\sigma}\left(\operatorname{grad}\operatorname{div}\underline{H} - \nabla^2\underline{H}\right). \qquad (1.22)$$

As $\operatorname{div}\underline{H} = 0$ this equation may be written

$$\frac{\partial \underline{H}}{\partial t} = \operatorname{curl}(\underline{v}\wedge\underline{H}) + \nu_M \nabla^2\underline{H}, \qquad (1.23)$$

where $$\nu_M = \frac{1}{4\pi\sigma}. \qquad (1.24)$$

Assume first that the material is at rest. Equation (1.3) then becomes

$$\frac{\partial \underline{H}}{\partial t} = \nu_M \nabla^2\underline{H} \qquad (1.25)$$

This has the form of a diffusion equation, and the quantity ν_M is often called the magnetic diffusivity. Thus this equation indicates that the field 'leaks' through the material from point to point. As a result of this, a decay of the field results, since oppositely directed fields at different points leak together and neutralize each other. The time of decay is of the order L^2/ν_M where L is a typical length.

As a different limiting case, suppose that the material is in motion but has infinite conductivity; equation (1.23) then becomes

$$\frac{\partial \underline{H}}{\partial t} = \operatorname{curl}\left(\underline{v} \wedge \underline{H} \right) \qquad (1.26)$$

This equation is identical with that satisfied by the vorticity in the theory of flow of non-viscous fluids and interpreted in that theory as implying that the vortex lines more with the fluid. Thus, equation (1.26) tells us that for any closed 'loop' moving through the fluid, the number of lines of force through this loop are constant. This idea was first put forward by Alfvén and is equivalent to saying that the lines of force are frozen into the material. Motion along the lines of force does not affect the field, but when the material moves transverse to the lines of force it carries them with it. An example of this effect will be seen later in that the magnetic field, transverse to the motion of a shock front, is increased by the passage of the shock.

When neither term on the right of equation (1.23) is negligible the time variation of $\underline{H}$ is the sum of the two parts given by equations (1.25) and (1.26). Thus the lines of force tend to be carried about with the moving material and at the same time they leak through it. In many laboratory experiments, though not those being considered here, the lines of force slip readily through the material, whereas in cosmic masses the leak is very slow and the lines of force can be regarded as very nearly frozen into the material.

2. Hydromagnetic waves

Let us consider the equations for a perfectly conducting non-viscous fluid. These equations are special cases of the more general equations stated previously, which may now be written

$$\frac{\partial \underline{H}}{\partial t} = \operatorname{curl}(\underline{v} \wedge \underline{H}), \tag{2.1}$$

$$\operatorname{div} \underline{H} = 0, \tag{2.2}$$

$$\rho \frac{D\underline{v}}{Dt} = -\nabla p + \frac{1}{4\pi}(\operatorname{curl}\underline{H}) \wedge \underline{H}, \tag{2.3}$$

$$\frac{\partial \rho}{\partial t} + \operatorname{div}(\rho \underline{v}) = 0 \tag{2.4}$$

We write
$$\underline{H} = \underline{H}_0 + \underline{h},$$
$$p = p_0 + p',$$
$$\rho = \rho_0 + \rho',$$

where the suffix o refers to the constant equilibrium value and $\underline{h}$, p' and ρ' are small variations in the wave. The velocity $\underline{v}$, which is zero in equilibrium, is a small quantity of the same order. Assuming that the flow is adiabatic we have

$$p' = a_0^2 \rho', \qquad (2.5)$$

where a is defined as the speed of sound in the media.

We shall seek solutions of these equations which are proportional to $\exp[i(\underline{k}\cdot\underline{r} - \omega t)]$ i.e. solutions which describe the propagation of plane waves with wave vector $\underline{k}$ and frequency ω. It is also convenient to introduce the phase velocity of the wave $u = \omega/k$. The simplest form of a hydromagnetic wave occurs for an incompressible flow in which the velocity $\underline{v}$ and the change $\underline{h}$ in the magnetic field are parallel to the y axis, but independent of y, while the mean magnetic field is parallel to the x axis. For this case equation (2.4) reduces to

$$\operatorname{div} \underline{v} = 0, \qquad (2.6)$$

and as

$$(\text{curl}\,\underline{H})\wedge\underline{H} = (\nabla.\underline{H})\underline{H} - \tfrac{1}{2}\nabla\underline{H}^2 , \qquad (2.7)$$

equation (2.3) may be written

$$\rho\frac{Dv}{Dt} = -\nabla q + \frac{1}{4\pi}(\underline{H}\,\nabla)\underline{H} , \qquad (2.8)$$

where

$$q = p + \frac{H^2}{8\pi} , \qquad (2.9)$$

$\frac{H^2}{8\pi}$ in this formula may be considered as a pressure due to the magnetic field and q as a total pressure. Taking the divergence of equation (2.8) we have that

$$\nabla^2 q = 0 . \qquad (2.10)$$

Outside the region affected by the disturbance H = a constant and from the equilibrium condition grad p = 0. Thus $q = p + \frac{H^2}{8\pi}$ is a solution of Laplace's equation which is constant outside a particular region and so must be a constant everywhere. Equations (2.1) and (2.8) may, therefore, be written.

$$\frac{\partial h}{\partial t} = H_0\frac{\partial v}{\partial x} , \qquad (2.11)$$

$$\frac{\partial v}{\partial t} = \frac{H_0}{4\pi\rho}\frac{\partial h}{\partial x} \qquad (2.12)$$

Combining these two equations we obtain the wave equation

$$\frac{\partial^2 h}{\partial t^2} = \frac{H_0^2}{4\pi\rho}\frac{\partial^2 h}{\partial x^2} \qquad (2.13)$$

The velocity of propagation of this wave is given by

$$u = \frac{\pm H_0}{\sqrt{4\pi\rho}} \quad . \tag{2.14}$$

Alfvén first discussed such waves in 1942 and, as a result, they are named after him, their velocity $\frac{H_0}{\sqrt{4\pi\rho}}$, being called the Alfvén velocity.

An Alfvén wave may be looked at as the vibration of a line of force. The stress system associated with the lines of force is a tensile stress $H^2/8\pi$ along the lines of force and a compressive stress $H^2/8\pi$ between the lines of force. This system is equivalent to a hydrostatic pressure ~~equal to~~ $H^2/8\pi$ and a tension $H^2/4\pi$ along the lines of force. If $y(x)$ is the displacement of the medium, the restoring force per cubic centimetre equals the tensile stress times $\frac{\partial^2 y}{\partial x^2}$, as shown in the theory of vibrating strings. Hence the equation of motion becomes

$$\rho \frac{\partial^2 y}{\partial t^2} = \frac{H^2}{4\pi} \frac{\partial^2 y}{\partial x^2} \quad , \tag{2.15}$$

which agrees with equation (2.13).

Returning now to the compressible flow equations (2.1) to (2.4), we may write these as

$$\operatorname{div} \underline{h} = 0 \quad , \tag{2.16}$$

$$\frac{\partial \underline{h}}{\partial t} = \operatorname{curl}(\underline{v} \wedge \underline{H}_0) \quad , \tag{2.17}$$

$$\frac{\partial \rho}{\partial t} + \rho \operatorname{div} \underline{v} = 0 \quad , \tag{2.18}$$

$$\frac{\partial \underline{v}}{\partial t} = -\frac{a_0^2}{\rho} \operatorname{grad} \rho' - \frac{\underline{H} \wedge \operatorname{curl} \underline{h}}{4\pi\rho} \quad , \tag{2.19}$$

where terms of higher order than the first have been neglected. For a pertubation periodic in time the first of these equations follows from the second and may be omitted.

Seeking solutions of the form exp$\left[\, i(\underline{k}.\underline{r} - \omega t) \,\right]$ again, the equations (2.17) to (2.19) may be written in ordinary vector form as

$$-\omega \underline{h} = \underline{k} \wedge (\underline{v} \wedge \underline{h}) \quad , \tag{2.20}$$

$$\omega \rho' = \rho\, \underline{k}.\underline{v} \quad , \tag{2.21}$$

$$-\omega \underline{v} + (a_0^2/\rho)\, \rho' \underline{k} = \underline{H}_0 \wedge (\underline{k} \wedge \underline{h})/4\pi\rho \tag{2.22}$$

The first of these shows that the vector $\underline{h}$ is perpendicular to the wave vector $\underline{k}$, which we shall take to be along the x axis, with the plane of $\underline{k}$ and $\underline{H}_0$ as the x - y plane. Eliminating ρ' from equation (2.22), by means of equation (2.21) and rewriting the result in components, we have

$$\left.\begin{aligned} u\, h_z &= -\, v_z H_{ox} \, , \\ u\, v_z &= -\, H_{ox} h_z / 4\pi\rho_0 \, , \end{aligned}\right\} \tag{2.23}$$

$$u h_y = v_x H_{oy} - v_y H_{ox} ,$$

$$u v_y = H_{ox} h_y / 4\pi\rho_o , \qquad (2.24)$$

$$v\left(u - \frac{a_o^2}{u}\right) = H_{oy} h_y / 4\pi\rho_o ,$$

where a suffix x, y, or z on a variable has been used to denote the appropriate component of that variable.

The equations have been split into two groups, the first involving only h_z and v_z and the second only h_y, v_x and v_y. It follows, therefore, that pertubations of the two groups of variables are propagated independently. The density, and therefore the pressure, belong to the second group, since

$$\rho' = a_o v_x / u . \qquad (2.25)$$

The compatibility condition for the first group is

$$u = u_1 = \pm \frac{H_{ox}}{(4\pi\rho_o)^{\frac{1}{2}}} . \qquad (2.26)$$

In these waves, shown in figure 2(a), the component of the magnetic field which is perpendicular to the directions of propagation and of the constant field H_o, oscillates, and with it the velocity v_z which is related to h_z by the equation

$$v_z = -\frac{h_z}{(4\pi\rho_o)^{\frac{1}{2}}} \qquad (2.27)$$

The dispersion relation between ω and $\underline{k}$ involves the direction of the wave vector

$$\omega = \frac{\underline{H}\,.\,\underline{k}}{(4\pi\rho_0)^{\frac{1}{2}}} , \qquad (2.28)$$

The physical velocity of propagation of the wave is called the group velocity V , and is given by the derivative $\frac{\partial\omega}{\partial\underline{k}}$. In the present case we have

$$V = \frac{\partial\omega}{\partial\underline{k}} = \frac{H_0}{(4\pi\rho_0)^{\frac{1}{2}}} , \qquad (2.29)$$

which does not involve the direction of $\underline{k}$. The direction of propagation of the wave, in the sense of its group velocity, is the direction of H_0 . ~~"These waves are longitudinal in character"~~.

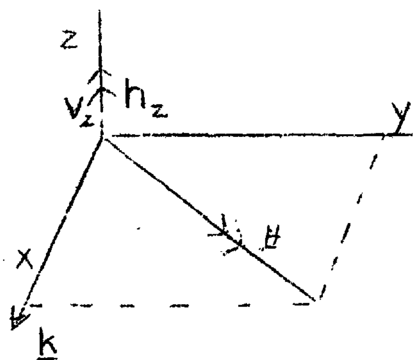

Fig. 2(a)

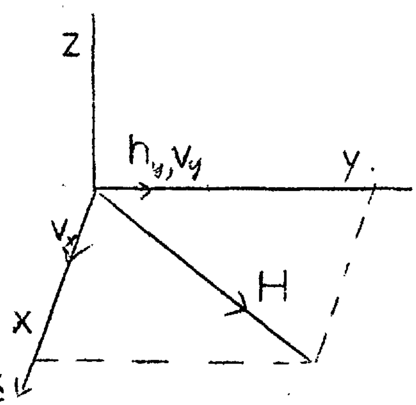

Fig. 2(b)

Let us now consider the waves described by the system of equations (2.24). Equating to zero the determinant of these equations, we obtain

$$\frac{u^2 H_{0y}^2}{4\pi\rho_0} = \left(u^2 - a_0^2\right)\left(u^2 - \frac{H_{0x}^2}{4\pi\rho_0}\right) . \qquad (2.30)$$

The roots of this quartic equation for U are

$$U_{2,3} = \pm\left\{\sqrt{a_0^2 + \frac{H_0^2}{4\pi\rho_0} + \frac{H_{0x}a_0}{\sqrt{\pi\rho_0}}} \pm \sqrt{a_0^2 + \frac{H}{4\pi\rho_0} - \frac{H_{0x}a_0}{\sqrt{\pi\rho_0}}}\right\} \qquad (2.31)$$

Thus we obtain two more types of wave. For these waves ~~are~~ ~~transverse, in which~~ the quantities h_y , v_x and v_y oscillate, the vectors $\underline{h}$ and $\underline{v}$ being in the plane of $\underline{H}$ and $\underline{k}$, as shown in figure 2(b)

Some interesting results follow when either $H^2 \gg$ or $\ll$ $4\pi\rho_0 a_0^2$, and the following results may be obtained, though the mathematical details have been omitted. In the limiting case where $H^2 \ll 4\pi\rho_0 a_0^2$ we have $U_2 \doteq a_0$ and it follows from equation (2.24) that $v_y \ll v_x$. In other words, in the limit, waves of this type become ordinary sound waves propagated with velocity a_0 . The weak transverse field in the wave is related to v by $h_y \doteq v_x H_{0y}/a_0$ In the same limiting case U_3 is the same as U_1 , to a first approximation, and $v_x \doteq 0$, $v_y \doteq -h_y/\sqrt{4\pi\rho_0}$ as in the wave of the first type, but with vectors $\underline{v}$ and $\underline{h}$ parallel to the plane of $\underline{k}$ and $\underline{H}$ instead of perpendicular to it.

When $H^2 \gg 4\pi\rho_0 a_0^2$ we have, in the first approximation, that $U_2 = H_0/\sqrt{4\pi\rho_0}$. Since this expression in independent of $\underline{k}$, the group velocity is of magnitude U_2 and its direction is that of $\underline{k}$. In this wave the vector $\underline{v}$ is perpendicular to $\underline{H}_0$ and its magnitude is given in terms of $h = h_y$ by $v \doteq h/\sqrt{4\pi\rho_0}$ For U_3 we have in this limiting case $U_3 \doteq a H_x/H_0$. The group velocity is $\frac{\partial\omega}{\partial k} = a_0 \underline{H}/H$ and the vector $\underline{v}$ in this case is antiparallel to $\underline{H}$, and its magnitude is given by $v = h^2 H^2/4\pi\rho_0 a_0 H_{0y}$

When the relation between H^2 and $\rho_0 a_0^2$ is arbitrary both U_2 and U_3 depend on the direction of the wave vector $\underline{k}$. As the angle between $\underline{k}$ and $\underline{H}$ increases, U_2 increases monatonically and U_3 decreases monatonically. If $\underline{k}$ is parallel to $\underline{H}$ (i.e. $H_y = 0$, $H_x = H$), U_1 and U_3 are respectively equal to the greater and smaller of a_0 and $U_1 = H/\sqrt{4\pi\rho_0}$. If $\underline{k}$ is perpendicular to $\underline{H}$ (i.e. $H_x = 0$, $H_y = H$), then

$$U_2 = \sqrt{a_0^2 + \frac{H_0^2}{4\pi\rho_0}}, \qquad (2.32)$$

while U_1 and U_3 are zero, i.e. only one type of wave exists.

Returning to an incompressible fluid it is interesting to note that the plane hydromagnetic wave given by the equation

$$U = \frac{H}{\sqrt{4\pi\rho}} \tag{2.33}$$

and

$$\underline{v} = \frac{h}{\sqrt{4\pi\rho}} \tag{2.34}$$

is, in fact, an exact solution of the equations, valid for any transverse field h not necessarily small. Consider again equations (2.1), (2.2), (2.6) and (2.8): if we seek a solution in which all the quantities depend on only one co-ordinate x and the time t, we find, from equation (2.6), that v_x is a constant and, by taking another co-ordinate system moving uniformly in the x direction, we can put $v_x = 0$. From the equation $\operatorname{div}\underline{H} = 0$ it follows that H_x = constant. Denoting the transverse component of H by h we obtain, from equations (2.1) and (2.8)

$$\frac{\partial h}{\partial t} = H_x \frac{\partial v}{\partial x}, \tag{2.35}$$

$$\frac{\partial v}{\partial t} = \frac{H_x}{4\pi\rho}\frac{\partial h}{\partial x}, \tag{2.36}$$

i.e. the exact equations necessarily reduce to the linear equations for a plane wave.

This section will be concluded with a brief discussion of the damping of hydromagnetic waves. There are two dissipative effects which must be considered, viscosity and electrical resistance. The basic equations, including these two effects may be written

$$\frac{\partial \underline{v}}{\partial t} = \frac{H}{4\pi\rho}\frac{\partial \underline{h}}{\partial x} + \nu \nabla^2 \underline{v} , \qquad (2.37)$$

$$\frac{\partial \underline{h}}{\partial t} = H_0 \frac{\partial \underline{v}}{\partial x} + \nu_M \nabla^2 \underline{h} . \qquad (2.38)$$

The relation between the kinematic viscosity ν and the ordinary coefficient of viscosity μ is that

$$\nu = \frac{\mu}{\rho} . \qquad (2.39)$$

Equations (2.37) and (2.38) may be written

$$\left(\frac{\partial}{\partial t} - \nu \nabla^2\right)\underline{v} = \frac{H_0}{4\pi\rho}\frac{\partial \underline{h}}{\partial x} , \qquad (2.40)$$

$$\left(\frac{\partial}{\partial t} - \nu_M \nabla^2\right)\underline{h} = H_0 \frac{\partial \underline{v}}{\partial x} . \qquad (2.41)$$

Eliminating $\underline{v}$ between these two equations gives,

$$\left(\frac{\partial}{\partial t} - \nu \nabla^2\right)\left(\frac{\partial}{\partial t} - \nu_M \nabla^2\right)\underline{h} = \frac{H_0^2}{4\pi\rho}\frac{\partial^2 \underline{h}}{\partial x^2}$$

$$= b^2 \frac{\partial^2 \underline{h}}{\partial x^2} , \qquad (2.42)$$

where b has been put equal to the Alfvén velocity. Assuming a plane wave again, $\underline{h}$ is proportional to $\exp\left[i(\underline{k}.\underline{r} - \omega t)\right]$ and thus equation (2.42) becomes

$$(-i\omega + \nu k^2)(-i\omega + \nu_M k^2) = k^2 b^2 ,$$

ie. $$-\omega^2 - i\omega k^2(\nu + \nu_M) + (\nu\nu_M k + b^2 k^2) = 0 , \qquad (2.43)$$

and thus

$$\omega = -i\frac{1}{2}(\nu + \nu_M)k^2 \pm \sqrt{b^2k^2 - \frac{1}{4}k^4(\nu - \nu_M)^2} \quad . \tag{2.44}$$

We assume that k is real and ω complex, and thus the time variation is sinusoidal with frequency $\doteq b\,k$, and the wave is damped exponentially with time constant T, where

$$T = \frac{2}{k^2(\nu + \nu_M)} \quad . \tag{2.45}$$

Thus the condition for waves not to be damped is that

$$\frac{2b}{k(\nu + \nu_M)} \gg 1 \quad . \tag{2.46}$$

3. Contact discontinuities

At an interface between two media various types of discontinuities may occur. In the next two sections of this chapter two kinds of discontinuities which occur at the interface between two perfectly conducting media will be discussed. Contact discontinuities will be considered in this section and shock fronts in the next.

The conservation laws (1.6) to (1.8) may be put in the following form, which is more convenient for this discussion.

$$\frac{\partial \rho}{\partial t} + \operatorname{div}(\rho \underline{v}) = 0 , \tag{3.1}$$

$$\frac{\partial}{\partial t}\rho\underline{v} + \operatorname{div}\left[\rho\underline{v}\,\underline{v} + p\overleftrightarrow{1} + \frac{1}{4\pi}\left\{\frac{1}{2}H^2\overleftrightarrow{1} - \overleftrightarrow{H}\,\overleftrightarrow{H}\right\}\right] = 0, \tag{3.2}$$

$$\frac{\partial}{\partial t}\left[\mathcal{E}\rho + \frac{1}{2}\rho v^2 + \frac{1}{8\pi}H^2\right] + \operatorname{div}\left[(i\rho + \frac{1}{2}\rho v^2)v + \frac{E\wedge H}{4\pi}\right] = 0, \tag{3.3}$$

where a double arrow, $\leftrightarrow$, above a quantity is used to denote a second order tensor. $\overleftrightarrow{1}$ denoting the unit tensor. $\left\{\frac{1}{2}H^2\overleftrightarrow{1} - \overleftrightarrow{H}\,\overleftrightarrow{H}\right\}$ is the Maxwell stress tensor, which Maxwell showed may be used to represent the electromagnetic force $\underline{j} \wedge \underline{H}$. Writing

$$\overleftrightarrow{S} = \rho\underline{v}\underline{v} - p\overleftrightarrow{1} + \frac{1}{4\pi}\left\{\frac{1}{2}H^2\overleftrightarrow{1} - \overleftrightarrow{H}\,\overleftrightarrow{H}\right\} , \tag{3.4}$$

equation (3.3) may be written

$$\frac{D}{Dt}(\rho v) + \operatorname{div}\overleftrightarrow{S} = 0 , \tag{3.5}$$

where $\overleftrightarrow{S}$ may be thought of as the momentum transport tensor.

By considering a suitable frame of reference the boundary between two media labelled 1 and 2 may be considered at rest. Let ΔQ represent the change in any physical variable Q across the interface, i.e.

$$\Delta Q = Q_2 - Q_1 . \tag{3.6}$$

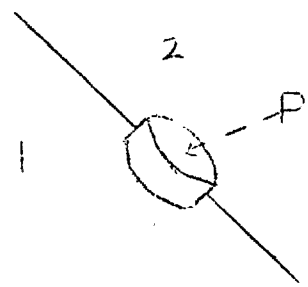

Fig. 2(c)

If no fluid crosses the boundary then

$$v_{n1} = v_{n2} = 0 \quad , \tag{3.7}$$

n here is used to denote the component normal to the interface; the suffix t will be used to denote the tangental component.

From equation (1.2) we have that

$$\mathrm{div}\, \underline{H} = 0 \ . \tag{3.8}$$

Applying this to the small pill box P in figure 2(c) and integrating, using Gauss' theorem, we have

$$0 = \int_V \mathrm{div}\, \underline{H}\, d\tau = \int_S \underline{H} \cdot \underline{dS} \quad , \tag{3.9}$$

where $d\tau$ and dS denote elements of volume and surface area respectively; ds will be used later to denote an element of arc. From equation (3.9) we, therefore, have that

$$\Delta H_n = 0 \ . \tag{3.10}$$

Equation (3.1) gives

$$\frac{\partial \underline{H}}{\partial t} = \mathrm{curl}(\underline{v} \wedge \underline{H}) \,. \qquad (3.11)$$

Integrating this equation and applying Stoke's theorem gives

$$\int_S \frac{\partial \underline{H}}{\partial t} \, dS = \int_S \mathrm{curl}(\underline{v} \wedge \underline{H}) \, dS \,,$$

$$= \oint (\underline{v} \wedge \underline{H}) \, ds \,. \qquad (3.12)$$

As dS tends to zero the left hand side of this equation tends to zero and therefore so does the right hand side, i.e.

$$\Delta(\underline{v} \wedge \underline{H})_t = 0 \,, \qquad (3.13)$$

or in order words

$$\Delta E_t = 0 \,. \qquad (3.14)$$

As

$$\underline{v}_t \wedge \underline{H}_t = \underline{v}_n \wedge \underline{H}_n = 0 \,,$$

$$(\underline{v} \wedge \underline{H})_t = \underline{v}_n \wedge \underline{H} + \underline{v}_t \wedge \underline{H}_n \,,$$

and as $v_{n1} = v_{n2} = 0$ we have that

$$\Delta(\underline{v}_t \wedge \underline{H}_n) = 0 \,,$$

$$\text{ie} \quad H_n \Delta v_t = 0 \,. \qquad (3.15)$$

Thus, equation (3.15) shows that

$$\left.\begin{array}{l} \text{either} \\ \qquad H_n = 0 \,, \\ \text{or } \; v_t \text{ is continuous.} \end{array}\right\} \qquad (3.16)$$

As $\Delta v_n = 0$ this condition may be rewritten as

$$\left.\begin{array}{ll} \text{either} & H_n = 0 , \\ \text{or} & \Delta \underline{v} = 0 . \end{array}\right\} \qquad (3.17)$$

By definition, an interface having $\Delta \underline{v} = 0$ is called a contact discontinuity.

Equation (3.5) may be written

$$\int_V \frac{D}{Dt}(\rho v)\, d\tau = -\int_V \operatorname{div} \overleftrightarrow{S}\, d\tau$$

$$= -\int \overleftrightarrow{S}\,\underline{n}\; dS , \qquad (3.18)$$

by Gauss' theorem, where $\underline{n}$ is the unit normal vector. As we let the volume V tend to zero, the left hand side tends to zero and, therefore,

$$\Delta\left(\overleftrightarrow{S}\cdot\underline{n}\right) = 0 . \qquad (3.19)$$

Now $\overleftrightarrow{S}\cdot\underline{n}$ is the normal component of stress, and thus this equation is equivalent to saying that the normal components of stress on either side of the interface are equal and opposite. Substituting for $\overleftrightarrow{S}$, from equation (3.4), gives that

$$\Delta\left[\rho \underline{v} v_n + p\,\underline{n} + \frac{1}{4\pi}\left(\frac{1}{2}H^2\underline{n} - \underline{H}\; H_n\right)\right]$$

$$= 0 . \qquad (3.20)$$

As $v_n = 0$, this equation may be rewritten

$$\Delta\left[p\underline{n} + \frac{1}{4\pi}\left(\frac{1}{2}H^2\underline{n} - \underline{H}\,H_n\right)\right] = 0 . \qquad (3.21)$$

Taking the scalar product of equation (3.21) with $\underline{n}$ yields, as $H_n = 0$, that

$$\Delta\left(p + \frac{H^2}{8\pi}\right) = 0 \qquad (3.22)$$

i.e. $\Delta q = 0$ across a contact discontinuity. Again taking the scalar product of equation (3.21) with $\underline{t}$, the unit vector in the tangental direction, yields that

$$\Delta\left(H_t\, H_n\right) = 0 \qquad (3.23)$$

As H_n is continuous we have that

$$H_n\, \Delta H_t = 0\,, \qquad (3.24)$$

$$\text{i.e. either } \Delta H_t = 0\,, \quad \text{or } H_n = 0\,. \qquad (3.25)$$

Because H_n is continuous this condition may be rewritten

$$\text{either } H_n = 0 \quad \text{or } \underline{H} \text{ is continuous.} \qquad (3.26)$$

Summarizing these results we have that, at a contact discontinuity, either

$$\left.\begin{aligned} \Delta H &= 0, \\ \Delta v &= 0, \\ \Delta q &= 0, \\ H_n &\neq 0. \end{aligned}\right\} \qquad (3.27)$$

or

$$\left.\begin{aligned} H_n &= 0 \\ \Delta q &= 0, \\ \Delta v_n &= 0 \end{aligned}\right\} \qquad (3.28)$$

A discontinuity of the kind given by the equations of (3.27) is called a tangental discontinuity.

The theory, as given in this section, has assumed that both media are perfectly conducting. If we assume that one of the media is an insulator or has finite conductivity, then equation (3.13) is no longer valid, as the concept of a moving line of force is no longer true.

4. Magnetohydrodynamic shock waves

A shock wave is a different type of discontinuity from a contact discontinuity in that whereas in the latter no fluid crosses the interface, in a shock wave fluid does cross the discontinuity. In normal shock hydrodynamics it is well known that the motion in a shock proceeds perpendicularly to the shock front, but in magnetohydrodynamics this is no longer necessarily so. When treating shocks whose direction of propagation is parallel or perpendicular to the magnetic force lines, one obtains solutions to the shock equations if one assumes that all motion is parallel to the direction of shock propagation. These shocks are called longitudinal. Discontinuities in which the motion of the material is along the surface of the discontinuity, and therefore perpendicular to the direction of propagation are called transverse shocks. The work in the remaining chapters is concerned with longitudinal shocks, and thus oblique shocks will not be considered in any great detail.

As $\operatorname{div} \underline{H} = 0$ we again have that

$$\Delta H_n = 0 \,, \qquad (4.1)$$

$$\text{i.e.} \quad H_{n1} = H_{n2} \,. \qquad (4.2)$$

If $H_{n1} = H_{n2} = 0$ then the shock is perpendicular. Such a shock is illustrated in figure 2(d) and has the

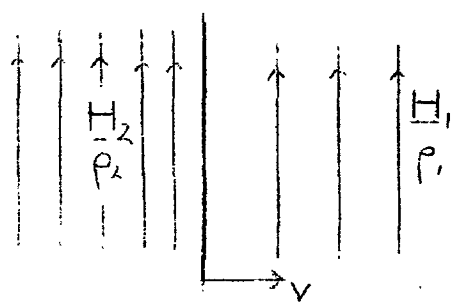

Fig. 2(d) A perpendicular shock

property that the lines of force are parallel to the shock front. A shock in which the magnetic lines of force are parallel to the direction of propagation is called a parallel shock. For such a shock as this the magnetic field does not affect the motion which may be taken as an ordinary hydrodynamical shock.

From equation (3.13) we have that

$$\Delta(\underline{v} \wedge \underline{H})_t = 0 ;$$

$$\text{i.e. } \Delta(\underline{v} \wedge \underline{H}) \wedge \underline{n} = 0 , \tag{4.3}$$

$$\text{or } \Delta(v_n \underline{H}_t - H_n \underline{v}_t) = 0 . \tag{4.4}$$

Writing $\underline{H} = \underline{H}_t + \underline{H}_n$ and $\underline{v} = \underline{v}_t + \underline{v}_n$ this equation may be written

$$\Delta(v_n \underline{H}_t - H_n \underline{v}_t) = 0 . \tag{4.5}$$

If $H_n = 0$ then

$$\Delta(v_n \underline{H}_t) = 0 . \tag{4.6}$$

$(v_n \underline{H}) = (v_n \underline{H}_t)$ may be considered as the rate at which lines of force are being taken across the shock front. Although we have specified that the frame of reference be perpendicular to the shock we have not yet specified the transverse frame of reference. In the most general case when H_n is not zero this frame of reference is best chosen such that $\underline{H}$ is parallel to $\underline{v}$ on side 1, i.e.

$$\frac{\underline{H}_1}{H_{n1}} = \frac{\underline{v}_1}{v_{n1}} ,$$

$$\text{i.e. } (v_n \underline{H} - H_n \underline{v})_1 = 0 . \tag{4.7}$$

From equation (4.4) we, therefore, have that

$$(v_n \underline{H} - H_n \underline{v})_2 = 0 , \tag{4.8}$$

i.e. $\underline{H}$ and $\underline{v}$ are parallel in region 2. We conclude, therefore, that it is possible to choose a frame of reference for an oblique shock in such a way that the flow is always along the lines of force.

From the conservation of mass, equation (3.1), in the steady state we have $\operatorname{div}(\rho v) = 0$ and thus

$$\Delta\,(\rho v_n) = 0\,, \tag{4.9}$$

$$\text{i.e. } \rho_1 v_{n1} = \rho_2 v_{n2} = m\,, \tag{4.10}$$

where m is a measure of the mass flow crossing unit area of the shock front per unit time.

The momentum transport equation (3.2) yields that

$$\Delta\left[\underline{n}\cdot\left(\rho\underline{v}\,\underline{v} - p\,\overleftrightarrow{1} + \frac{1}{8\pi}\overleftrightarrow{1}\,H^2 - \frac{1}{4\pi}\underline{H}\,\underline{H}\right)\right] = 0\,, \tag{4.11}$$

$$\text{i.e. } \Delta\left(q\,\underline{n} + \rho v\,\underline{v} - \frac{1}{4\pi}H_n\,\underline{H}\right) = 0 \tag{4.12}$$

For a perpendicular shock the transverse and normal components of this equation yield that

$$\Delta\, v_t = 0 \quad \text{as } H_n = 0\,, \tag{4.13}$$

$$\text{and } \Delta\left(q + \rho v_n^2\right) = 0 \tag{4.14}$$

The former of these two equations implies that by a suitable choice of the frame of reference v_t may be taken as zero.

The energy conservation equation gives

$$\Delta\left[\left(\tfrac{1}{2}\rho v^2 - \rho i\right)\underline{v} + \frac{\underline{E}\wedge\underline{H}}{4\pi}\right]_n = 0 \qquad (4.15)$$

Now $\underline{E} = -\underline{v}\wedge\underline{H}$ and thus

$$\left[\underline{E}\wedge\underline{H}\right]_n = \left[(\underline{v}\wedge\underline{H})\wedge\underline{H}\right]_n ,$$

$$= v_{\perp} H^2 , \qquad (4.16)$$

where $v_{\perp}$ is the component of $\underline{v}$ perpendicular to the magnetic field. Thus

$$\Delta\left[\left(\tfrac{1}{2}\rho v^2 + i\rho\right)v_n + \frac{v_{\perp}H^2}{4\pi}\right] = 0 . \qquad (4.17)$$

For a perpendicular shock, the frame of reference has been chosen in such a way that this reduces to

$$\Delta\left[\tfrac{1}{2}\rho v^2 + \rho i + \frac{H^2}{4\pi}\right]v_n = 0 , \qquad (4.18)$$

or
$$\left[\tfrac{1}{2}\rho v^2 - \rho i^*\right]v_n = 0 . \qquad (4.19)$$

where
$$i^* = i + \frac{H^2}{4\pi\rho} . \qquad (4.20)$$

In the case of an oblique shock equation (4.17) reduces to

$$\Delta\left(\tfrac{1}{2}\rho v^2 - \rho i\right)v_n = 0 , \qquad (4.21)$$

because, as a result of the choice of the frame of reference, $v_{\perp} = 0$.

5. Perpendicular shocks

This chapter will be concluded with a detailed consideration of a perpendicular shock as illustrated in figure 2(d). The basic equations (4.9), (4.14), (4.19) and (4.6) may be written

$$\Delta(\rho v) = 0 , \tag{5.1}$$

$$\Delta(q + \rho v^2) = 0 , \tag{5.2}$$

$$\Delta(i^* \rho v + \tfrac{1}{2}\rho v^3) = 0 , \tag{5.3}$$

$$\Delta(H v) = 0 . \tag{5.4}$$

Defining τ as $1/\rho$ and putting $\rho v = m$ = constant we have

$$v_1 = m\tau_1 , \qquad v_2 = m\tau_2 , \tag{5.5}$$

$$\Delta(q + m^2\tau) = 0 , \tag{5.6}$$

$$\Delta(i^* + \tfrac{1}{2}m^2\tau^2) = 0 , \tag{5.7}$$

$$H_1\tau_1 = H_2\tau_2 = A , \tag{5.8}$$

where A is a constant. The equations (5.5) to (5.7) are the same as those for a non-magnetic shock with the internal energy $\mathcal{E}$ replaced by the total internal energy $\mathcal{E}^* = \mathcal{E} + \frac{H^2}{8\pi\rho}$ and the pressure p replaced by the total pressure $q = p + \frac{H^2}{8\pi}$. Equations (5.6) and (5.7) yield that

$$\frac{\Delta q}{\Delta \tau} = -m^2 = \frac{\Delta i^*}{\frac{1}{2}\Delta \tau^2} = \frac{\Delta i^*}{\frac{\tau_1+\tau_2}{2}\Delta\tau} \quad (5.9)$$

As we are considering a shock $\Delta\tau \neq 0$, and thus we have

$$\bar{\tau}\,\Delta q = \Delta i^* , \quad (5.10)$$

where $$\bar{\tau} = \tfrac{1}{2}(\tau_1 + \tau_2) . \quad (5.11)$$

If the magnetic field H is zero then, from the definition of q and i^* , we have

$$i_2 - i_1 = \tau(p_2 - p_1) . \quad (5.12)$$

Now $i = i(p,\tau)$, hence if we know p_1 , ρ_1 and hence i_1 , the above equation may be written

$$H(p_2\,\tau_2) = 0 , \quad (5.13)$$

where $H(p,\tau)$ is defined as the Hugoniot function. For a polytropic gas, i.e. a perfect gas for which the specific heats at constant volume and pressure are constant,

$$i = \frac{\gamma}{\gamma - 1}\,p\,\tau , \quad (5.14)$$

where γ is the ratio of the specific heat at constant pressure to that at constant volume. Thus we have

$$H(p,\tau) = (\alpha\tau - \tau_1)p - (\tau_1\alpha - \tau)p_1 , \quad (5.15)$$

where $$\alpha = \frac{\gamma + 1}{\gamma - 1} . \quad (5.16)$$

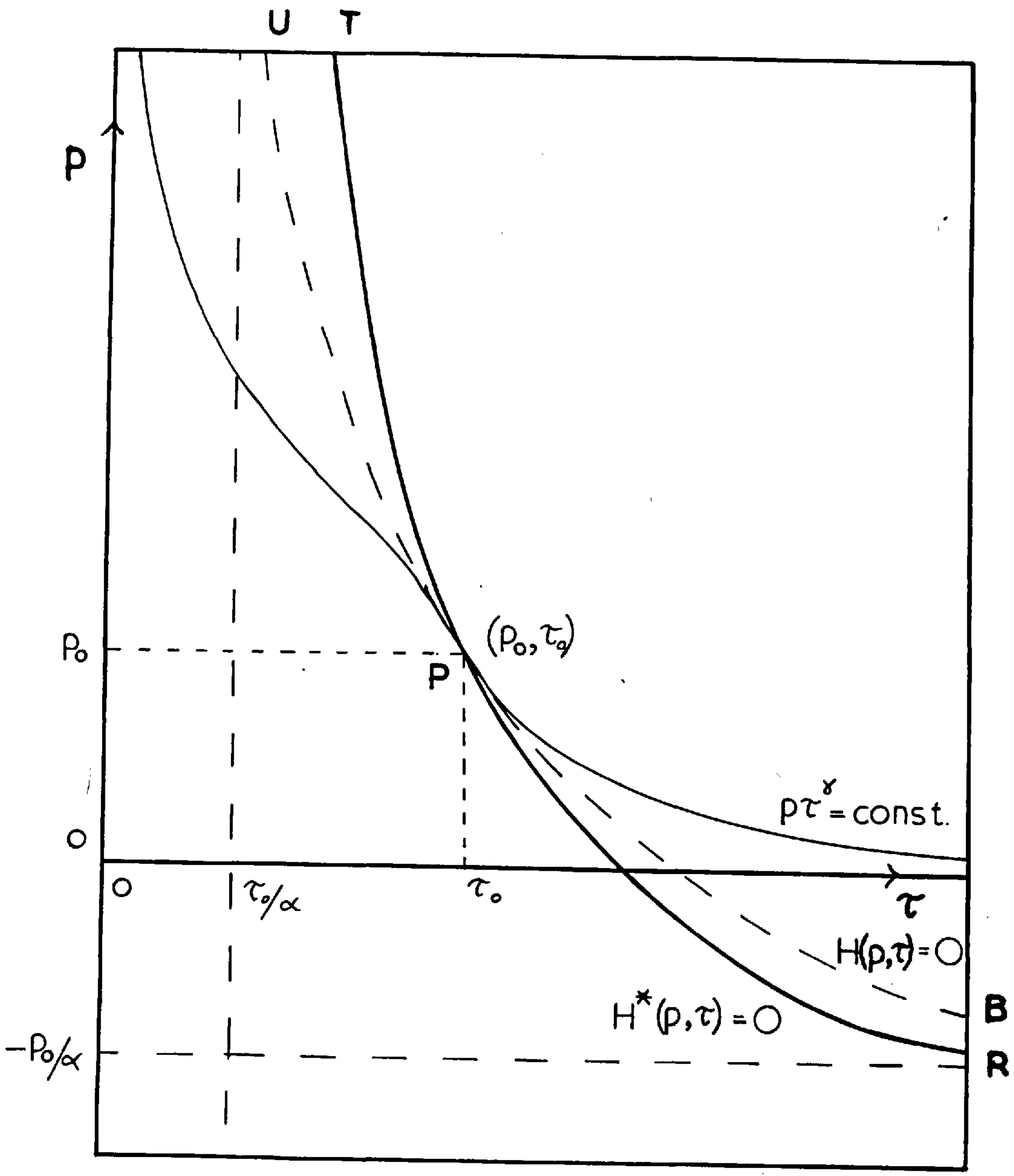

FIG. 3. HUGONIOT CURVES

Thus $H(p, \tau)$ is a hyperbola, as shown in figure 3. For given initial conditions (p_1, τ_1) the curve represents the locus of all possible final states (p_2, τ_2). Explicitly we have that

$$p_2 = \frac{p_1(\tau_2 - \alpha \tau_1)}{\tau_1 - \alpha \tau_2} . \qquad (5.17)$$

The well known feature of α being the maximum compression possible for an ordinary hydrodynamic shock is easily seen in this figure. Shown also in this figure is the adiabatic curve $p \tau^{\gamma}$ = constant which touches the curve $H(p, \tau) = 0$ at (p_1, τ_1). As we are considering an ideal gas this adiabatic curve represents the constant entropy curve $S = S_1$. In the region above this curve $S > S_1$, and below it $S < S_1$. Now through a shock wave the entropy must increase, and thus the part PB of the curve $H(p, \tau)$ is not a permissible part of the locus for the final state $(p_2 \ \tau_2)$. Thus

$$\tau_2 < \tau_1 , \qquad (5.18)$$

and
$$p_2 > p_1 \qquad (5.19)$$

illustrating the well known fact that shocks are compressive.

We can now consider what effect a magnetic field has on this theory. A generalized Hugoniot function $H^*(p, \tau)$ may be defined by

$$H^*(p, \tau) = \Delta i^*(p, \tau) - \bar{\tau} \Delta p^* . \qquad (5.20)$$

which may be written

$$H^*(p,\tau) = H(p,\tau) + \frac{1}{8\pi}\left[\Delta 2 H^2 \tau - \bar{\tau} \Delta H^2 \right] . \quad (5.21)$$

Manipulating this equation algebraically and using the fact that $A = H\tau$ we have

$$H^*(p,\tau) = H(p,\tau) - \frac{A(\tau_2 - \tau_1)^3}{16\pi\tau_1^2\tau_2^2} , \quad (5.22)$$

Putting $H^*(p,\tau) = 0$ gives

$$p_2 = \frac{p_1(\tau_2 - \alpha\tau_1)}{\tau_1 - \alpha\tau_2} + \frac{A^2(\tau_2 - \tau_1)^2}{16\pi\tau_1^2\tau_2^2(\tau_1 - \alpha\tau_2)} \quad (5.23)$$

The curve $H^*(p,\tau)$ is also shown in figure 3 and we again see that the maximum compression is still α. Again the part PR of the curve $H^*(p,\tau) = 0$ is not admissible and thus a magnetic shock is still compressive, though as the curve $H^*(p\,\tau) = 0$ is above the curve $H(p,\tau) = 0$ we see that a magnetic shock is more irreversible than an ordinary hydrodynamic shock.

An ordinary strong hydrodynamic shock transforms a considerable part of its kinetic energy into heat. It is of interest to determine whether, in the presence of a magnetic field, this continues to be true or whether the magnetic field can act as a sort of cushion producing elastic recoil, where normal hydrodynamics would predict a strongly inelastic collision.

Let us assume that there is such a cushioning effect and see whether such an assumption would be consistant. As we are considering a strong shock we do not have that

$$|v_1 - v_2| \ll |v_1| , \tag{5.24}$$

but we do have that

$$\left.\begin{aligned} \mathcal{E}_1 &\ll \rho_1 v_1^2 , \\ p_1 &\ll \rho_1 v_1^2 . \end{aligned}\right\} \tag{5.25}$$

and we are going to assume that

$$\left.\begin{aligned} \mathcal{E}_2 &\ll \rho_2 v_2^2 , \\ p_2 &\ll \rho_2 v_2^2 . \end{aligned}\right\} \tag{5.26}$$

In the light of assumptions (5.25) and (5.26) equations (5.6) and (5.7) may be written

$$\frac{H_1^2}{8\pi} + \rho_1 v_1^2 = \frac{H_2^2}{8\pi} + \rho_2 v_2^2 , \tag{5.27}$$

$$\frac{H_1^2 v_1}{4\pi} + \frac{1}{2}\rho_1 v^3 = \frac{H_2^2 v_2}{4\pi} + \frac{1}{2}\rho_2 v_2^3 . \tag{5.28}$$

Now $\rho = \dfrac{m}{V}$ and $H = \dfrac{Am}{V}$, thus (5.27) and (5.28) may be written

$$V_2 - V_1 = \frac{A^2 m}{8\pi}\left[\frac{1}{V_1^2} - \frac{1}{V_2^2}\right], \qquad (5.29)$$

$$V_2^2 - V_1^2 = \frac{A^2 m}{2\pi}\left[\frac{1}{V_1} - \frac{1}{V_2}\right] \qquad (5.30)$$

Dividing (5.29) into (5.30) gives that

$$V_2 + V_1 = \frac{4 V_1 V_2}{V_1 + V_2}, \qquad (5.31)$$

$$\text{i.e. } (V_1 - V_2)^2 = 0,$$

$$\text{i.e. } V_1 = V_2 \qquad (5.32)$$

This condition is inconsistent with the condition given in equation (5.24) for a strong shock, and thus we conclude that in a magnetic shock, as in an ordinary shock, a considerable portion of the kinetic energy is still transferred into heat.

CHAPTER III

The Flow in a Shock Tube with no Magnetic Fields

1. The mathematical model

To investigate the flow which develops in a T-tube following a discharge at low pressure, it is necessary to adopt a model which is amendable to mathematical analysis. Such a model is the sudden release of a high temperature gas in a shock tube under the influence of constant transverse magnetic fields. In this model the magnetic field resulting from the return path of the current is assumed to be equivalent to a uniform magnetic field throughout the high pressure region. Mitchner[11] has considered the solution of the steady state equations for various cases of a similar model, thus obtaining the initial motion. Here, however, the motion is examined up to the time at which the rarefaction wave reaches the shock front, and the model is generalized to cover the case of an initial uniform magnetic field in front of the shock wave, i.e. a constant external magnetic field across the side arm. In this chapter, the flow in a shock tube when there are no magnetic fields is examined; in the following chapter the extension to a magnetohydrodynamic flow is considered.

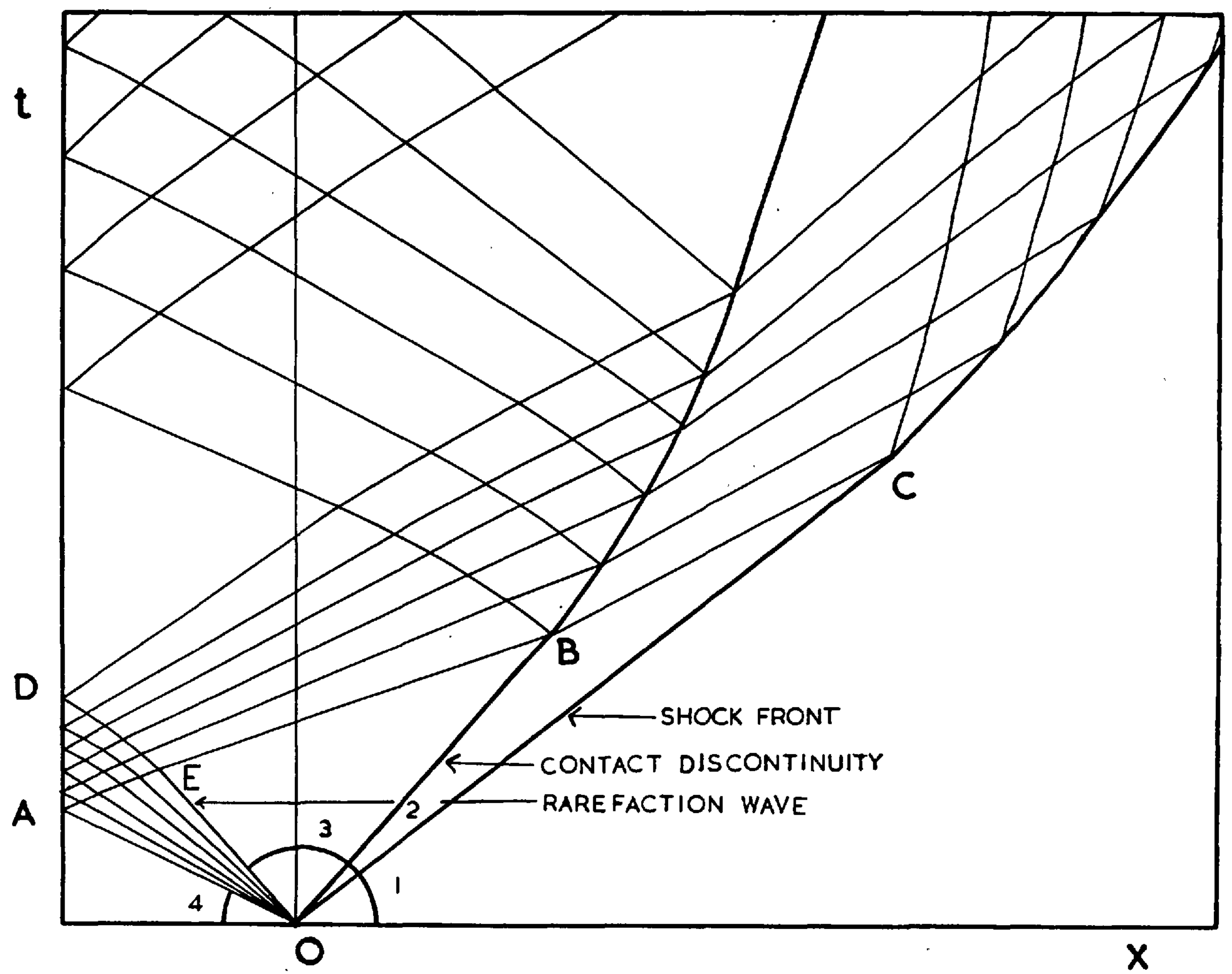

FIG. 1. SHOCK TUBE FLOW

Figure 1 shows the flow pattern in the x - t plane that develops when a release, such as has been discussed, takes place. There are four regions in which all the variables are constant and these are labelled 1 to 4 as shown in the figure. A variable with one of these numbers as a suffix will be used to denote the value of the variable in that region. O C represents the shock front which advances with speed U into the undisturbed low pressure gas. The region 2 behind the shock front, containing the high temperature plasma, is terminated by a contact discontinuity O B , which separates the gas which was initially on the right of the plane of release from that on the left. The head of the rarefaction wave is represented by O A and its tail by O E , the position of the latter being determined in such a way that the rarefaction wave and region 3 join with continuity of velocity, density and pressure.

2. One dimensional flow

The equations of conservation of mass, momentum and energy (1.6) to (1.8) of chapter II, for the flow in one dimension without any magnetic fields may be written

$$\frac{\partial \rho}{\partial t} + u\frac{\partial \rho}{\partial x} + \rho\frac{\partial u}{\partial x} = 0 , \qquad (2.1)$$

$$\rho\frac{\partial u}{\partial t} + \rho u\frac{\partial u}{\partial x} + \frac{\partial p}{\partial x} = 0, \qquad (2.2)$$

$$\frac{\partial}{\partial t}\left(\tfrac{1}{2}\rho u^2 + \rho\varepsilon\right) + \frac{\partial}{\partial x}\left[\rho v\left(\tfrac{1}{2}v^2 + i\right)\right] = 0, \qquad (2.3)$$

u throughout this chapter, and the next, will be used to denote the velocity relative to a system of co-ordinates which is at rest. Following the motion, the entropy S is constant and thus

$$\frac{\partial S}{\partial t} + u\frac{\partial S}{\partial x} = 0 \qquad (2.4)$$

The equation of state may be written

$$p = f(\rho, S) \qquad (2.5)$$

and, by definition

$$a^2 = \frac{\partial p}{\partial \rho} \qquad (2.6)$$

Equations (2.5) and (2.6) yield that

$$\frac{\partial p}{\partial t} = a^2\frac{\partial \rho}{\partial t} + \frac{\partial f}{\partial S}\frac{\partial S}{\partial t}, \qquad (2.7)$$

and

$$\frac{\partial p}{\partial x} = a^2\frac{\partial \rho}{\partial x} + \frac{\partial f}{\partial S}\frac{\partial S}{\partial x}. \qquad (2.8)$$

Thus equation (2.4) may be written

$$\frac{\partial p}{\partial t} + u\frac{\partial p}{\partial x} + \rho a^2\frac{\partial u}{\partial x} = 0. \qquad (2.9)$$

Adding and subtracting from equation (2.9) equation (2.2) multiplied by a, we find that

$$\left\{\frac{\partial p}{\partial t} + (u + a)\frac{\partial p}{\partial x}\right\} + \rho a\left\{\frac{\partial u}{\partial t} + (u + a)\frac{\partial u}{\partial x}\right\} = 0, \qquad (2.10)$$

$$\left\{\frac{\partial p}{\partial t} + (u-a)\frac{\partial p}{\partial x}\right\} - \rho a\left\{\frac{\partial u}{\partial t} + (u-a)\frac{\partial u}{\partial x}\right\} = 0 . \tag{2.11}$$

From equations (2.10), (2.11) and (2.4) we see that at any point in the flow three characteristic directions may be defined C_+, C_- and C_o, by

$$dx = (u+a)\,dt , \tag{2.12}$$

$$dx = (u-a)\,dt , \tag{2.13}$$

$$dx = u\,dt . \tag{2.14}$$

Along these directions, equations (2.10), (2.11) and (2.4) may be written

$$dp + \rho a\,du = 0 , \tag{2.15}$$

$$dp - \rho a\,du = 0 , \tag{2.16}$$

$$dS = 0 . \tag{2.17}$$

The C_+ and C_- directions represent the lines followed by small disturbances and the C_o direction represents the actual particle paths.

These characteristic directions will define three families of curves in the x - t plane, $\alpha(x, t) = 0$, $\beta(x, t) = 0$ and $\delta(x, t) = 0$, the curves being defined by the equations

$$\frac{\partial x}{\partial \alpha} = (u+a)\frac{\partial t}{\partial \alpha} , \tag{2.18}$$

$$\frac{\partial x}{\partial \beta} = (u-a)\frac{\partial t}{\partial \beta} , \tag{2.19}$$

$$\frac{\partial x}{\partial \delta} = u \frac{\partial t}{\partial \delta} \qquad (2.20)$$

It is now natural to introduce new independent variables α and β in such a way that α is constant along the C_+ curves and β is constant along the C_- curves. A function of the density ω is introduced, defined by

$$\omega = \int_0^\rho a \frac{d\rho}{\rho} \qquad (2.21)$$

With this definition, and with the new independent variables, equations (2.10), (2.11), and (2.4) may be written

$$\frac{\partial u}{\partial \alpha} + \frac{\partial \omega}{\partial \alpha} = \frac{1}{\rho a} \frac{\partial p}{\partial S} \frac{\partial S}{\partial \alpha}, \qquad (2.22)$$

$$\frac{\partial u}{\partial \beta} - \frac{\partial \omega}{\partial \beta} = -\frac{1}{\rho a} \frac{\partial p}{\partial S} \frac{\partial S}{\partial \beta}, \qquad (2.23)$$

$$\frac{\partial S}{\partial \alpha} \frac{\partial t}{\partial \beta} + \frac{\partial t}{\partial \alpha} \frac{\partial S}{\partial \beta} = 0 . \qquad (2.24)$$

For a perfect gas the equation of state (2.5) may be written

$$p = \rho^{\gamma} \exp(S/C_v), \qquad (2.25)$$

where C_v is the specific heat of the gas at constant volume, and in this case the integration of equation (2.21) may be carried out to give

$$\omega = \frac{2}{\gamma - 1} a . \qquad (2.26)$$

Thus (2.22) and (2.23) reduce to

$$\frac{\partial u}{\partial \alpha} + \frac{2}{\gamma - 1}\frac{\partial a}{\partial \alpha} = \frac{a}{c_v \gamma(\gamma - 1)}\frac{\partial S}{\partial \alpha}, \tag{2.27}$$

$$\frac{\partial u}{\partial \beta} - \frac{2}{\gamma - 1}\frac{\partial a}{\partial \beta} = -\frac{a}{c_v \gamma(\gamma - 1)}\frac{\partial S}{\partial \alpha}. \tag{2.28}$$

For an isentropic flow the right hand side of these two equations vanishes, and they may be integrated to give

$$u + \frac{2}{\gamma - 1} a = 2 r(\alpha), \tag{2.29}$$

$$u - \frac{2}{\gamma - 1} a = - 2 s(\beta). \tag{2.30}$$

$r(\alpha)$ and $s(\beta)$ are arbitrary functions of α and β respectively and are frequently called Riemann invariants. A wave having either $r(\alpha)$ or $s(\beta)$ constant throughout is called a simple wave. There are two types of simple waves, rarefaction waves and compression waves. In the former the pressure and density of a gas particle decreases crossing the wave, whereas in the latter the pressure and density increases. Suppose $r(\alpha)$ = constant throughout a wave, then along a C_- characteristic $s(\beta)$ will be constant and from (2.29) and (2.30), we therefore see that both u and a will be constant along a C_- characteristic; i.e. the C_- characteristics will be straight lines in the x - t plane, their slope being given by equation (2.13). Similarly if $s(\beta)$ is a constant throughout a wave then the C_+ characteristics will be straight lines.

3. The steady state equations

The state of the gas behind the shock is dependent on the state in front through the well known shock conservation equations. These may be deduced from equations (1.6) to (1.8) of chapter II, and for a polytropic gas may be written

$$\rho_2(U - u_2) = \rho_1 U \qquad (3.1)$$

$$p_2 + \rho_2(U - u_2)^2 = p_1 + \rho_1 U^2, \qquad (3.2)$$

$$\frac{\gamma}{\gamma-1}\frac{p_2}{\rho_2} + \frac{1}{2}(U - u_2)^2 = \frac{\gamma}{\gamma-1}\frac{p_1}{\rho_1} + \frac{1}{2}U^2, \qquad (3.3)$$

where u_2 is the actual velocity of the gas behind the shock relative to a co-ordinate system at rest. ρ_2 and U may be eliminated from these equations to give an expression for p_2 in terms of u_2,

$$p_2 = p_1 - \rho_1 u_2\left[\frac{\gamma-1}{2}u_2 + \sqrt{\frac{1}{4}\left(\frac{\gamma+1}{2}\right)^2 u_2^2 + a_1^2}\right]. \qquad (3.4)$$

The rarefaction wave is a simple wave having the property that the Riemann invariant r is a constant throughout the wave, and thus, from the theory of the preceding section, for a perfect isentropic flow

$$\frac{u}{2} + \frac{a}{\gamma-1} = \frac{a_4}{\gamma-1}, \qquad (3.5)$$

as when $u = 0$, $a = a_4$. As the flow is isentropic

$$p_3 = p_4 \left(\frac{a_3}{a_4} \right)^{\frac{2\gamma}{\gamma-1}} . \tag{3.6}$$

At the contact discontinuity we have continuity of velocity and pressure, i.e.

$$u_3 = u_2 , \tag{3.7}$$

$$p_3 = p_2 , \tag{3.8}$$

p_3, a_3 and u_3 may be eliminated from equations (3.5) to (3.8) to give

$$p_2 = p_4 \left(1 - \frac{\gamma-1}{2} \frac{u_2}{a_4} \right)^{\frac{2\gamma}{\gamma-1}} . \tag{3.9}$$

Equations (3.4) and (3.9) are thus two simultaneous equations for p_2 and u_2, which may be solved quite easily, leading to a complete determination of the steady state conditions.

4. Reflection of the rarefaction wave at the wall

The attenuation of the shock front is investigated by the method of characteristics whereby the conditions at any point in the flow may be determined. There are three separate problems involved in the construction of the characteristics for the flow: the reflection of the rarefaction wave at the wall, and the interactions of the reflected rarefaction wave both with the contact discontinuity and with the shock front. The most suitable method for constructing the characteristics in these interaction zones is a finite difference technique, similar to that used by Courant and Friedrichs.[10] In this method the curved characteristics are replaced by a series of straight line segments.

The reflection of the rarefaction wave at the wall, illustrated in figure 2, will be considered first. As the gas is assumed to be perfect and the flow isentropic the initial rarefaction wave has the property that

$$u + \frac{2}{\gamma-1} a = 2 r_0 = \text{constant throughout the wave} \qquad (4.1)$$

and

$$u - \frac{2}{\gamma-1} a = -2 s_i = \text{constant along the } i^{th}\ C_- \text{ characteristic of slope } (u-a) \qquad (4.2)$$

where $i = 0(1)n$, the number n being assigned arbitrarily, depending on the accuracy of the construction that is required. These C_- characteristics will be straight until they meet the first reflected C_+ characteristic L_0 (figure 2). In the interaction zone $A\ D\ A_n$ we have

$$u + \frac{2}{\gamma-1} a = 2 r_j = \text{constant along the } j^{th}\ C_+ \text{ characteristic}, \qquad (4.3)$$

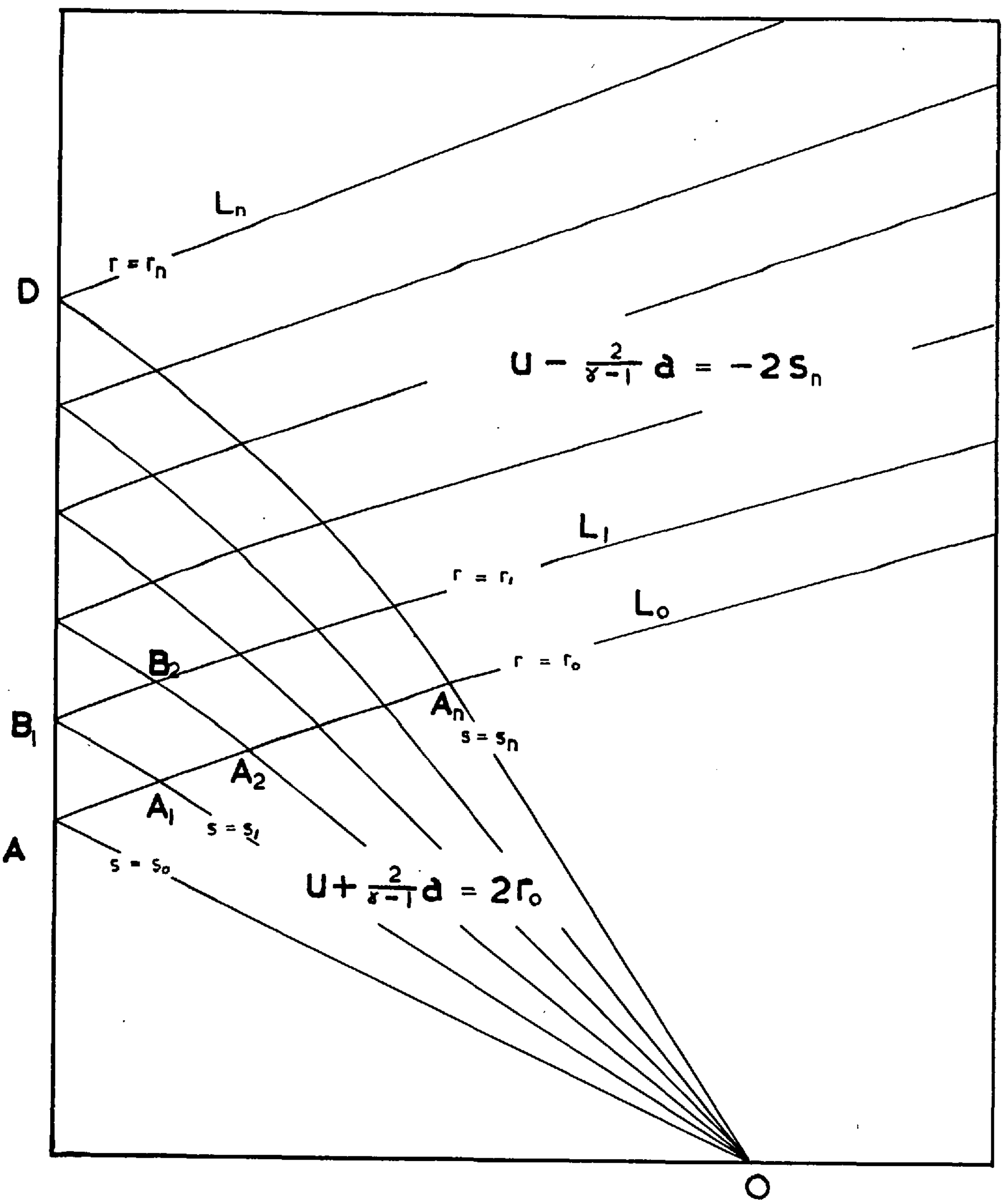

FIG. 2. REFLECTION OF THE RAREFACTION WAVE

$$u - \frac{2}{\gamma - 1} a = -2 s_i = \text{constant along the } i^{th} \; C_- \text{characteristic,} \qquad (4.4)$$

where again, $j = O(1)n$

$$\left(\frac{dx}{dt}\right)_{C_+} = u + a \,, \qquad (4.5)$$

and $$\left(\frac{dx}{dt}\right)_{C_-} = u - a \,. \qquad (4.6)$$

Neither of the two Riemann invariants will be constant throughout the region A D A_n , though the final wave which emerges will again be a simple wave, having the property that $u - \frac{2}{\gamma - 1} a = -2 s_n =$ a constant throughout the wave. Thus the C_+ characteristics of the reflected wave will be straight lines.

At the intersection of the j^{th} C_+ and i^{th} C_-characteristic r_j = constant and s_i = constant, and thus at this point u , a , $\left(\frac{dx}{dt}\right)_{C_+}$ and $\left(\frac{dx}{dt}\right)_{C_-}$ may be found. The equations (4.5) and (4.6) may be approximated to by

$$\Delta_s x = (\bar{u} + \bar{a}) \Delta_s t \quad \text{along } r_j = \text{constant} \,, \qquad (4.7)$$

$$\Delta_r x = (\bar{u} - \bar{a}) \Delta_r t \quad \text{along } s_i = \text{constant} \,, \qquad (4.8)$$

where Δ_r means the difference between two successive net points of s = constant along r = constant, and Δ_s has a similar meaning. $\bar{u} + \bar{a}$ or $\bar{u} - \bar{a}$ denotes the average of $u + a$ or $u - a$ at two successive net points. The equations (4.3) to (4.6) together with the boundary condition that $u = 0$ at the wall, may thus be used to construct the characteristics in the interaction zone, the characteristic curves being approximated to by a series of straight line segments.

To illustrate how the characteristics for these interaction zones are drawn, this particular construction will be explained in some detail. Similar methods must be used for the interactions described later. OA and OA_n are determined by the steady state conditions, the slope of the former being $-a_4$, as u is zero in region 4, and that of the latter being $(u_3 - a_3)$. The steady state conditions also yield that

$$r_o = \frac{1}{\gamma - 1} a_4 \tag{4.9}$$

$$s_o = \frac{1}{\gamma - 1} a_4 \tag{4.10}$$

and
$$s_n = \frac{1}{2}\left(u_3 - \frac{2}{\gamma - 1} a_3\right) \tag{4.11}$$

The remaining C_- characteristics of the initial wave are each characterized by a Riemann invariant s_i, where

$$s_o > s_1 > s_2 > - - - - > s_{n-1} > s_n \tag{4.12}$$

As $u + \frac{2}{\gamma - 1} a = \frac{2}{\gamma - 1} a_4$ throughout the wave the position of the other C_- characteristics in the $x - t$ plane are easily found once the s_i's have been specified.

L_0 is the first reflected characteristic to be determined. It is a C_+ characteristic with $r = r_0 = a$ constant along it, and is found as follows. At A_1 we have,

$$u + \frac{2}{\gamma - 1} a = 2 r_0 \tag{4.13}$$

$$u - \frac{2}{\gamma - 1} a = -2 s_1 \tag{4.14}$$

Thus u, a, $\left(\frac{dx}{dt}\right)_{C+}$ and $\left(\frac{dx}{dt}\right)_{C-}$ may all be found at A_1, and the segment $A A_1$ of L_0 may be drawn, its slope being given by

$$\frac{dx}{dt} = \bar{u} + \bar{a} \tag{4.15}$$

where $\bar{u} + \bar{a}$ is the mean of $u + a$ between the two points A and A_1, A_2, A_3 etc., and thus the whole of L_0, may be constructed in a similar manner. Both u and a at A_1 are now known and, as $u = 0$ at B_0 and the value of a at B_1 is given by $a = \frac{s_1}{\gamma - 1}$ the segment $A_1 B_1$ may be drawn, its slope being given by the mean of $(u - a)$ between A_1 and B_{10}.

The characteristic L_1, has $u - \frac{2}{\gamma - 1} a = 2 r_1 = a$ constant along it, r_1, being given by

$$r_1 = s_1 \tag{4.16}$$

Thus L_1 may be drawn in exactly the same way as L_0 was constructed. In general we shall have

$$r_i = s_i \quad (0 \leq i \leq n), \tag{4.17}$$

and thus the characteristics for the whole of the interaction zone may be constructed.

An interesting case occurs if γ has the particular value 3. When this occurs we have,

$$u + a = 2r = \text{constant along the } C_+ \text{ lines}, \tag{4.18}$$

and $$u - a = -2s = \text{constant along the } C_- \text{ lines}. \tag{4.19}$$

Now the slopes of the characteristics are given by

$$\left(\frac{dx}{dt}\right)_{C_+} = u + a, \tag{4.20}$$

$$\left(\frac{dx}{dt}\right)_{C_-} = u - a. \tag{4.21}$$

Thus the characteristics will always be straight lines, even in the interaction zone of the incoming rarefaction wave and the reflected wave.

5. Interaction of the rarefaction wave with the contact discontinuity

The contact discontinuity separates two constant states with different values of entropy, temperature, and density, but with the same values of pressure and particle velocity. In the x - t plane the contact discontinuity is a straight line until it is met by the incoming rarefaction wave. The effect of this interaction is a gradual slowing down of the contact discontinuity, or in the x - t diagram a bending of the contact discontinuity line D , until D has crossed the entire width of the wave. This is shown in figure 3. The flow on both sides of D is isentropic and both the transmitted and reflected waves will be simple, i.e. we have

$$u - \frac{2}{\gamma - 1} a = -2s_0 = \text{constant throughout the incoming wave}, \tag{5.1}$$

$$u - \frac{2}{\gamma - 1} a = -2s_{10} = \text{constant throughout the transmitted wave}, \tag{5.2}$$

$$u + \frac{2}{\gamma - 1} a = 2r_n = \text{constant throughout the reflected wave}. \tag{5.3}$$

In the interaction zone the characteristics may be constructed by a similar method to that used for the reflection of the rarefaction wave at the wall. There is, however, a more complicated boundary condition to be satisfied, namely that along the contact discontinuity

$$\frac{dx}{dt} = u . \tag{5.4}$$

Using the notation of figure 3, where P_R represents any point on the right of the contact

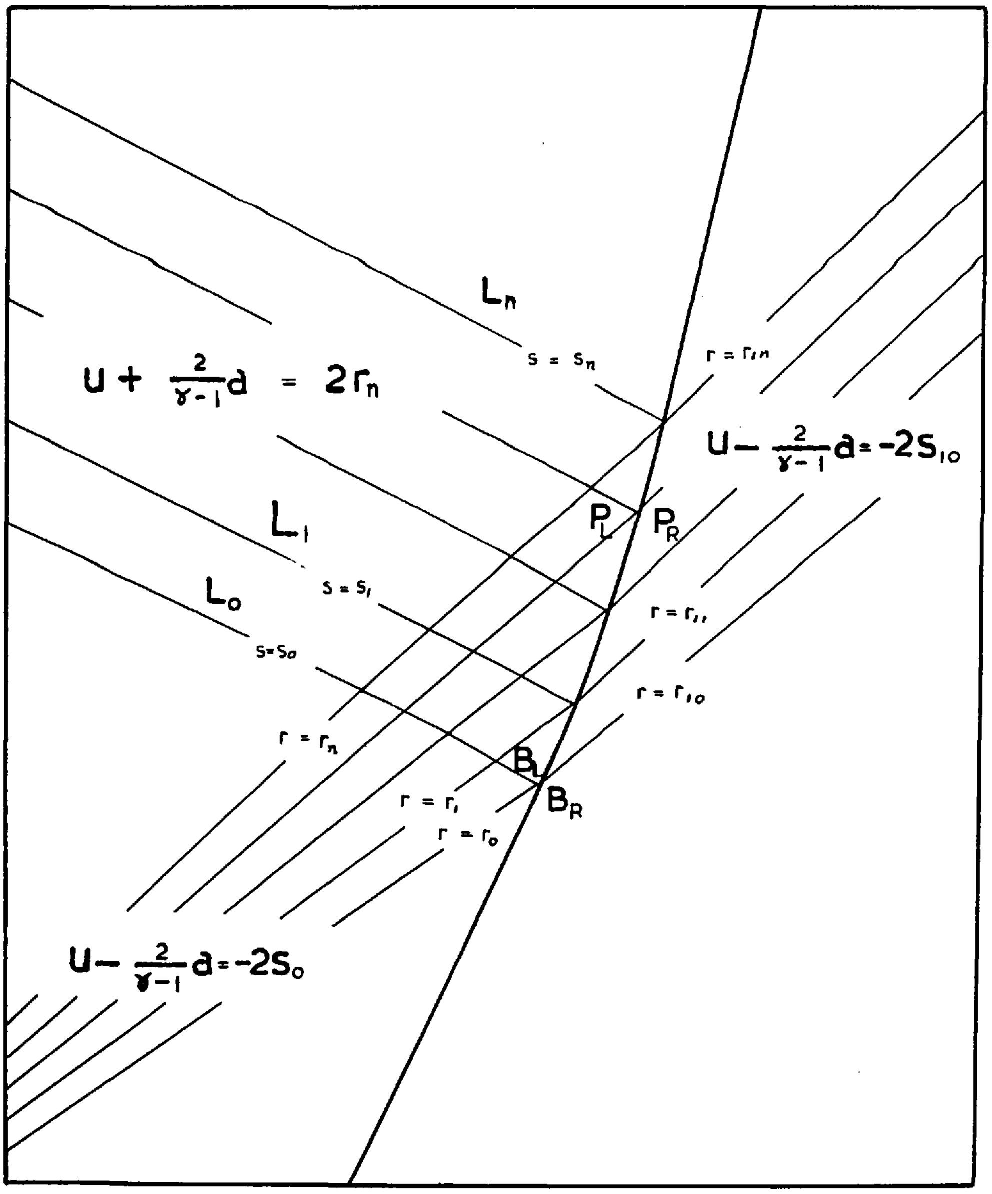

FIG. 3. INTERACTION OF THE RAREFACTION WAVE WITH THE CONTACT DISCONTINUITY

discontinuity, and P_L the corresponding point on the left, the continuity conditions (3.7) and (3.8) become

$$\rho(P_R) = \rho(P_L) , \tag{5.5}$$

$$u(P_R) = u(P_L) . \tag{5.6}$$

As the transmitted wave is simple we have from equation (5.2), in the notation of figure 3, that

$$u(P_R) - \frac{2}{\gamma_1 - 1} a(P_R) = a(A_{1R}) - \frac{2}{\gamma_1 - 1} a(A_{1R}) . \tag{5.7}$$

The flow is isentropic and thus

$$\frac{\rho(P_R)}{\rho(A_{1R})} = \left(\frac{a(P_R)}{a(A_1)}\right)^{\frac{2\gamma}{\gamma_1 - 1}} , \tag{5.8}$$

and

$$\frac{\rho(P_L)}{\rho(A_{1L})} = \left(\frac{a(P_L)}{a(A_{1L})}\right)^{\frac{2\gamma_4}{\gamma_4 - 1}} . \tag{5.9}$$

γ_1 and γ_4 are the ratios of the specific heats on either side of the contact discontinuity. Combining equations (5.5), (5.8) and (5.9) we have that

$$\frac{a(P_R)}{a(A_{1R})} = \left(\frac{a(P_L)}{a(A_{1L})}\right)^{\frac{\gamma_4(\gamma_1 - 1)}{\gamma_1(\gamma_4 - 1)}} . \tag{5.10}$$

Equations (5.6), (5.7) and (5.10) may, therefore, be combined to give $u(P_L)$ as a function of $a(P_L)$, being the relationship between u and a along the left hand side of the contact discontinuity. This relationship is

$$u(P_L) - a(A_{1L}) = \frac{2a(A_{1R})}{\gamma_1 - 1}\left[\left(\frac{a(P_L)}{a(A_{1L})}\right)^{\frac{\gamma_4(\gamma_1 - 1)}{\gamma_1(\gamma_4 - 1)}} - 1\right], \tag{5.11}$$

With equation (5.11) and the difference approximation to equation (5.4)

$$\Delta x = u \Delta t , \tag{5.12}$$

the position of the contact discontinuity and the characteristics of the flow may be found, in the order $L_0, L_1 - - - L_n$, by a similar process to that outlined in the last section. Again, if γ has the particular value 3 then all the characteristics will be straight lines.

6. Interaction of the rarefaction wave with the shock front.

The problem of a straight shock being overtaken by a rarefaction wave is more complex than the two interactions considered previously. During the penetration, the shock gradually weakens in intensity and speed until it eventually emerges as a weakened constant shock.

Because of the decay of the shock the isentropic character of the process is lost and we, therefore, have three families of characteristics $\alpha(x\ t) = 0$, $\beta(x, t) = 0$ and $\delta(x, t) = 0$ defined by equations of the form

$$\frac{\partial x}{\partial \alpha} = (u + a)\frac{\partial t}{\partial \alpha}, \qquad (6.1)$$

$$\frac{\partial x}{\partial \beta} = (u - a)\frac{\partial t}{\partial \beta}, \qquad (6.2)$$

$$\frac{\partial x}{\partial \delta} = u \frac{\partial t}{\partial \delta}. \qquad (6.3)$$

The equations of one dimensional non-steady flow involving entropy changes and in terms of the variables α and β were derived in section 2 of this chapter and, for an ideal gas, are

$$\frac{\partial u}{\partial \alpha} + \frac{2}{\gamma - 1}\frac{\partial a}{\partial \alpha} = \frac{a}{\gamma(\gamma - 1)C_v}\frac{\partial S}{\partial \alpha}, \qquad (6.4)$$

$$\frac{\partial u}{\partial \beta} - \frac{2}{\gamma - 1}\frac{\partial a}{\partial \beta} = -\frac{a}{\gamma(\gamma - 1)C_v}\frac{\partial S}{\partial \beta}, \qquad (6.5)$$

$$\frac{\partial t}{\partial \beta}\frac{\partial S}{\partial \beta} + \frac{\partial t}{\partial \alpha}\frac{\partial S}{\partial \beta} = 0 \qquad (6.6)$$

These equations determine the C_+, C_- and C_0 characteristics. If the Riemann invariants $r(\alpha)$ and $s(\beta)$ for non-isentropic flow are defined as follows

$$r(\alpha) = u + \frac{2}{\gamma - 1}a - \frac{a}{\gamma(\gamma - 1)C_v}S, \qquad (6.7)$$

$$s(\beta) = u - \frac{2}{\gamma - 1}a + \frac{a}{\gamma(\gamma - 1)C_v}S, \qquad (6.8)$$

Then the equations (6.1), (6.2) and (6.6) to (6.8) may be written in difference form as

$$\Delta_s x = (\bar{u} + \bar{a}) \Delta_s t \quad \text{along } r(\alpha) = \text{constant}, \tag{6.9}$$

$$\Delta_r x = (\bar{u} - \bar{a}) \Delta_r t \quad \text{along } s(\beta) = \text{constant}, \tag{6.10}$$

$$\Delta_s\left(u - \frac{2}{\gamma - 1} a\right) = \frac{a}{\gamma(\gamma - 1)C_v} \Delta_s S \text{ along } r(\alpha) = \text{constant}, \tag{6.11}$$

$$\Delta_r\left(u - \frac{2}{\gamma - 1} a\right) = \frac{a}{\gamma(\gamma - 1)C_v} \Delta_r S \text{ along } s(\beta) = \text{constant}, \tag{6.12}$$

$$\Delta_s S \, \Delta_r t + \Delta_r S \, \Delta_s t = 0 \tag{6.13}$$

Figure 4 shows the flow pattern for this interaction. The incoming C_+ characteristics will have $r(\alpha)$ = constant and the reflected C_- characteristics, $L_0, L_1 - - - - L_n$, will have $S(\beta)$ = constant along them. The characteristic L_0 and the distribution of u, a and S along it may be found quite easily in the usual way. At the shock front the relevant boundary conditions come from the shock relations connecting the steady state (1) in front of the shock with the conditions behind the shock. These relations may be used to express the shock velocity $\frac{dx}{dt}$ in terms of the particle velocity u, the sound speed a and the entropy S, i.e.

$$\frac{dx}{dt} = h(u) \tag{6.14}$$

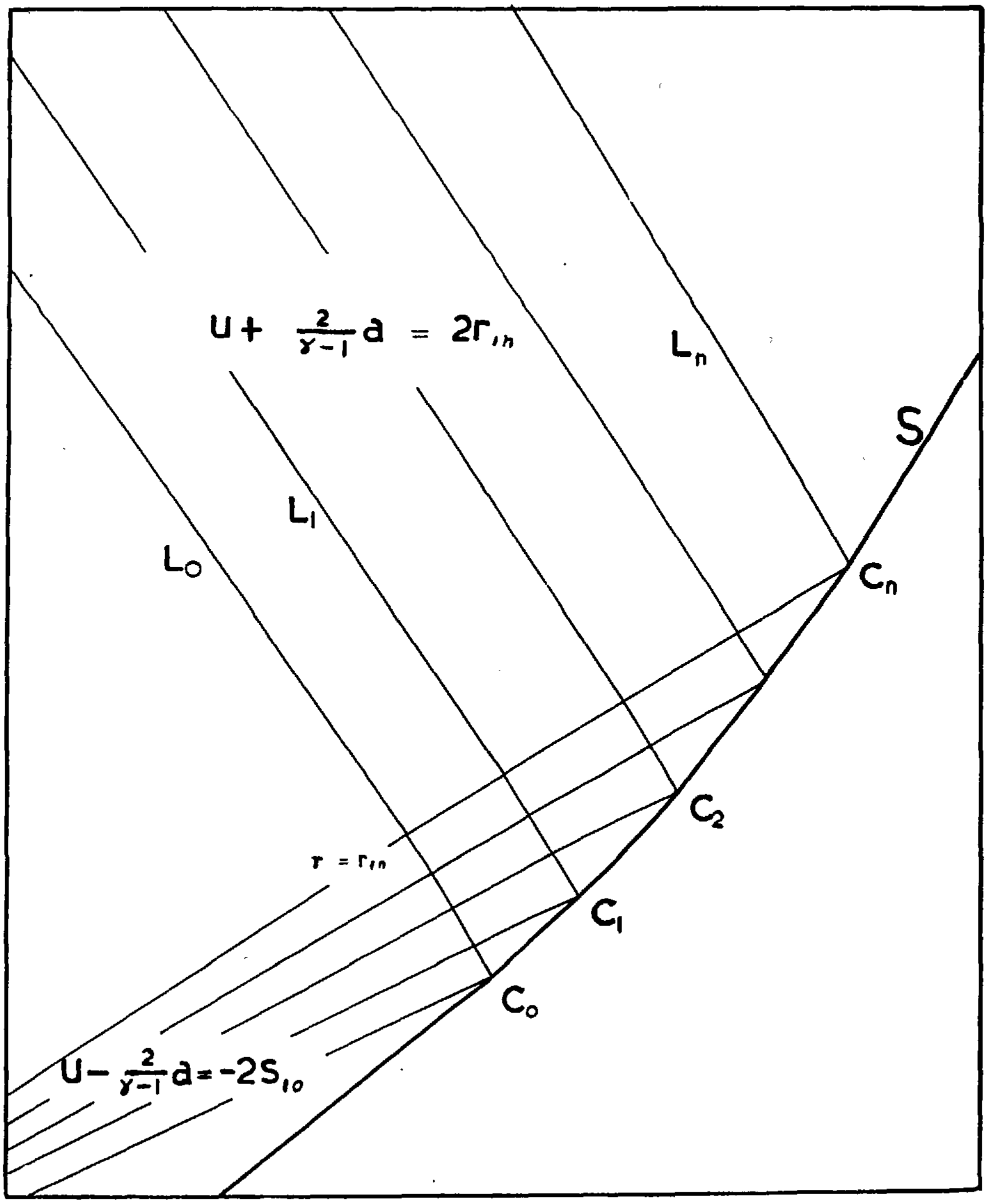

FIG. 4. INTERACTION OF THE RAREFACTION WAVE WITH THE SHOCK FRONT

$$\frac{dx}{dt} = g(a) \quad , \tag{6.15}$$

$$\frac{dx}{dt} = k(S) \quad . \tag{6.16}$$

For a normal shock the functions $h(u)$, $g(a)$ and $k(S)$ are fairly complicated, but for strong shocks they have the following simple form

$$h(u) = \frac{\gamma+1}{2} u \quad , \tag{6.17}$$

$$g(a) = \frac{\gamma+1}{2\gamma(\gamma-1)} a \quad , \tag{6.18}$$

$$k(S) = \left(\frac{\gamma+1}{\gamma}\right)^{\frac{1}{2}} \left(\frac{\gamma+1}{\gamma-1}\right)^{\frac{\gamma}{2}} \exp\left[\frac{S - S_1}{2C_v}\right] . \tag{6.19}$$

Consider first the determination of u and a at C_1 and the co-ordinates of C_1 . These may be found by an iterative procedure using equations (6.10), (6.12) and (6.13) together with equations (6.14) to (6.16) expressed in a difference form. First assume that $\Delta S = 0$ and then solve the relevant equations to give a first approximation to x , t , u and a at C_1. Equation (6.13) will now determine a new value of S at C which can then be used to obtain new values of x , t , u , a and S at C . This iteration can be continued until the pro cess converges.

The conditions at points not on the shock front may be found in a similar way, though all of the equations (6.9) to (6.13) must be used instead of using equations (6.14) to (6.16). Thus the characteristics of the flow and the position of the shock front for this interaction may be determined.

In figure 5 the complete construction for $\gamma = 3$ for the following initial conditions is shown

$$p_1 = 4.10^2 \text{ dynes/cm.}^2,$$
$$T_1 = 320^\circ K,$$
$$p_4 = 5.10^6 \text{ dynes/cm.}^2,$$
$$T_4 = 10^6 \,{}^\circ K.$$

To simplify the interaction of the rarefaction wave with the shock front entropy changes have been neglected, i.e. only the first approximation has been taken. The pressure and density at any point in the wave may be found from these calculations, and in figure 6 pressure profiles, for this wave, at various instants of time are shown.

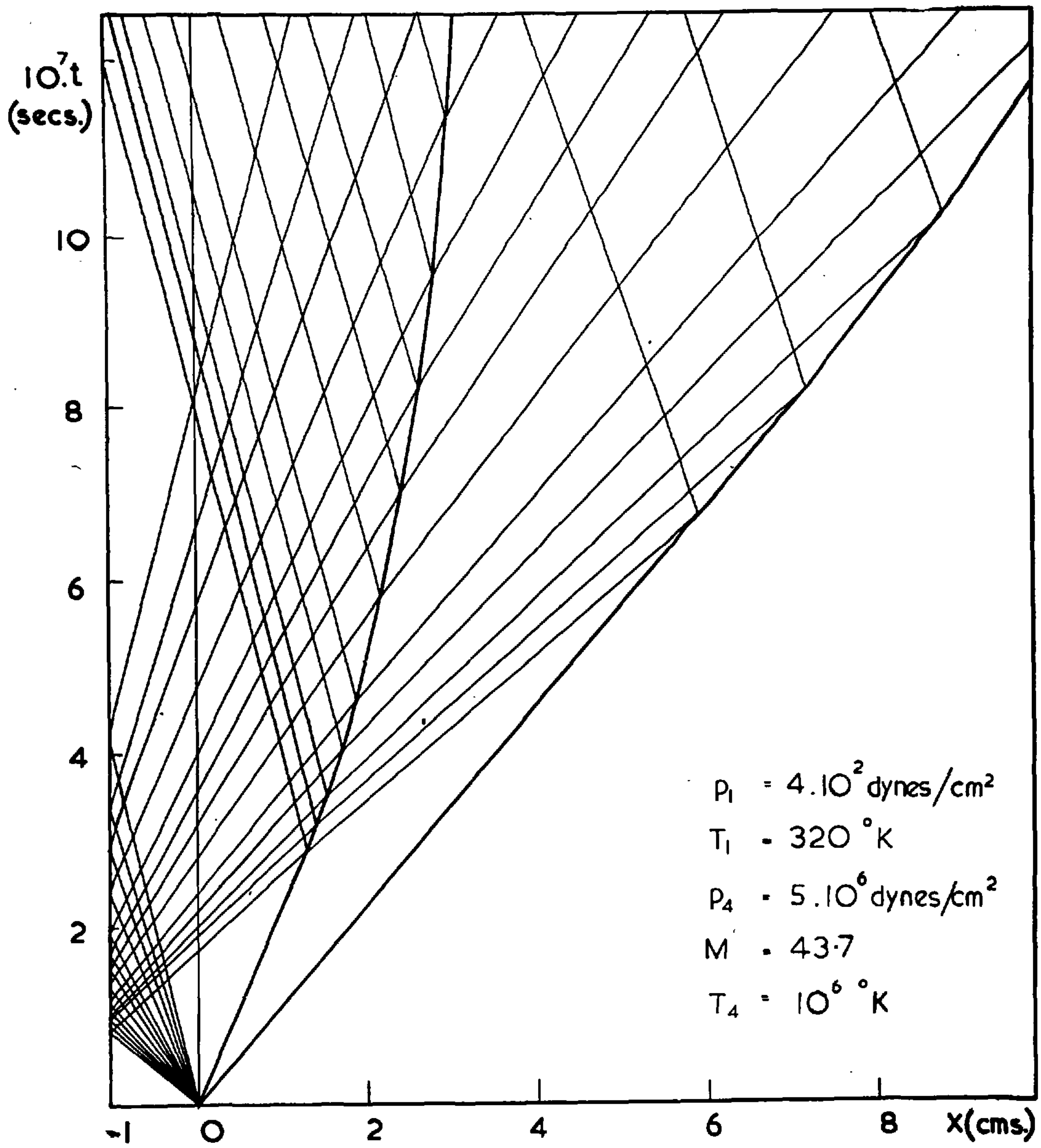

FIG. 5. CONSTRUCTION OF THE CHARACTERISTICS FOR $\gamma = 3$

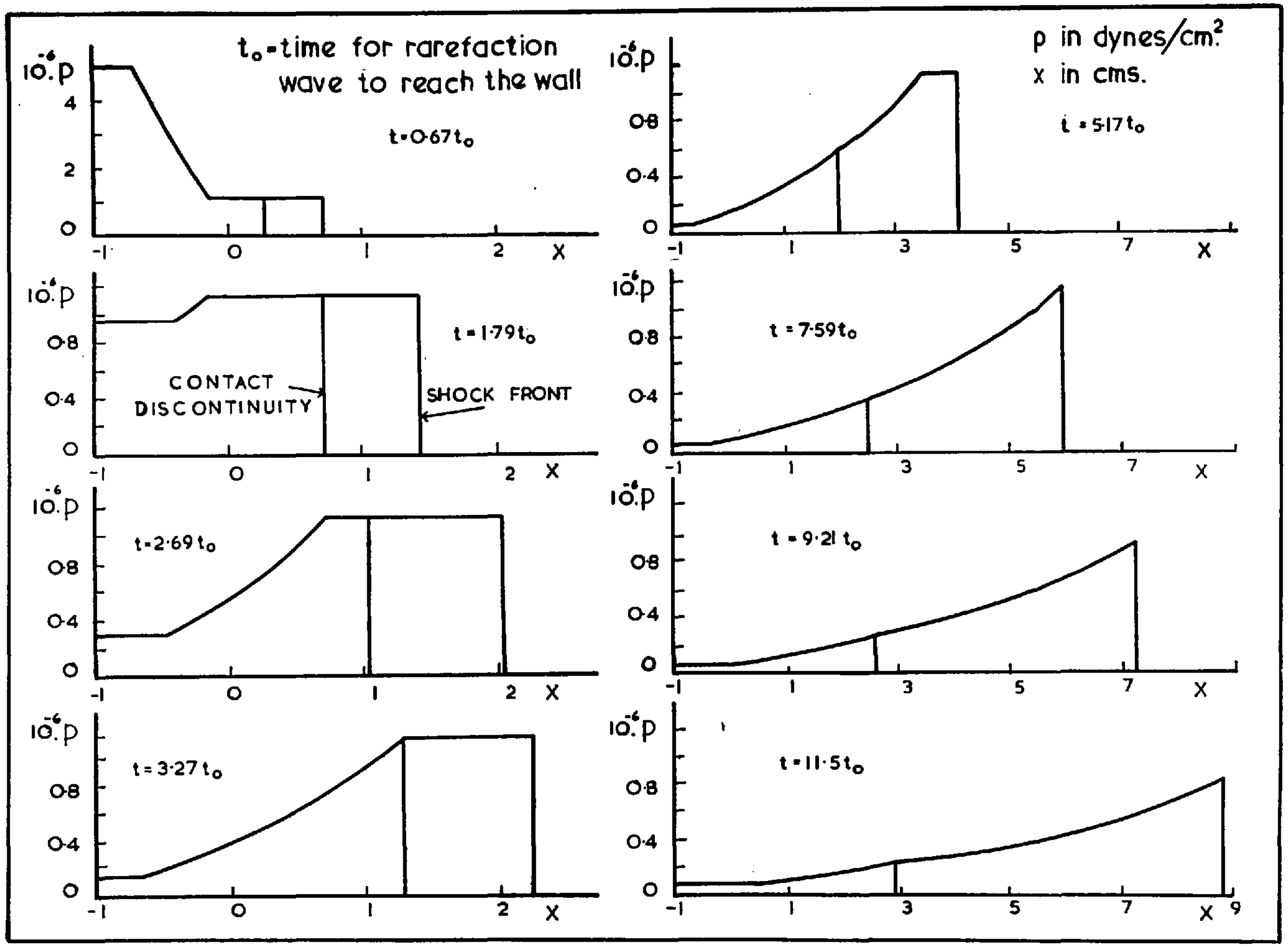

FIG. 6. PRESSURE PROFILES FOR $\gamma = 3$

CHAPTER IV

Magnetohydrohynamic Flow in a Shock Tube

1. Generalized Riemann invariants

We now consider the flow in a shock tube under the influence of transverse magnetic fields, this being the model which has been adopted for the discharge in a T-tube apparatus. If the line of flow is chosen parallel to the x axis and the magnetic field parallel to the z axis, then the hydromagnetic equations of continuity and motion for an isentropic flow may be written,

$$\frac{\partial \rho}{\partial t} + u \frac{\partial \rho}{\partial x} + \rho \frac{\partial u}{\partial x} = 0 , \tag{1.1}$$

$$\frac{\partial u}{\partial t} + u \frac{\partial \rho}{\partial x} = -\frac{1}{\rho} \frac{\partial p}{\partial x} - \frac{H}{4\pi} \frac{\partial H}{\partial x} . \tag{1.2}$$

Introducing the total pressure q into equation (1.2) we may rewrite this equation as

$$\frac{\partial u}{\partial t} + u \frac{\partial u}{\partial x} = -\frac{1}{\rho} \frac{dq}{d\rho} \frac{\partial \rho}{\partial x} = -\frac{c^2}{\rho} \frac{\partial \rho}{\partial x}, \tag{1.3}$$

where

$$c^2 = \frac{dq}{d\rho} . \tag{1.4}$$

These equations are now in their usual hydrohynamic form, though c has replaced the normal speed of sound a. Thus, these equations may be written

$$\left\{ \frac{\partial}{\partial t} + (u + c) \frac{\partial}{\partial x} \right\} \left\{ u + \omega \right\} = 0 , \tag{1.5}$$

$$\left\{ \frac{\partial}{\partial t} + (u - c) \frac{\partial}{\partial x} \right\} \left\{ u - \omega \right\} = 0 \quad , \qquad (1.6)$$

where $\pm\frac{1}{2}(u \pm \omega)$ are the generalized Riemann invariants, ω now being defined by

$$\omega = \int_0^\rho c \frac{d\rho}{\rho} \quad . \qquad (1.7)$$

Being of the same form as the ordinary hydrohynamic equations, the analysis of the previous chapter, with suitable modifications, will still be valid.

The gas in the discharge tube, and that in the region behind the shock front, will be at a high temperature and thus it is reasonable to assume that the electrical conductivity is infinite. With this assumption we have, from Maxwell's equations and the generalized Ohm's law, that

$$H = \beta \rho \qquad (1.8)$$

where β is a constant. Using equation (1.8), equation (1.4) may be written

$$c^2 = a^2 + b^2 \quad , \qquad (1.9)$$

where a = the ordinary hydrohynamic speed of sound

and $b = \left(\frac{\beta^2 \rho}{4\pi} \right)^{\frac{1}{2}}$ = the Alfvén speed. (1.10)

The isentropic relation for a perfect gas is

$$p = A \rho^{\gamma_4} \quad , \qquad (1.11)$$

where A is a constant. We put

$$n = \frac{2}{\gamma_4 - 1} \qquad \text{i.e.} \qquad \gamma_4 - 1 = \frac{2}{n} , \qquad (1.12)$$

and from equation (1.11), and the definition of a we have that

$$a^2 = A \gamma_4 \rho^{2/n} . \qquad (1.13)$$

Expressing b in terms of ρ , equations (1.10) and (1.12) give

$$b^2 = k^2 a^n , \qquad (1.14)$$

where

$$k^2 = \frac{\beta^2}{4\pi (A\gamma_4)^{\frac{n}{2}}} \qquad (1.15)$$

Thus the integral ω becomes

$$\omega = \int_0^\rho c \frac{d\rho}{\rho} = \int_0^\rho (a^2 + k^2 a^n)^{\frac{1}{2}} \frac{d\rho}{\rho}$$

$$= \int_0^a (1 + k^2 y^{n-2})^{\frac{1}{2}} dy , \qquad (1.16)$$

and putting $x = y/a$ we have

$$\omega = \frac{2a}{\gamma_4 - 1} \int (1 + \alpha^2 x^{n-2})^{\frac{1}{2}} dx , \qquad (1.17)$$

where

$$\alpha^2 = \frac{H^2}{4\pi\rho a^2} = \frac{b^2}{a^2} = k^2 a^{n-2} . \qquad (1.18)$$

We may, therefore, write

$$\omega = \frac{2a}{\gamma_4 - 1} I_n(\alpha) , \qquad (1.19)$$

where

$$I_n(\alpha) = \int_0^1 (1 + \alpha^2 x^{n-2})^{\frac{1}{2}} dx \quad (1.20)$$

Because n depends on γ, it will not necessarily be an integer, and thus it will not always be possible to evaluate this integral without resorting to numerical techniques. For n = 2, 3 or 4, corresponding to γ = 2, 5/3 and 3/2 respectively, the integral may be evaluated exactly and we have

$$I_2(\alpha) = (1 + \alpha^2), \quad (1.21)$$

$$I_3(\alpha) = \frac{2}{3\alpha}\left[(1 + \alpha^2)^{3/2} - 1\right], \quad (1.22)$$

$$I_4(\alpha) = \frac{1}{2\alpha}\left[\sin^{-1}\alpha - \alpha(1 + \alpha^2)^{1/2}\right] \quad (1.23)$$

The value n = 3 corresponds to the value of γ for a monatomic gas and this integral is shown in figure 1

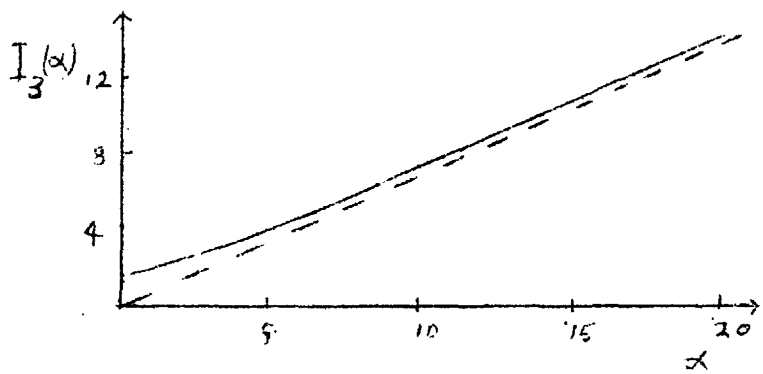

Fig. 1. <u>The Riemann Invariant Integral</u>

For $\alpha \gg 1$ the integral has an asymptotic form, which is

$$I_n(\alpha) = (\gamma - 1)\,\alpha \, . \quad (1.24)$$

When there is no magnetic field $I_n(\alpha)$ has the value unity.

Behind the shock front the gas will be highly ionized and may thus be taken as a monatomic gas, consequently we shall take $\gamma_1 = \gamma_4 = 5/3$ for numerical work. The ratio of the magnetic pressure $H^2/8\pi$ to the gas pressure p is a useful parameter to define, and this ratio will be denoted by λ , i.e.

$$\lambda = \frac{H}{8\pi p} , \tag{1.25}$$

With this definition, and for $\gamma = 5/3$, we have

$$k_4^2 = \frac{6}{5} \frac{\lambda_4}{a_4} , \tag{1.26}$$

$$\alpha_4^2 = \frac{6}{5} \lambda_4 . \tag{1.27}$$

2. Magnetic field in the high pressure region only.

Where a magnetic field is established initially in the high pressure region only, $(H_1 = 0 \quad H_4 \neq 0)$, the energy created by the resulting shock, although supplied in part from the magnetic field, appears entirely in the usual hydrodynamical forms of increased internal heat and translational energy. In this case the magnetic field is entirely behind the contact discontinuity, and the state of the gas behind the shock is related to the state in front through the usual shock conservation laws. For a polytropic gas and a strong shock, these may be written,

$$\frac{u_2}{a_1} = \frac{2}{\gamma_1 + 1} M , \tag{2.1}$$

$$\frac{p_2}{p_1} = \frac{2\gamma_1}{\gamma_1 + 1} M , \tag{2.2}$$

$$\frac{\rho_2}{\rho_1} = \frac{\gamma_1 + 1}{\gamma_1 - 1} , \tag{2.3}$$

where M is the Mach number of the shock.

As for the flow in the absence of a magnetic field, the rarefaction wave is a simple wave having one of the generalized Riemann invariants constant throughout the wave. Thus the velocities u and a at the tail of the rarefaction wave are connected by the relation

$$\frac{u_3}{2} + \frac{a_3}{\gamma_4 - 1} I_n(\alpha_3) = \frac{a_4}{\gamma_4 - 1} I_n(\alpha_4) , \tag{2.4}$$

as when $u = 0$, $a = a_4$. The conditions to be satisfied at the contact discontinuity are

$$u_3 = u_2 , \tag{2.5}$$

$$q_3 = q_2 = p_2 \tag{2.6}$$

As the expansion is isentropic we have

$$p_3 = p_4 \left(a_3/a_4 \right)^{\frac{2\gamma_4}{\gamma_4 - 1}} , \tag{2.7}$$

and thus, using equations (2.7) and (1.8), q reduces to

$$q_3 = p_4 \left(\frac{a_3}{a_4} \right)^{n+2} + \frac{H_4^2}{8\pi} \left(\frac{a_3}{a_4} \right)^{2n} \tag{2.8}$$

Elimination of q_3 and p_2 between (2.2), (2.6) and (2.8) gives

$$\frac{p_4}{p_1} = \frac{2\gamma_1}{\gamma_1+1} M^2\left[\left(\frac{a_3}{a_4}\right)^{n+2} + \lambda_4\left(\frac{a_3}{a_4}\right)^{2n}\right]. \quad (2.9)$$

Using (2.5), u_2 may be eliminated between (2.1) and (2.4) to give

$$M = \left(\frac{\gamma_1+1}{\gamma_4-1}\right)\frac{a_4}{a_1}\left[I_n(\alpha_4) - \frac{a_3}{a_4} I_n(\alpha_3)\right] \quad (2.10)$$

Finally M can be eliminated from equations (2.9) and (2.10) to give an equation for a_3

$$\left[\left(\frac{a_3}{a_4}\right)^{n+2} + \lambda_4\left(\frac{a_3}{a_4}\right)^{2n}\right] =$$

$$\left[\frac{2(\gamma_1-1)\gamma_4}{(\gamma_4-1)}\frac{\rho_1}{\rho_2}\right]\left[I_n(\alpha_4) - \frac{a_3}{a_4} I_n(\alpha_3)\right]^2 \quad (2.11)$$

As we are considering a monatomic gas $\gamma_1 = \gamma_4 = 5/3$ and equation (1.22) may be used for $I_n(\alpha)$, whence equation (2.11) simplifies to the following equation for $z = a_3/a_4$

$$z^3\left(1 + \frac{1}{\lambda_4 z}\right)^{\frac{1}{2}} = A_1 - B_1\left(1 + \frac{6}{5}\lambda_4 z\right)^{3/2}, \quad (2.12)$$

where

$$A_1 = \left(\frac{20}{\lambda_4}\frac{\rho_1}{\rho_4}\right)^{\frac{1}{2}}\left(I_3(\alpha_4) + \frac{5}{9\lambda_4}\right), \quad (2.13)$$

and

$$B_1 = \left(\frac{20}{\lambda_4}\frac{\rho_1}{\rho_4}\right)^{\frac{1}{2}} \frac{5}{9\lambda_4} \quad (2.14)$$

It should be noted that when $\alpha \gg 1$ this theory is considerably simplified as the asymptotic form of the integral $I_n(\alpha)$ may be taken, leading to an explicit formula for M in terms of the initial conditions. In this case equations (2.9) and (2.10) may be written

$$\left(\frac{a_3}{a_4}\right)^n = \frac{4 \gamma_1 p_1 M}{\gamma_4(\gamma_1 - 1) p_4 \alpha_4} , \qquad (2.15)$$

$$\left(\frac{a_3}{a_4}\right)^{\frac{n}{2}} = 1 - \frac{a_1}{(\gamma_1 + 1) a_4 \alpha_4} M . \qquad (2.16)$$

a_3/a_4 may be eliminated between (2.15) and (2.16) and the subsequent quadratic equation solved for M to give

$$M = \left(\frac{2}{\gamma_4}\right)^{\frac{1}{2}} \lambda_4^{\frac{1}{2}} (\gamma_1 + 1) \frac{a_4}{a_1} \left[1 + y - \left\{ (1+y)^2 - 1 \right\}^{\frac{1}{2}} \right] \qquad (2.17)$$

where
$$y = \left[\frac{\gamma_1 (\gamma_1 + 1) p_1}{\gamma_4 \; p_4} \right]^{\frac{1}{2}} \frac{a_4}{a_1} . \qquad (2.18)$$

For equation (2.17) to be valid we must have

$$\left(\frac{a_3}{a_4}\right)^{n-2} \lambda_4 \gg 1 , \qquad (2.19)$$

and
$$\alpha_4 \left(\frac{a_3}{a_4}\right)^{\frac{n}{2}-1} \gg 1 . \qquad (2.20)$$

In the numerical cases which are relevant to T-tube experimental conditions, (2.19) is satisfied fairly well but (2.20) is not so readily satisfied and is a borderline case.

These steady state equations were derived by

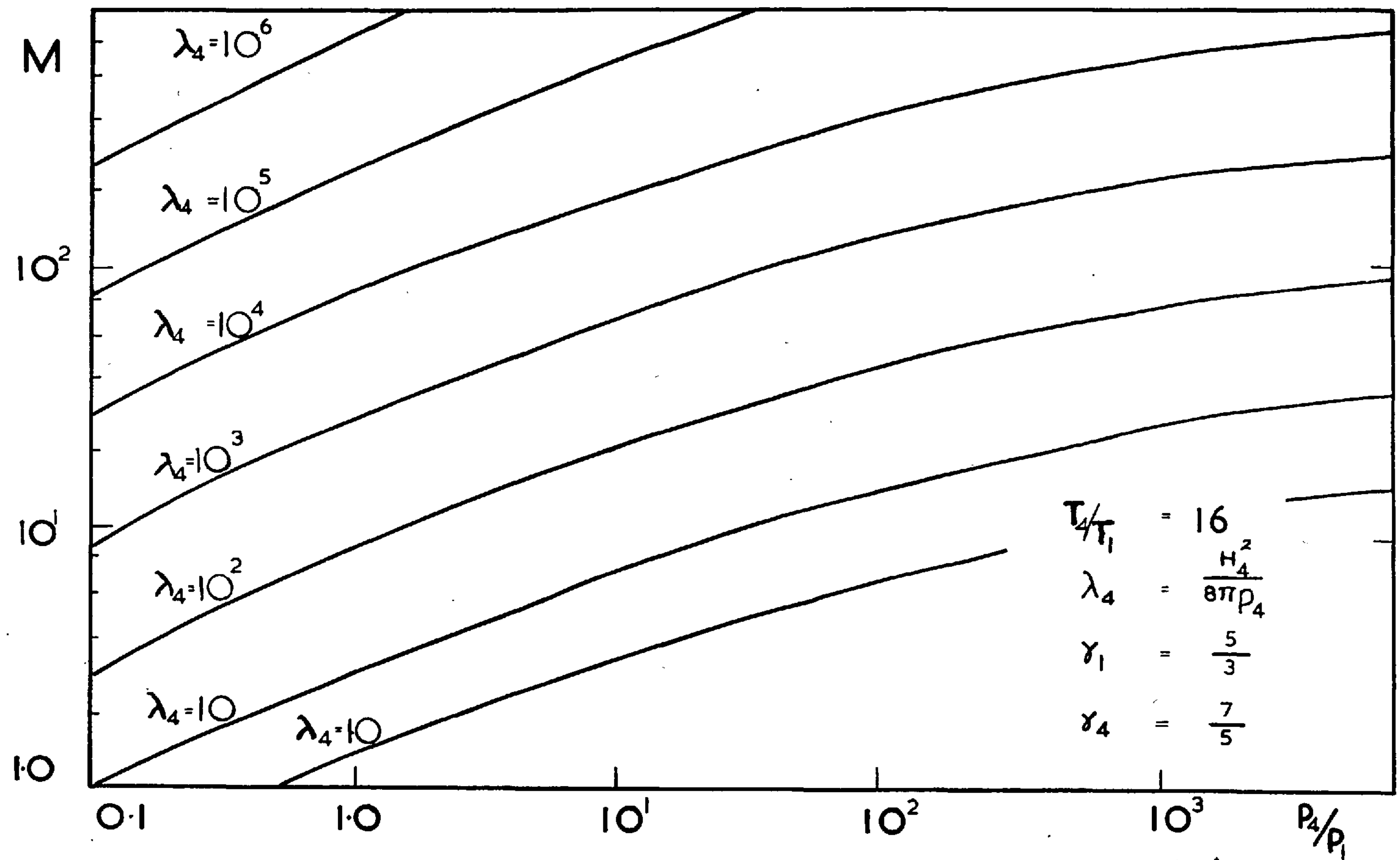

FIG. 2. M AS A FUNCTION OF λ_4 & P_4/P_1

Mitchner in a slightly different form and a graph, similar to the one obtained by him, is shown in figure 2 showing the dependence of the Mach number M on the pressure ratios P_4/P_1 and λ_4. The calculations have been carried out for $\gamma_1 = 5/3$, $\gamma_4 = 7/5$ and $a_4/a_1 = 4$. In ordinary hydrodynamics increasing the ratio P_4/P_1 would increase the speed of the shock, however, in magnetohydrodynamics, where strong magnetic fields are involved, the magnetic pressure provides most of the driving force for the shock, and consequently the driving power is not greatly affected by a change in the ordinary gas pressure. As may be seen from figure 2, increasing p_4, but keeping H_4 and T_4 fixed, actually decreases the speed of the shock. This is because the driving force has remained more or less constant, but the inertia of the gas has been increased.

The general construction of the characteristics is basically the same as for the non-magnetic case, and qualitatively the resulting pattern of characteristics is exactly the same as that shown in figure 1 of chapter III. When there is a magnetic field, however, the definition of ω is slightly different, and the velocity $c = \sqrt{a^2 + b^2}$ replaces the ordinary sound speed a. Referring to this figure we have that, in region O A E, the flow is a simple wave and

$$u + \frac{2a}{\gamma - 1} I_n(\alpha) = 2r = \text{constant throughout } ODE, \tag{2.21}$$

$$u - \frac{2a}{\gamma - 1} I_n(\alpha) = -2s = \text{constant along the } C- \text{ characteristic of slope } (u - c). \tag{2.22}$$

The slope of OA is $-c_4$ and that of OE $(u_3 - c_3)$ where u_3 and c_3 are calculated from the steady state equations. Throughout the region ADE we have the equations

$$u + \frac{2a}{\gamma - 1} I_n(\alpha) = \text{constant along the } C+ \text{ characteristics}, \tag{2.23}$$

$$u - \frac{2a}{\gamma - 1} I_n(\alpha) = \text{constant along the } C- \text{ characteristics}, \tag{2.24}$$

$$\left(\frac{dx}{dt}\right)_{C+} = u + c, \tag{2.25}$$

$$\left(\frac{dx}{dt}\right)_{C-} = u - c. \tag{2.26}$$

These equations, together with the boundary condition $u = 0$ at the wall, as before, serve to determine u, c, $\left(\frac{dx}{dt}\right)_{C+}$ and $\left(\frac{dx}{dt}\right)_{C-}$ at a complete net of points throughout the interaction zone, whence the characteristics may be constructed by the usual finite difference technique.

The reflected rarefaction wave will catch up and interact with the contact discontinuity which is advancing with speed u , as shown in figure 3 of chapter III. This interaction is again similar to the non-magnetic one, except in that the condition to be satisfied along the contact discontinuity is altered. Again, using the notation of this figure, the equations (2.5) and (2.6), which are to be satisfied at the contact discontinuity, become

$$p_4\left[\left(\frac{a(P_L)}{a_4}\right)^{n+2} + \lambda_4\left(\frac{a(P_L)}{a_4}\right)^{2n}\right] = p_2\left(\frac{a(P_R)}{a_2}\right)^{n+2}, \qquad (2.27)$$

and

$$u(P_R) = u(P_L). \qquad (2.28)$$

As the transmitted wave is again simple, we have the relation s = constant throughout this wave, and thus

$$u(B_L) - \frac{2}{\gamma_1 - 1}\, a(P_R) = u(B_R) - \frac{2}{\gamma_1 - 1}\, a(B_R). \qquad (2.29)$$

Equations (2.27) to (2.29) combine to give the boundary condition which must be satisfied along the left hand side of the discontinuity,

$$\frac{p_4}{p_1}\left[\left(\frac{a(P_L)}{a_4}\right)^{n+2} + \lambda_4\left(\frac{a(P_L)}{a_4}\right)^{2n}\right] = \left[\frac{\gamma_1 - 1}{2}\,\frac{u(P_L) - u_2}{a_2} - 1\right]^{n+2} \qquad (2.30)$$

There is no magnetic field to the right of the contact discontinuity and thus the construction of the characteristics in this region will be exactly the same as for the non-magnetic case. The actual position in the x - t plane of the contact discontinuity and the shock front, determined by their velocities, will not, of course, be the same as for a similar case in the absence of a magnetic field.

3. Magnetic field in the high and low pressure region

Where a magnetic field is established initially in both the high and low pressure regions, the state of the gas behind the shock is related to the state in front through the hydromagnetic shock conservation equation, together with equation (2.8) which expresses the fact that H/ρ is a constant across the shock front. For a polytropic gas these equations may be written

$$\rho_2(U - u_2) = \rho_1 U \tag{3.1}$$

$$p_2 + \frac{H_2^2}{8\pi} + \rho_2(U - u_2)^2 = p_1 + \frac{H_1^2}{8\pi} + \rho_1 U^2, \tag{3.2}$$

$$\frac{\gamma}{\gamma-1}\frac{p_2}{\rho_2} + \frac{H_2^2}{4\pi\rho_2} + \frac{1}{2}(U - u_2)^2 = \frac{\gamma}{\gamma-1}\frac{p_1}{\rho_1} + \frac{H_1^2}{4\pi\rho_1} + \frac{1}{2}U^2, \tag{3.3}$$

$$\frac{H_2}{\rho_2} = \frac{H_1}{\rho_1}. \tag{3.4}$$

Since the velocity of a small longitudinal disturbance in front of the shock wave now has the value c, given by equation (2.9), a new Mach number N must be defined, being equal to U/a. Simplification of equations (3.1) to (3.4) yields

$$\lambda_1 = \frac{\left(N - \frac{1}{N} - \frac{\gamma+1}{2}\frac{u_2}{a_1}\right)\left(N - \frac{u_2}{a_1}\right)}{1 - \frac{\gamma_1}{2}\frac{u_2}{a_1}\frac{1}{N}}, \qquad (3.5)$$

and

$$\frac{T_2}{T_1} = (\gamma_1 - 1)\left[\left(\frac{u}{a}\right)^2 \frac{1}{2}\,\frac{\left(1 + \frac{2}{N}\frac{a_1}{u_2}\right)}{\left(1 - \frac{\gamma_1}{2}\frac{u_2}{a_1}\frac{1}{N}\right)} - \left\{\frac{1}{2}\left(\frac{u_2}{a_1}\right)^2 - \frac{1}{\gamma_1 - 1}\right\}\right] \qquad (3.6)$$

For the experimental cases of interest $\frac{1}{N} \ll 1$, $1 \ll T_2/T_1$ and $\left(\frac{a}{u_2}\right)^2 \ll 1$ and thus terms of these orders may be neglected in equations (3.5) and (3.6), which may be rewritten

$$\lambda_1 = \frac{\frac{\gamma_1}{2}\left(N - \frac{\gamma_1+1}{2}\frac{u_2}{a_1}\right)\left(N - \frac{u_2}{a_1}\right)}{1 - \frac{\gamma_1}{2}\frac{u_2}{a_1}\frac{1}{N}}, \qquad (3.7)$$

$$N = \frac{\gamma_1(\gamma_1 - 1)}{4}\left[\frac{2}{\gamma_1 - 1}\frac{u_2}{a_1} + \frac{T_2}{T_1}\left(\frac{u}{a_1}\right)^3\right]. \qquad (3.8)$$

Substituting N from equation (3.8) into equation (3.7) gives

$$\lambda_1 = \frac{\gamma_1}{2}\left(\frac{u_2}{a_1}\right)\left[\frac{2}{\gamma_1 - 1} + \left(\frac{u_2}{a_2}\right)^2\right]\left[\frac{\gamma_1(\gamma_1 - 1)}{4}\left(\frac{u_2}{a_2}\right)^2 - \frac{2-\gamma_1}{2}\right] \times \left[\frac{\gamma_1(\gamma_1 - 1)}{4}\left(\frac{u_2}{a_2}\right)^2 - \frac{1}{2}\right] \qquad (3.9)$$

Equations (2.4) and (2.5) are still valid, even though there is a magnetic field in the low pressure region, and u_3 may be eliminated between these two equations to give

$$u_2 = \frac{2a_4}{\gamma_4 - 1}\left[I_n(\alpha_4) - \frac{a_3}{a_4} I_n(\alpha_3) \right] \tag{3.10}$$

To complete the solution of the steady state equations, without the algebra becoming too complex, it is necessary to take the asymptotic form of $I_n(\alpha)$. On this basis equation (3.10) reduces to

$$u_2 = 2k_4 a_4^{\frac{n}{2}}\left[1 - \left(\frac{a_3}{a_4}\right)^{\frac{n}{2}} \right]. \tag{3.11}$$

The continuity of the total pressure q at the contact discontinuity, represented by equation (2.6) gives, with the aid of (3.8) and (2.8), that

$$p_4\left[\left(\frac{a_3}{a_4}\right)^{n+2} + \lambda_4\left(\frac{a_3}{a_4}\right)^{2n} \right] = p_1\left\{ (1+\lambda_1) + \left(\frac{u_2}{a_1}\right)^2 \frac{\gamma_1^2(\gamma-1)}{4}\left[\frac{2}{\gamma_1 - 1} + \left(\frac{u_2}{a_2}\right)^2\right]\right\}. \tag{3.12}$$

Again $\lambda_1 \gg 1$ and $\lambda_4\left(\frac{a_3}{a_4}\right)^{n-2} \gg 1$ and this equation may be written

$$p_4\lambda_4\left(\frac{a}{a}\right)^{2n} = p_1\left\{ \lambda_1 + \left(\frac{u_2}{a_1}\right)^2 \frac{\gamma_1^2(\gamma_1-1)}{4}\left[\frac{2}{\gamma_1 - 1} + \left(\frac{u_2}{a_2}\right)^2\right]\right\}. \tag{3.13}$$

Setting $\gamma_1 = \gamma_4 = 5/3$, putting $x = \left(u_2/a_2\right)^2$ and eliminating a_3/a_4 from (3.11) and (3.13) gives an equation in x and u_2

$$\left[1 - \frac{u_2}{2 k_4 a_4^{\frac{n}{2}}} \right] = \left[\frac{H_1}{H_4} \right]^{\frac{1}{2}} \left[1 + \left(\frac{u_2}{a_1} \right)^2 \frac{25}{54 \lambda_1} (3 + x) \right]^{\frac{1}{4}} \qquad (3.14)$$

Expressing equation (3.9) in terms of the variables x and u_2 , and putting $\gamma_1 = 5/3$ gives

$$u_2^2 = \frac{18^2 \, 6}{5} \lambda_1^2 a_1^2 \left[\frac{x}{(3 + x)(5x - 3)(5x - 9)} \right] \qquad (3.15)$$

u_2 may be easily eliminated from equations (3.14) and (3.15) to give a single equation for the variable x .

$$A_2 - B_2 \left[\frac{x}{(3 + x)(5x - 9)(5x - 3)} \right]^{\frac{1}{2}} \left[1 + \frac{180 x}{(5x - 3)(5x - 9)} \right]^{\frac{1}{4}}, \qquad (3.16)$$

where $$A_2 = \left[\frac{H_4}{H_1} \right]^{\frac{1}{2}}, \qquad (3.17)$$

and $$B_2 = \left[\frac{H_4}{H_1} \right]^{\frac{1}{2}} \lambda_1^{\frac{1}{2}} \frac{9 \cdot 86 a_1}{k_4 a_4^{\frac{n}{2}}} . \qquad (3.18)$$

The construction of the characteristics is basically the same as before, when there was no magnetic field in the low pressure region, though now the formula $\omega = \frac{2a}{\gamma - 1} I_n(\alpha)$, where $I_n(\alpha) \neq 1$ must be used throughout the flow. From actually solving equation

(3.16) for a few cases it is evident that the shock moves a little faster, the contact discontinuity a little slower and the temperature behind the shock front falls when $\lambda_1 \neq 1$. These results are illustrated in the third and eighth columns of table 1. Behind the shock front we shall have the speed of sound replaced by c_2 where

$$c_2 = (a_2^2 + b_2^2)^{\frac{1}{2}} \tag{3.19}$$

which may be reduced to

$$c_2 = a\left(1 + \lambda_1 \frac{2}{\gamma_1} \frac{\rho_2}{\rho_1} \frac{T_1}{T_2}\right)^{\frac{1}{2}} \tag{3.20}$$

At the contact discontinuity the boundary conditions will be slightly different from the case when $H_1 = 0$. The pressure continuity (2.27) will be replaced by the equation

$$P_4\left[\left(\frac{a(P_R)}{a_4}\right)^{n+2} + \lambda_4\left(\frac{a(P_L)}{a_4}\right)^{2n}\right] = P_2\left[\left(\frac{a(P_R)}{a_2}\right)^{n+2} + \lambda_1\left(\frac{a(P_R)}{a_2}\right)^{2n}\right], \tag{3.21}$$

and the Riemann invariant equation (2.29) by

$$u(P_L) - \frac{2a(P_R)}{\gamma_1 - 1} I_n(\alpha_{P_R}) = u_2 - \frac{2a_2}{\gamma_1 - 1} I_n(\alpha_2) \tag{3.22}$$

Theoretically $a(P_R)$ can be eliminated between equations

(3.21) and (3.22) to give a relation between $u(P_L)$ and $a(P_L)$ along the contact discontinuity, whence the position of the contact discontinuity in the $x - t$ plane can be found in the usual way. However, these equations are rather complicated and unnecessary if we only require the most important feature of this construction, namely the co-ordinates of the point C in the $x - t$ plane, where the rarefaction wave commences to weaken the shock front. The co-ordinates of this point C may be found by a partial construction of the characteristics as shown in figure 3. A case where $\lambda_1 = 0$ and a suitable non-zero λ_1 are shown together for comparison.

4. Discussion of the results

The calculation of the steady state conditions and partial construction of the characteristics has been carried out for several initial conditions, and the results are shown in table 1. All the calculations are for hydrogen at an initial pressure $p = 1.4.10^3$ dynes/cm^2. (or 1 mm. of mercury) and $H = 10^5$ gauss, the latter corresponding to a discharge current of about 10^5 amps/sq.cm. The temperature of the discharge is difficult to estimate, but for purposes of comparison this has been taken as 10^5 °K. This can be shown to be not unreasonable

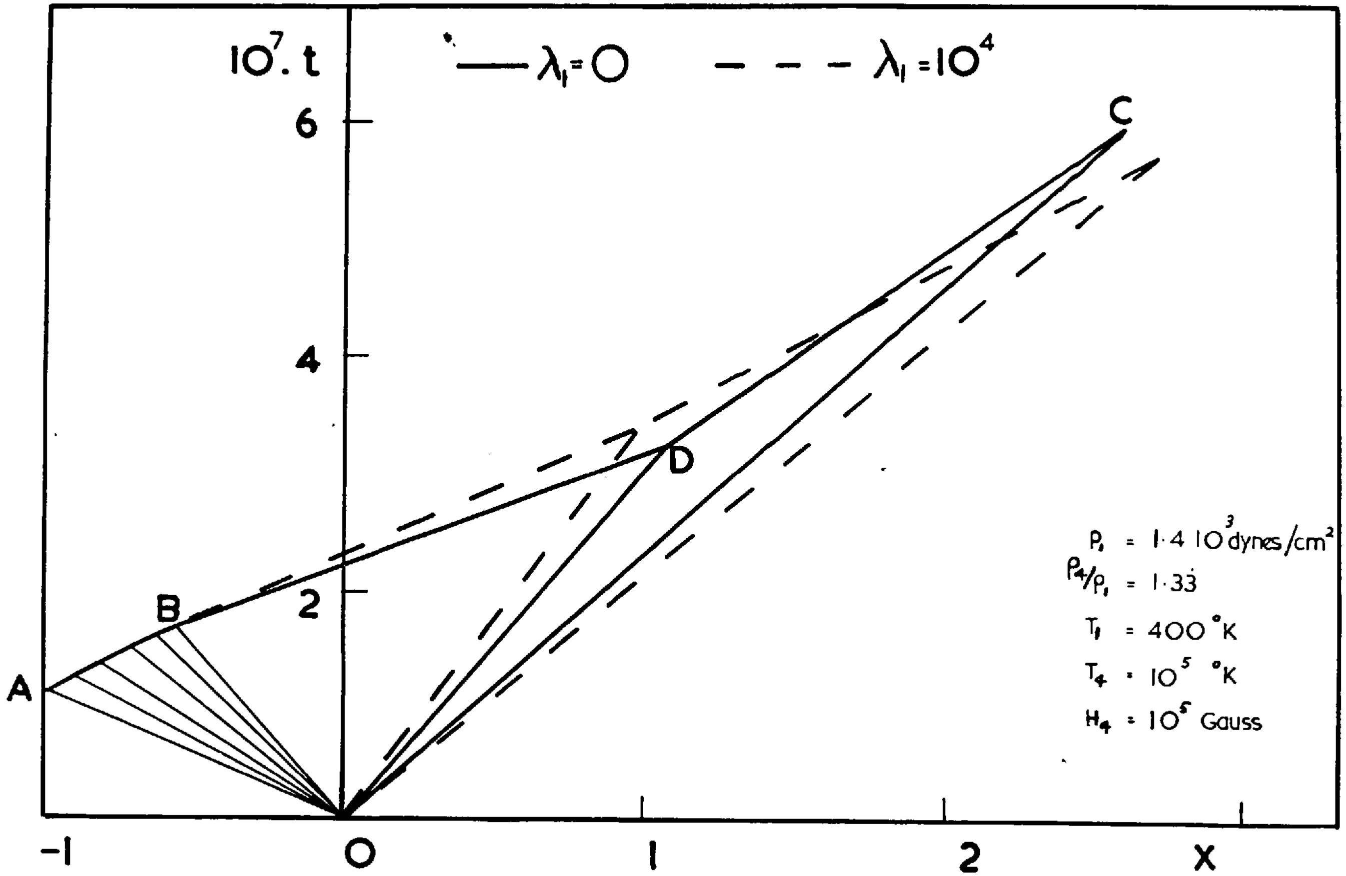

FIG. 3. PARTIAL CONSTRUCTION OF THE CHARACTERISTICS

by the following approximate calculation, which uses for the details of the electrical circuit the kind of values attained by Kolb in his experiments.

We let L = inductance of circuit,

j = current,

C = capacitance of the condenser bank = 0.52 μf.

Q = charge on the condenser,

V = voltage on the condenser = 50 k V,

R = resistance of the gas,

f = frequency of discharge = 700 k.c./sec,

τ = period of the discharge.

The 'rise time' of the current is $\tau/4$ and in this time the amount of energy liberated by the electrical circuit is

$$E_1 = \int_0^{\tau/4} R\, j^2 dt \,, \tag{4.1}$$

where

$$j = \frac{Q}{\sqrt{LC}} \sin\left(\frac{t}{\sqrt{LC}} + \varepsilon \right), \tag{4.2}$$

ε being the phase angle. Assuming that R is independent of time this integrates to

$$E_1 = \frac{1}{8} \frac{RCV^2}{L} \tau \,. \tag{4.3}$$

To evaluate this energy it is necessary to know the resistance R of the gas in the discharge tube, which implies a knowledge of the resistivity η . The electrical conductivity, equal to the reciprocal of the resistivity, is discussed fully in the next chapter. For this calculation we shall take the value of the resistivity of a gas transverse to a strong magnetic field, due to Spitzer,

$$\eta = 1{\cdot}29\,10^{3}\,\frac{\log\Lambda}{T^{3/2}} \quad \text{e.m.u.,} \qquad (4.4)$$

where $\log \Lambda$ is the so-called Coulomb logerithm which, for present purposes, may be assumed to have the value 8. If the discharge tube is taken to be of length ℓ cm. and radium 1 cm. then we conclude that the energy liberated is given by

$$E_1 = \frac{7{\cdot}95.10^{14}\,\ell}{T^{3/2}} \quad \text{ergs.} \qquad (4.5)$$

The heat gained by the gas is given by

$$E_2 = m\,c_v T \quad \text{ergs,} \qquad (4.6)$$

m being the mass of gas in the discharge tube, the initial temperature of the gas having been neglected in comparison with the final temperature. Equating the heat liberated by the electrical circuit to that gained by the gas gives

$$4{\cdot}63\,T\,\ell = \frac{7{\cdot}95\,10^{14}\,\ell}{T^{3/2}} \qquad (4.7)$$

This equation leads to a temperature of the discharge of $T = 8.10^4$ ^oK which is not inconsistent with an assumption of $T = 10^5$ ^oK.

It has been assumed that the distance from the plane of release to the back wall is 1 cm. If this were not so, and the distance was ℓ_1 cm. then both the time taken for the rarefaction wave to reach C, and the distance travelled by the shock in this time would have to be multiplied by ℓ_1 .

Different results can be obtained by cooling the discharge tube and/or heating the side arm, before the discharge is sparked. In table 1 the column T'_4 $^{\circ}K$ gives the initial temperature of the gas in the discharge tube. Cooling the discharge tube increases ρ_4 , and heating the side arm lowers ρ_1 ; thus a density difference is set up which could be considered as replacing the diaphragm in the conventional shock tube. As there is actually no physical boundary to separate the two regions, before the high temperature gas is released there is certain to be some mixing in the vicinity of the plane of release and thus, in this region, we cannot expect the equations to be exact. It is assumed, as indicated by the approximate calculation, that the temperature of the discharge is not affected to any great degree by the initial cooling of the discharge tube.

Cooling the discharge tube prior to the discharge taking place has the effect of increasing the pressure p_4

TABLE 1

Results for the Reflection

of the Rarefaction Wave

T_4^1 °K	T_1 °K	T_2 °K	Time to reach C t in secs.	Distance travelled by shock in time t in cms.	Non-magnetic shock width in cms.	H_1 Gauss	U $cm^2/sec.$
300	300	$8.84.10^6$	$5.85.10^{-8}$	2.59	19.0	0	$4.43.10^7$
300	300	$5.03.10^6$	$5.85.10^{-8}$	2.82		$2.06.10^4$	$4.79.10^7$
30	300	$3.25.10^6$	$2.74.10^{-7}$	7.35	2.6	0	$2.68.10^7$
30	300	$2.08.10^6$	$2.70.10^{-7}$	8.25		$1.32.10^4$	$3.06.10^7$
300	400	$1.07.10^7$	$6.10.10^{-8}$	2.98	28.0	0	$4.87.10^7$
300	400	$6.20.10^6$	$5.85.10^{-8}$	3.09		$1.98.10^4$	$5.30.10^7$
30	400	$3.70.10^6$	$2.89.10^{-7}$	8.26	3.3	0	$2.86.10^7$
30	400	$2.33.10^6$	$2.79.10^{-7}$	9.04		$1.20.10^4$	$3.23.10^7$
40	400	$4.30.10^6$	$2.47.10^{-7}$	7.62	4.6	0	$3.09.10^7$
40	400	$2.30.10^6$	$2.44.10^{-7}$	8.48		$1.29.10^4$	$3.47.10^7$

of the gas which drives the shock. In the absence of a magnetic field this would have the effect of increasing the speed of the shock, but for a magnetically driven shock this does not always follow. For magnetic fields of the order 10^5 gauss the magnetic pressure is much greater than the ordinary gas pressure and, for the numerical cases shown in table 1, it can be seen that the shock velocity actually decreases when the gas pressure p_4 is increased due to the increased inertia.

Increasing ρ_4 puts more thermal energy into the system but this goes towards raising the mass of gas heated in the shock wave rather than raising its temperature. This, however, is quite a good feature because the relative amount of heat lost by radiation will be less if more of the gas is heated.

The increase in the distance travelled by the shock before the rarefaction wave reaches it is due to a decrease in the speed of the rarefaction wave. The head of the latter travels with speed c_4 back into the high pressure region. That c_4 is reduced can easily be seen by noting that increasing ρ_4 decreases the Alfvén speed $b_4 = \left(\frac{H_4^2}{4\pi\rho_4}\right)^{\frac{1}{2}}$ which in turn decreases $c_4 = (a_4^2 + b_4^2)^{\frac{1}{2}}$. Both c_3 and c_2, the later speeds of the rarefaction wave are also reduced by increasing ρ_4, but this cannot be seen without actually solving the equations. Comparing the results of the first two cases given in table 1, where the pressure p_4 is greater by a factor 10 in the second case, shows that c_4 is decreased by a factor of approximately $\sqrt{10}$. This is because the Alfvén speed dominates the ordinary sound speed; c_3 and c_2 are decreased by factors 4.0 and 1.6 respectively.

From the figures shown in table 1 it can be seen that the temperature of the plasma behind the shock front is higher if the discharge tube is not cooled. On the other hand, without cooling, the rarefaction wave returns to the shock front before the steady state conditions have been established.

CHAPTER V

The Transport Coefficients

1. Viscosity

The viscosity of a gas is essentially a measure of the rate of transfer of momentum. For unit velocity gradient, the coefficient of viscosity μ is defined to be exactly equal to the rate of transfer of momentum across unit area. This rate of transfer of momentum may be calculated by using a simple kinetic theory.

We suppose that the velocity is in the y direction and that there is a positive velocity gradient $\frac{d v_0}{d x}$, v_0 being the mass velocity, as shown in figure 1. The momentum carried by the molecules across a

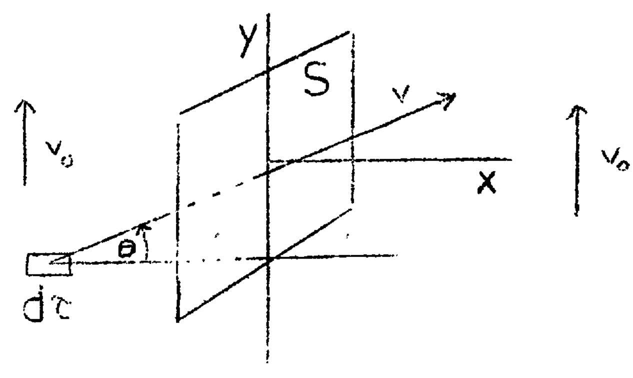

Figure 1

small plane, S, perpendicular to the x axis has to be considered. As $\frac{d v_0}{d x}$ is assumed to be positive, molecules crossing S from left to right come from regions where the mass velocity v_0 is less than it is in the region into which they go, and so tend to arrive in their new positions with less than the average amount of y momentum. Similarly, those crossing to the left carry out an excessive share of such momentum. In this way the gas lying to the right of S tends to suffer a loss of y momentum, and this is equivalent to the action of a force directed towards $-y$, while the gas on the left tends similarly to gain momentum and so experiences a force towards $+y$.

Now the velocity of a molecule is determined as a result of its last collision, and we must, therefore, consider the distribution of velocities among those molecules which collide in a given element of volume $d\tau$. It is assumed that the average velocity of the molecules after their collision in $d\tau$ is equal to the mass velocity of the gas at that point. If x denotes the distance of $d\tau$ from S, and v_{os} the value of the mass velocity at S, its value at $d\tau$ may be written $v_{os} + x \dfrac{dv_{os}}{dx}$.
Thus the average momentum carried away by the molecules that collide in $d\tau$ is given by $m\left(v + \bar{x}\dfrac{dv_{os}}{dx}\right)$ where m is the mass of a molecule and $\bar{x}$ denotes the mean value of x. The total momentum carried towards +x across unit area per second is given by the product of this expression and the number of molecules crossing dS; the resulting expression for the momentum is, therefore

$$\frac{1}{4} n\bar{v}m\left(v + \bar{x}\frac{dv_o}{dx}\right) \qquad (1.1)$$

where n is the number of molecules in a unit volume, and $\overline{V}$ is the mean molecular speed.

The average value of x for molecules with a Maxwellian velocity distribution is given by

$$\overline{x} = -\frac{2}{3}\ell \;, \tag{1.2}$$

where ℓ is the mean free path. Equation (1.1), therefore, gives the rate of transfer of y momentum crossing from left to right, M_+ as

$$M_+ = \frac{1}{4} n m v \left(v_{os} - \frac{2}{3}\ell \frac{d v_o}{d x} \right). \tag{1.3}$$

In the same way we find that molecules crossing towards the left carry y momentum out of the region lying on the right of S, at the rate, M_- , where

$$M_- = \frac{1}{4} n m v \left(v_{os} + \frac{2}{3}\ell \frac{d v_o}{d x} \right). \tag{1.4}$$

Subtracting this expression from the previous one we have, finally, that the net rate of transfer of y momentum across towards +x per unit second is

$$M_+ - M_- = -\frac{1}{3} n m v \ell \frac{d v_o}{d x} \;. \tag{1.5}$$

Thus

$$\mu = \frac{1}{3} \rho \overline{v} \ell \;, \tag{1.6}$$

for a gas of density ρ .

This formula was obtained by Maxwell in 1860 and is now only of historical interest. It has several errors, for example the mean free path is not strictly independent of speed as has been assumed, which, although they do not affect the form of the result, will affect the numerical factor involved. Corrections for these errors can be made, however, though they are rather tedious and a superior method is now used to derive the coefficient of viscosity and the other transport coefficients which was derived by Chapman and Enskog in 1915. This method starts with the Boltzman equation

$$\frac{\partial f}{\partial t} + \sum_i \frac{\partial f}{\partial x_i} v_i + \sum_i \frac{F_i}{m} \frac{\partial f}{\partial v_i} = \left(\frac{\partial f}{\partial t}\right)_{collisions}, \quad (1.7)$$

where i takes the values 1, 2, 3, x_1, x_2, x_3 represent the cartesian axes; v_1, v_2, v_3 are the three components of the velocity $\underline{v}$; F_i is the i^{th} component of the external force and $f = f(\underline{v})$ is the velocity distribution function; $\left(\frac{\partial f}{\partial t}\right)$ collisions represent the change in $\frac{\partial f}{\partial t}$ due to collisions. Approximations to the transport coefficients are generated through a series expansion of the distribution function, together with solutions to the subsequent linear integral equations.

Chapman's final formula for μ is

$$\mu = 0.491(1+\varepsilon)\rho \bar{v} l_{vc}, \quad (1.8)$$

where $$l_{vc} = \frac{1}{\sqrt{2}\, n\, S_{vc}}, \quad (1.9)$$

and S_{vc} is defined as the mean equivalent cross-section for molecular collisions, and is given by quite a complicated integral. ε is a very small number whose maximum value is 0.016, its value for the model of a gas composed of molecules which are assumed to be hard elastic spheres. For such a model $S_{vc} = \pi\sigma^2$ where σ is the ordinary collision diameter and $\bar{v} = 2\left(\frac{2kT}{\pi m}\right)^{\frac{1}{2}}$, where k is the Boltzman constant, and in this case equation (1.8) reduces to

$$\mu = \frac{0.998(mkT)^{\frac{1}{2}}}{\pi^{3/2}\sigma^2} \quad \text{dyne sec/cm}^2 \qquad (1.10)$$

The value of μ for hydrogen may be found by inserting the appropriate numerical constants into equation (1.10) to give

$$\mu = 5.15.10^{-6}\, T^{\frac{1}{2}} \text{ dyne sec/cm}^2 \qquad (1.11)$$

In an ionized gas electrostatic forces play a dominant role in molecular encounters and the formula for the viscosity will consequently be modified. The viscosity of such a gas is mainly due to encounters between the ions and has been found very accurately by Chapman. For present purposes, however, we need only consider his first approximation which gives

$$\mu = \frac{5}{16 A_2(2)}\left(\frac{mkT}{\pi}\right)^{\frac{1}{2}}\left(\frac{2kT}{e^2}\right)^2, \qquad (1.12)$$

where $$A_2(2) = 2\left[\log(1+\Lambda^2) - \frac{\Lambda^2}{1+\Lambda^2}\right], \quad (1.13)$$

and $$\Lambda = \overline{(h/p_0)} \quad . \quad (1.14)$$

The bar in (1.14) denotes a mean, h is the Debye shielding length and p_0 is the value of the impact parameter (the distance of closest approach of two colliding particles) such that the deflection in the orbital plane is $\pi/2$. Substituting the accepted values for h and p_0 into Λ, and taking mean values gives

$$\Lambda = \left[\frac{3}{2Z^2e^2}\left(\frac{k^3T^3}{\pi n}\right)^{\frac{1}{2}}\right], \quad (1.15)$$

where Z is the ionic charge, e the charge on an electron and n_e the electron number density. Λ is usually large and thus $A_2(2)$ may be written

$$A_2(2) = 4\log\Lambda - 2, \quad (1.16)$$

where $\log\Lambda$ is the so-called Coulomb logarithm. Spitzer gives a table of $\log\Lambda$ as a function of T and n_e, but for present purposes it may be taken as constant having the value 10, that is assuming that the gas has an ionic charge Z = 1. For ionized hydrogen equation (1.12) gives the following numerical value for μ.

$$\mu = 1.54.10^{-16} \text{ dyne sec/cm.}^2 \quad (1.17)$$

Electron encounters have been neglected in this formula for μ . Taking these into account by using Chapman's more accurate formula would reduce μ by a factor 1.042. This is a negligible effect for the purposes of this work, and is less than the error introduced by taking $A_2(2)$ as a constant. A magnetic field will not have any appreciable effect on the viscosity, as the viscosity is due principally to the ion encounters and not the electron encounters.

A graph of log μ as a function of log T, for hydrogen, is shown in figure 2, using the values for μ given in equations (1.11) and (1.17). It can be seen that the transition from the ordinary gas to the ionized gas occurs at about $T = 2.10^5$ ^oK. There will not, of course, be a sudden transition from one formula to the other, as shown in this figure, but a gradual transition over quite a range of T, corresponding to a partially ionized gas.

2. Thermal conductivity

The thermal conductivity λ of a gas is a measure of the rate of transfer of energy within a gas by the molecules. By substituting the average heat energy of a molecule in place of the y momentum, the simple calculation to find the viscosity may be used to give a value for λ . This theory yields that

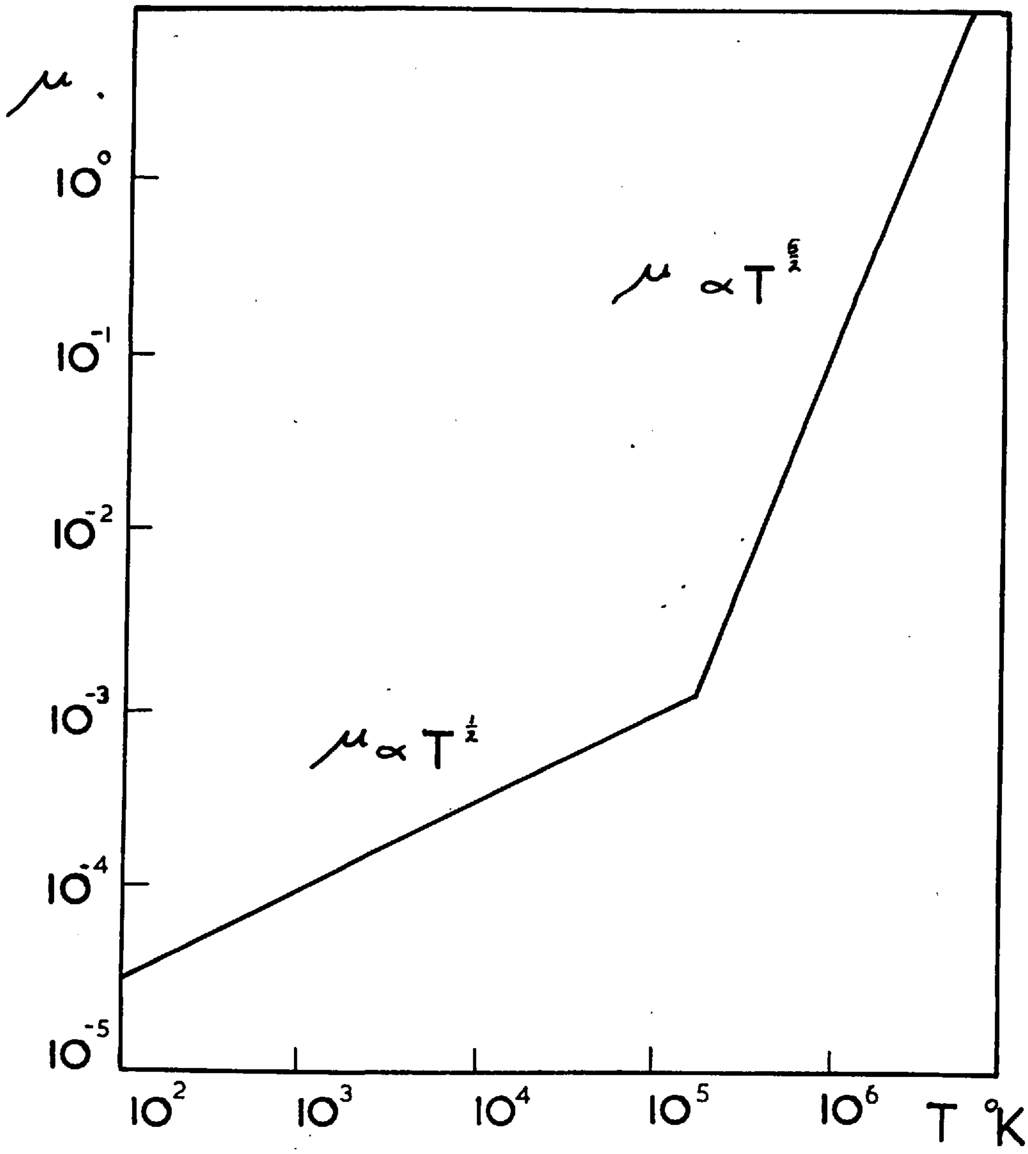

FIG. 2. VISCOSITY OF HYDROGEN

$$\lambda = \frac{1}{3} \rho \bar{v} \ell c_v , \qquad (2.1)$$

i.e. $$\lambda = \mu c_v , \qquad (2.2)$$

where C_v is the specific heat at constant volume. Using the more sophisticated theory of Chapman gives

$$\lambda = (1 + \delta) \frac{5}{2} \mu C_v , \qquad (2.3)$$

where μ is defined by equation (1.8) and δ is a very small number having the value 0.01 for the hard elastic sphere model.

For the thermal conductivity of an ionized gas the electron encounters are more important than ion encounters. Chapman has given a theory for the thermal conductivity of an ionized gas and his final result is

$$\lambda = 0{\cdot}342 \lambda_e , \qquad (2.4)$$

where λ_e is the value of λ for a gas in which the ions are neglected and is given by

$$\lambda_e = \frac{15 k \quad 5}{4 m_e A_2(2)} \left(\frac{kT}{\pi}\right) \left(\frac{2kT}{e^2}\right)^2 \qquad (2.5)$$

m_e being the mass of an electron and $A_2(2)$ is again given by equation (1.10)

3. Electrical conductivity

The electrical conductivity σ is usually defined as the ratio of the electrical current density $\underline{j}$

to the electric field $\underline{E}$. However, in the presence of a magnetic field the usual definition is rather unsuitable, as the relationship between $\underline{j}$ and $\underline{E}$ is quite complicated. A better way of defining σ is as the ratio of j to P_{ei} ; P_{ei} being the rate at which the electrons in a unit volume gain momentum by impact with positive ions, i.e.

$$\sigma = \frac{e\, n_e}{c} \frac{j}{P_{ei}} \tag{3.1}$$

The power dissipated into heat per unit volume equals the force on the electrons, resulting from ion impact, times the mean drift velocity of the electrons relative to the ions. The first of these two quantities is simply P_{ei} , while the latter is $c\, j / n_e e$. Using the definition of σ given in equation (3.1) yields directly that the Joule heating is $\frac{1}{\sigma} j^2$, which is analagous to the ordinary definition of σ .

To compute σ , in order of magnitude, we may use the most elementary form of kinetic theory in which each collision is assumed to produce a large deflection. The momentum gained by an electron in each collision is $m_e(v_i - v_e)$, on the average, where v_e and v_i are the macroscopic velocities of electrons and positive ions. The number of such collisions per cubic centimetre may be set equal to $\nu\, n_e$, where ν is the collision frequency for each electron. The current density is $n_e e(v_i - v_e)/c$. Combining these quantities into equations (3.1) we obtain

$$\sigma = \frac{n_e e^2}{m_e c^2 \nu} \qquad (3.2)$$

This is the familiar equation for σ though it is only approximate. In a fully ionized gas there is some uncertainty as to the appropriate value of ν to use in equation (3.2). To compute σ with any accuracy it is necessary to consider the manner in which the contributions to j and P_{ei} vary with the velocity of the electrons. To investigate this the same method as before is used. A velocity distribution function for the electrons of the following form, as suggested by Chapman and Cowling is introduced

$$f_e(w) = f_e^{(o)}\{1 + D(\ell_e w)\}\cos\theta, \qquad (3.3)$$

where w is the electron velocity, θ is the polar angle in velocity space, the polar axis being in the direction of the current and $f_e^{(o)}(w)$ is the Maxwellian distribution function for the electron velocities. $D(\ell_e w)$, where $\ell_e = \frac{m_e}{2kT}$ is, in general, a complicated function chosen in such a way that $f_e(w)$ satisfies the Boltzman equation.

With this definition of $f_e(w)$

$$j_e = -\frac{e}{c}\int f_e(w)\, w\cos\theta\, d^3\underline{w}, \qquad (3.4)$$

the integral being over all velocity space. It may be evaluated to give

$$j_e = -\frac{4 e n_e}{3\sqrt{\pi}\,\ell_e c} I_3'(\infty), \quad (3.5)$$

where, in general

$$I_n'(\infty) = \int_0^\infty x^n D(x) e^{-x^2} dx \quad (3.6)$$

P_{ei} may be written

$$P_{ei} = m_e \int f_e(w) \langle \Delta \xi \rangle d^3\underline{w} \quad (3.7)$$

where $\langle \Delta \xi \rangle$ is the average rate of change of the electron velocity measured in a direction along which the electron is moving and the integral is again overall velocity space. Taking the formula for $\langle \Delta \xi \rangle$ given by Cohen, Spitzer and Routley,[14] P_{ei} may be evaluated to give

$$P_{ei} = \frac{e^4 n_e^2 Z \sqrt{6}\, \pi^{\frac{1}{2}} \log \Lambda\, I_0'(\infty)}{m_e \ell_e (\overline{v^2})^{3/2}} \quad (3.8)$$

$\overline{v^2}$ is the mean square electron velocity and $\log \Lambda$ is the same Coulomb logarithm as defined in equation (1.15). Substituting (3.5) and (3.8) into equation (3.1) yields

$$\sigma = \frac{2(2kT)^{3/2}}{Z \pi^{3/2} m_e e^2 c^2 \log \Lambda} \frac{\sqrt{\pi}}{8} \frac{I_3'(\infty)}{I_0'(\infty)}, \quad (3.9)$$

as $m_e \overline{v^2} = 3kT$ this equation may be written

$$\sigma = \sigma_L \alpha \quad (3.10)$$

where

$$\alpha = \frac{\sqrt{\pi}\, I_3(\infty)}{8\, I_0(\infty)}, \quad (3.11)$$

and σ_L is the conductivity of a so-called Lorentz gas, a hypothetically fully ionized gas in which the electrons do not interact with each other and the positive ions are at rest, i.e. for a Lorentz gas

$$\frac{I_0'(\infty)}{I_3'(\infty)} = \frac{\sqrt{\pi}}{8} \quad . \tag{3.12}$$

When electron-electron encounters are taken into account the form of $D(\ell_e w)$, which was proportional to $(\ell_e w)^4$ for a Lorentz gas, is altered leading to a value of α differing from unity. This new value of α has been calculated by Chapman and Cowling, and for a gas with an ionic charge $Z = 1$, they give

$$\alpha = 0.582 \quad . \tag{3.13}$$

In the presence of a magnetic field, transverse to an electric field, these values of α are no longer valid, since the distribution of current over electrons of different velocities is altered. As the conductivity is defined in terms of energy dissipation it is evident that this quantity depends on microscopic collisions and is not directly dependent on $\underline{H}$ provided a microscopic analysis is valid. This is so provided that the mean free path between collisions is very much greater than the radius of gyration of the particles, i.e. provided that the particles are spiralling freely. The condition for this may be written

$$\left[\frac{(3kT)^2}{\pi n_e e^4}\right]\frac{1}{Z_i^4} \gg \frac{m_e v c}{Z_i e H} \qquad (3.14)$$

which is satisfied under many astrophysical and laboratory conditions.

The exact manner in which the magnetic field affects the distribution function $f_e(\mathbf{w})$ has been investigated by Spitzer. 17 His final value for α is

$$\alpha = 0.296 \qquad (3.15)$$

By comparing equations (3.15) and (3.13) we can see that the transverse conductivity is 0.518 times the normal conductivity for currents parallel to a magnetic field.

CHAPTER VI

The Structure of the Shock Front

1. Previous work

Magnetohydrodynamic shock waves have been considered in the preceding chapters utilizing the shock conservation equations. These equations give the relationship between the values of the velocity, temperature, density and magnetic field for the states of uniform flow on either side of the shock front. Here in this chapter, the nature of the flow inside the transition region connecting these two uniform states is considered, particular attention being paid to the width of this transition region.

J. M. Burgers[18] investigated the structure of the shock front but his work neglected the viscosity, except in so far as it was needed, in certain cases, to lead to a final discontinuity which was required to establish the steady state conditions in the complete shock wave. In this chapter his theory is discussed and given a more detailed treatment.

W. Marshall[22] has considered the problem of the structure of the shock front of a wave advancing into a preionized gas. This is discussed briefly here but for experiments such as Kolb's, the gas ahead of the shock is not in this state, being at room temperature. The structure of the front of a shock wave advancing into a cold gas is considered in some detail and the results are compared with those of Marshall. The consequence of assuming that the gas is initially at room temperature is that the shock front is much sharper in the initial stages, where the compression is due solely to viscous and heat conduction effects. Two natural units of length occur, as in Marshall's work, namely for the range of dissipation of Joule heat and one determining the range of the viscous forces. These are not of the same order of magnitude, and the interplay between the two is examined.

2. Basic equations

The case of an infinite plane shock moving with velocity v_1 into an undisturbed gas at room temperature in which there is a transverse magnetic field is examined. A co-ordinate system moving with the shock is chosen and thus we see a gas streaming into the shock with velocity v_1. If the line of flow is chosen parallel to the x axis, and the magnetic field parallel to the z axis, then the electromagnetic equations become

$$j = \frac{dH}{dx} , \tag{2.1}$$

$$\frac{dE}{dx} = 0 , \tag{2.2}$$

$$j = \sigma(E - vH) . \qquad (2.3)$$

Equations (2.1) to (2.3) may be combined to give

$$E = vH - \frac{1}{4\pi\sigma}\frac{dH}{dx} ,$$
$$= \text{constant} = E_1 ,$$

i.e. $$\frac{1}{4\pi\sigma}\frac{dH}{dx} = vH - E_1 . \qquad (2.4)$$

The conservation of mass, momentum and energy, equations (1.6) to (1.8) of chapter II, including dissipative effects may be written

$$\frac{d}{dx}(\rho v) = 0 , \qquad (2.5)$$

$$\rho\frac{dv}{dx} = -\frac{dp}{dx} + \frac{d}{dx}\left(\frac{4}{3}\mu\frac{dv}{dx}\right) + \frac{H}{4\pi}\frac{dH}{dx} , \qquad (2.6)$$

$$\frac{d}{dx}\left[\rho v\left(\tfrac{1}{2}v^2 + \varepsilon + p/\rho\right) - \tfrac{4}{3}\mu v\frac{dv}{dx} - \lambda\frac{dT}{dx} + \frac{E_1 H}{4\pi}\right] = 0 , \qquad (2.7)$$

where $4/3\,\mu\,\dfrac{dv}{dx}$ represents the viscous forces. These equations may be expressed in a slightly different form as

$$\rho v = \text{constant} = m , \qquad (2.8)$$

$$p + \rho v^2 - \tfrac{4}{3}\mu\frac{dv}{dx} + \frac{H^2}{8\pi} = \text{constant} , \qquad (2.9)$$

$$m\left(\tfrac{1}{2}v^2 + \varepsilon + p/\rho\right) - \tfrac{4}{3}\mu v\frac{dv}{dx} - \lambda\frac{dT}{dx} + \frac{E_1 H}{4\pi} = \text{constant}. \qquad (2.10)$$

The constants in equations (2.9) and (2.1) are determined by the conditions in the initial and final steady states when $\frac{dv}{dx}$ and $\frac{dT}{dx}$ are zero. We assume that we are again dealing with a polytropic gas, whence we have the additional equations

$$\frac{p}{\rho} = RT \quad , \tag{2.11}$$

$$\varepsilon = \frac{1}{\gamma - 1}\,\frac{p}{\rho} \quad . \tag{2.12}$$

From equations (2.8) to (2.10), by neglecting viscous and magnetic effects, we can see that the width of the shock front is of the order λ'/mR. Again, by neglecting heat conduction and magnetic effects, we conclude that the width of the shock is of the order μ/m. Using the numerical values which have been given in chapter V for the transport coefficients, it can be seen that $\frac{\lambda}{mR} \Big/ \frac{\mu}{m}$ is always much less than one. Thus heat conduction will have a far smaller effect on the width of the shock than viscous forces and, for this reason, in the remainder of the chapter, heat conduction will be neglected. A paper by D. Gilbarg[19] on ordinary hydrodynamic shocks, discusses the existence and uniqueness of shock transitions in some detail. He also gives a more mathematically rigid proof than given above that heat conduction may be neglected. Equation (2.10) may now be written

$$m\left(\tfrac{1}{2}v^2 + \varepsilon + p/\rho\right) - \tfrac{4}{3}\mu v\frac{dv}{dx} + \frac{E_1 H}{4\pi} = \text{constant} \quad . \tag{2.13}$$

To simplify the equations, it is convenient to put $\theta_1 = \frac{1}{\gamma M^2}$ and to introduce non-dimensional variables h, z and τ according to the scheme

$$\left.\begin{aligned} v &= v_1 z \,, \qquad \text{i.e.} \quad \rho = \rho_1/z \,, \\ H &= (8\pi\rho_1 v_1^2)^{\frac{1}{2}} h \,, \\ T &= T_1 \tau \,. \end{aligned}\right\} \qquad (2.14)$$

With the appropriate elimination and substitution of the new variables, equations (2.4), (2.8), (2.9) and (2.13) become

$$\frac{dh}{dx} = 4\pi\sigma v_1 (zh - c) \,, \qquad (2.15)$$

$$\frac{4}{3}\frac{\mu}{m} z \frac{dz}{dx} = \frac{1}{2}(\gamma+1)z^2 - \gamma(1 + \theta_1 + (h_1^2 - h^2))z$$
$$\frac{1}{2}(\gamma - 1) + \gamma\theta_1 - 2(\gamma - 1)c(h - h_1) \,, \qquad (2.16)$$

$$\tau = \frac{1}{2}\frac{(\gamma-1)}{\theta_1}\{(1 - z)^2 - 2(\theta_1 + h_1^2 - h^2)z$$
$$- 4c(h - h_1) + 1 \,. \qquad (2.17)$$

In these equations c is an unknown constant equal to $E_1/v_1^2\sqrt{8\pi\rho_1}$ and μ and σ depend on τ as described in chapter V. Note that for fairly strong shocks $\theta_1 = \frac{1}{\gamma M^2}$ may be neglected. The boundary conditions which determine the physically admissible solutions are $\frac{dh}{dx} = 0$ and $\frac{dz}{dx} = 0$ at $x = \pm\infty$.

For the analysis in later sections it is convenient to introduce into equations (2.15) and (2.16) two functions f(h, z, c) and g(h, z, c) defined as follows

$$f(h, z, c) \equiv z\,h - c, \qquad (2.18)$$

$$g(h, z, c) \equiv \tfrac{1}{2}(\gamma+1)z^2 - \gamma(1+\theta_1+h_1^2-h^2)z + \tfrac{1}{2}(\gamma-1)\gamma\theta_1 + 2(\gamma-1)c(h-h_1). \qquad (2.19)$$

Equations (2.15) and (2.16) will now read

$$\frac{dh}{dx} = 4\pi\sigma v_1 f(h,z,c), \qquad (2.20)$$

and

$$\frac{dz}{dx} = \frac{3}{4}\frac{m}{\mu z} g(h,z,c), \qquad (2.21)$$

3. The non-magnetic case

In the case of strong shocks the temperature behind the shock front will be very high, and consequently the width of the shock, which was shown to be of the order μ/m, may be of the same order of magnitude as the experimental apparatus being used to produce the shock. The actual shock profile may be found by integrating equation (2.21): neglecting magnetic effects, the relevant equations are

$$\frac{dz}{dx} = \frac{3}{4}\frac{m}{\mu z}\left[\frac{\gamma+1}{2}z^2 - \gamma z - \frac{\gamma-1}{2} + \gamma\theta_1(1-z)\right] \qquad (3.1)$$

$$\tau = \frac{1}{2}\frac{(\gamma-1)}{\theta_1}\left[(1-z)^2 - 2\theta_1 z\right] + \gamma \qquad (3.2)$$

Equation (3.1) was first obtained by Lord Rayleigh[23] in 1910 and was integrated exactly by him, on the assumption that μ was constant. Writing equation (3.1) in the form

$$\frac{3}{4}\,\frac{m}{\mu}\int dx = \int \frac{z\,dz}{\left[\frac{\gamma+1}{2}z - \left(\frac{\gamma-1}{2} - \gamma\theta_1\right)\right]\left[z-1\right]} \quad (3.3)$$

it may be integrated to give

$$x = \frac{4}{3}\,\frac{\mu}{m(1+\gamma\theta_1)}\left[\left(\frac{\gamma-1}{\gamma+1} - \frac{2\gamma\theta_1}{\gamma+1}\right)\log\left(\frac{\gamma+1}{2}z - \frac{\gamma-1}{2} + \gamma\theta_1\right) - \log(1-z)\right]. \quad (3.4)$$

This solution, however, does neglect the vital variation of viscosity with temperature. For a monatomic gas $\gamma = 5/3$ and, for fairly strong shocks, equations (3.1) and (3.2) reduce to

$$\frac{dz}{dx} = \frac{3m}{4\mu z}(4z-1)(z-1) \quad , \quad (3.5)$$

where $\mu = \mu(\tau)$ and

$$\tau = \frac{5}{9}M^2(1-z)^2 \quad (3.6)$$

These equations have been integrated numerically using the values of μ shown in figure 2 of chapter V, and a typical result is shown in figure 1. The shock is moving from the right to the left in this figure and both non dimensional density and temperature profiles are shown. For both the density and temperature the same feature of a rapid change in the initial stages followed by a wide region in which z and τ change slowly can be seen.

Rayleigh's formula (3.4) may be used to show the

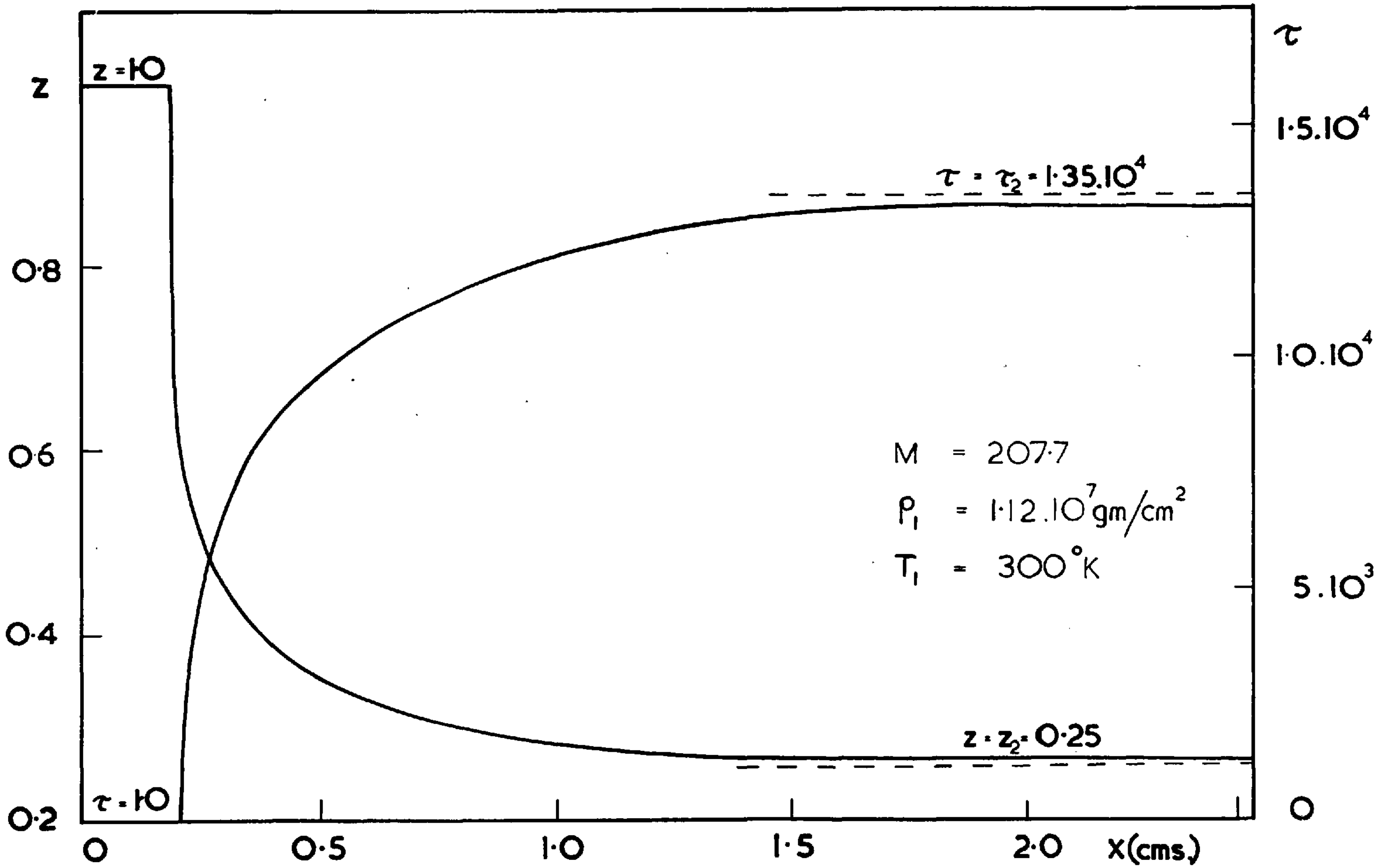

FIG. 1. SHOCK PROFILE FOR A STRONG HYDRODYNAMIC SHOCK

manner in which the wave profile tends to $x = \pm\infty$, because near these limits we can take μ to be constant. As $z \rightarrow z_2$ we have

$$x = + \frac{4}{3}\frac{\mu}{m}\frac{1}{1+\gamma\theta_1}\left[\left(\frac{\gamma-1}{\gamma+1} - \frac{2\gamma\theta_1}{\gamma+1}\right)\log\left(\frac{\gamma+1}{2}z_2 - \frac{\gamma-1}{2} + \gamma\theta_1\right)\right] + A_1, \quad (3.7)$$

and as $z \rightarrow z_1 = 1$

$$x = - \frac{4}{3}\frac{\mu}{m}\frac{1}{1+\gamma\theta_1}\log(1-z) + A_2, \quad (3.8)$$

where A_1 and A_2 are the arbitrary constants, which depend on the choice of origin.

If an initial temperature of 300°K, a pressure of about 10^3 dynes/cm.^{2} and a Mach number of 250 are taken, then the total width of the shock is about 10 cm. Hence, for shocks of this kind, the width of the front is of the same order of magnitude as the dimensions of the experimental apparatus which is being used to produce them. It is unlikely, in such cases, that the steady state, and thus the final high temperature will ever be reached. There is, however, the possibility that the introduction of a transverse magnetic field may reduce the width of the shock.

4. Shock wave advancing into a medium with finite conductivity

Burgers theory of a shock wave in a conducting medium considers the basic equations, which were set out in section 2, in the $h - z$ plane on the assumption that the viscosity is small enough to be neglected. A more thorough mathematical analysis than that attempted by Burgers is given here on the basis of the same approximation. Being able to neglect the viscosity implies that we are dealing with fairly weak shocks, when the temperatures involved are not very great.

As the wave is considered to be advancing into a medium of finite conductivity σ is never zero and thus the steady state conditions far ahead and far behind the shock wave (equations (2.20) and (2.21)) give that

$$f(h, z, c) = z\,h - c = 0 \qquad (4.1)$$

and

$$g(h, z, c) = 0 \qquad (4.2)$$

From the state far ahead of the shock wave, equation (4.1) gives that

$$c = h_1 \qquad (4.3)$$

Thus the definitions of $f(h, z, c)$ and $g(h, z, c)$ given in equations (2.18) and (2.19) become

$$f(h, z) = z\,h - c \qquad (4.4)$$

and

$$g(h,z) = \tfrac{1}{2}(\gamma+1)z^2 - \gamma\left(1 + \theta_1 + h_1^2 - h^2\right)z + \tfrac{1}{2}(\gamma - 1) + \gamma\theta_1 - 2(\gamma - 1)\,h_1(h - h_1) \qquad (4.5)$$

Assuming that the viscosity is zero $g(h, z) = 0$ throughout the flow, and the basic equations may be written

$$\frac{dh}{dx} = 4\pi\sigma v_1 f(h, z), \qquad (4.6)$$

$$g(h, z) = 0 \qquad (4.7)$$

Consider these equations in the $h - z$ plane. There are two cases as shown in figures 2(a) and 2(b), the final conditions in both cases being given by the intersection of $g(h, z) = 0$ with the hyperbola $z h = h_1$. With a strong initial magnetic field we can follow $g(h, z) = 0$ until it reaches the hyperbola for a second time (figure 2(a)), the point of intersection determining z_2 and h_2. For the case of a weak initial magnetic field (figure 2(b)), however, the part of the curve along which $\frac{dh}{dz}$ is positive cannot be used. This can be seen by showing that the slope of $g(h, z) = 0$ at (h_2, z_2) cannot be positive.

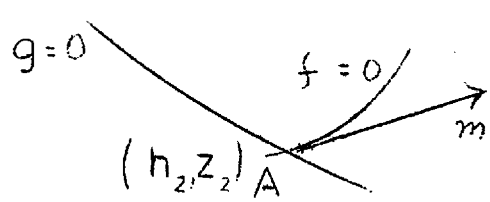

Figure 2(d)

Taking equation (4.6) and integrating it over the whole range gives

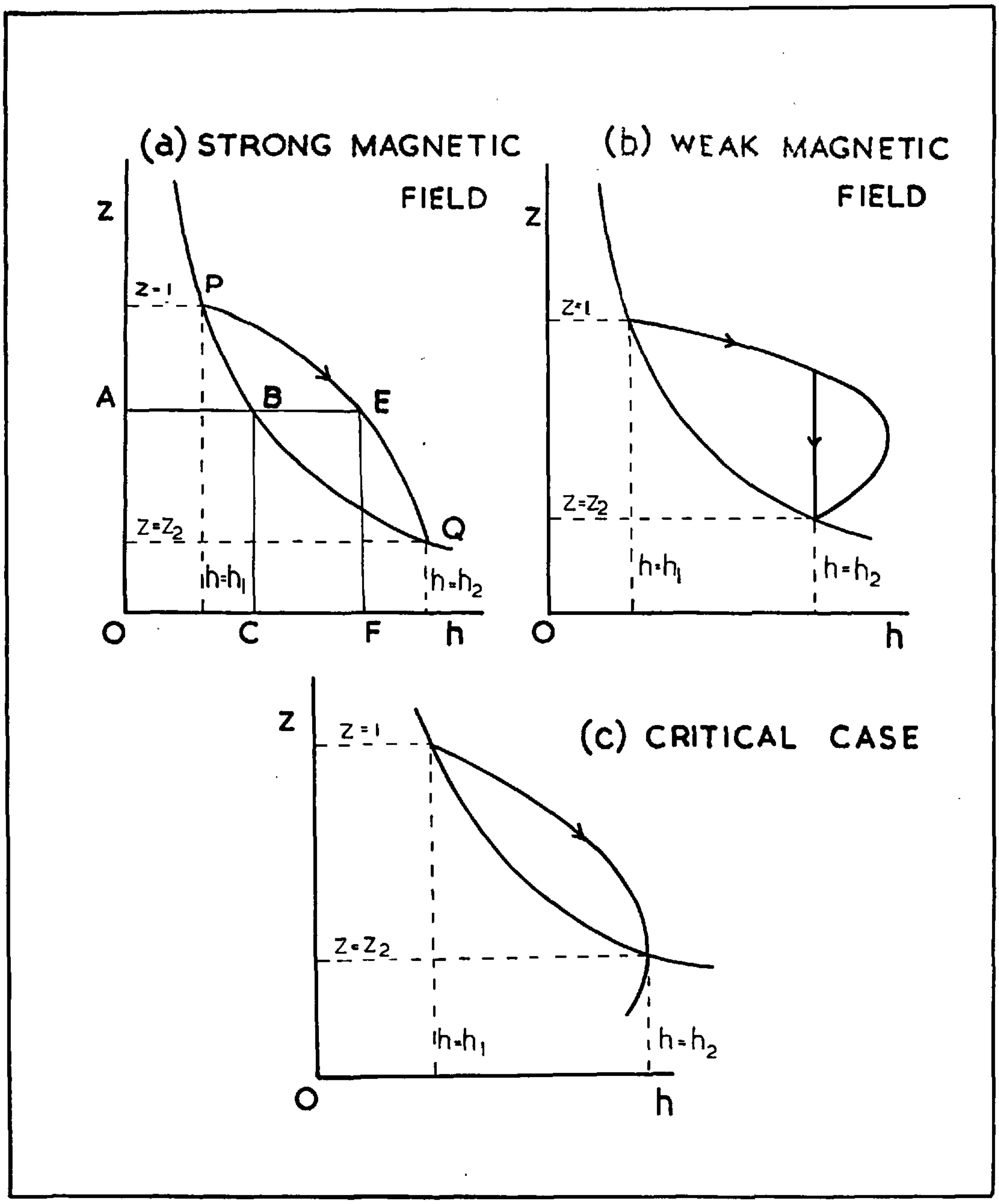

FIG. 2. h-z CURVES (FOR A WAVE ADVANCING INTO A PRE-IONIZED GAS)

$$[x]_1^2 = \frac{1}{4\pi\sigma v_1}\int_{h_1}^{h_2}\frac{dh}{zh - h_1} \quad (4.8)$$

We are at present only interested in the behaviour of the integral near $h = h_2$, and in this neighbourhood we may put

$$z = z_2 + m(h - h_2) \quad (4.9)$$

Defining I to be the integral from $h_2 + \mathcal{E}$ to h, where $\mathcal{E}$ is small, and by substituting z from equation (4.8) into the integral we therefore have that

$$I = \frac{1}{m}\int_{h_2+\varepsilon}^{h_2}\frac{dh}{h^2+2Bh+A}, \quad (4.10)$$

where
$$A = -\frac{h_1}{m}, \quad (4.11)$$

and
$$B = \frac{1}{2}\left[\left(\frac{h_1}{h_2}\right)\frac{1}{m} - h_2\right]. \quad (4.12)$$

Equation (4.10) can be written

$$I = \frac{1}{m}\int_{h_2+\varepsilon}^{h_2}\frac{dh}{(h+B)^2 + A - B^2}. \quad (4.13)$$

Now
$$A - B^2 = -\frac{1}{2}\left[\left(\frac{h_1}{h_2}\right)\frac{1}{m} + h_2\right]^2, \quad (4.14)$$

thus $(A - B^2)$ is always negative and, therefore

$$I = -\frac{1}{m}\frac{1}{\sqrt{B^2-A}}\left[\coth^{-1}\frac{h+B}{\sqrt{B^2-A}}\right]_{h_2+\varepsilon}^{h_2} \quad (4.15)$$

Now initially at $z = 1$, $h = h_1$, x starts from $x = -\infty$ and if we now consider what happens at the upper limit we see that, if m is positive, the final value of x is $-\infty$

Thus if $\left(\frac{dh}{dz}\right)_{h=h_2}$ is positive the solution does not represent an infinite wave.

The conclusion is, therefore, that in the case of a weak initial magnetic field there is first a change from $z = 1$, $h = h_1$ to $z = z'$, $h = h_2$, given by the point on $g(h, z) = 0$ situated vertically above the second point of intersection of $g(h, z) = 0$ with the hyperbola. At this stage the magnetic field has reached its final value but the velocity has not. Thus an ordinary shock is needed with a constant value of the magnetic field to bring the velocity down to its final value as represented by z . The former case is called a pure magnetic shock because it will take place entirely in a width of the order $\frac{1}{4\pi\sigma v_1}$, whereas the shock in the latter case could not be completed without some consideration of the viscosity.

There will be a critical value of h_1 such that the shock will just be purely magnetic. This critical case is shown in figure 2(c) and is determined ~~mathematically~~ by the condition that

$$\left(\frac{d\,h}{d\,z}\right)_{h=h_2} = 0 \tag{4.16}$$

Mathematically the final conditions (h_2, z_2) are given by the equations

$$z_2 h_2 = h_1 \quad , \tag{4.17}$$

$$\tfrac{1}{2}(\gamma+1)z_2 - \gamma(1+\theta_1+h_1^2-h_2^2)z + \gamma\theta_1 - 2(\gamma-1)h_1(h_2-h_1)$$
$$\tfrac{1}{2}(\gamma-1) = 0 \qquad (4.18)$$

Eliminating h_2 gives

$$h_1^2 = \frac{(\gamma-1)z_2^2 - (2\gamma\theta_1+\gamma-1)z_2}{2\gamma z_2 - 2(\gamma-2)}, \qquad (4.19)$$

Thus, for a given Mach number, this equation implies that there is a whole range of values of h_1 and z_2 which will satisfy the equations. However, the addition of equation (4.16) will determine the critical value of h_1 denoted by h_1^*, and a unique z_2. Condition (4.16), together with equation (4.17), may be written

$$h_1^2 = \frac{z_2^2\gamma(1+\theta_1) - (\gamma+1)z_2^3}{(1-z^2)\gamma} \qquad (4.20)$$

Equations (4.19) and (4.20) may be considered as giving h_1^* as a function of θ_1, or h_1^* as a function of the Mach number M; the latter is shown in figure 3. From this figure we see that h_1^* rises rapidly to a maximum and then tends to a limit. The value of this limit can be found theoretically from equation (4.19) and (4.20) by putting $\theta_1 = 0$, i.e. $M = \infty$. Corresponding to this h_1^* is a certain value of z_2, the equation for which is

$$\gamma(\gamma+1)z^3 - (3\gamma-4)(\gamma+1)z^2 + 3\gamma(\gamma-1)z - \gamma(\gamma-1) = 0$$
$$(4.21)$$

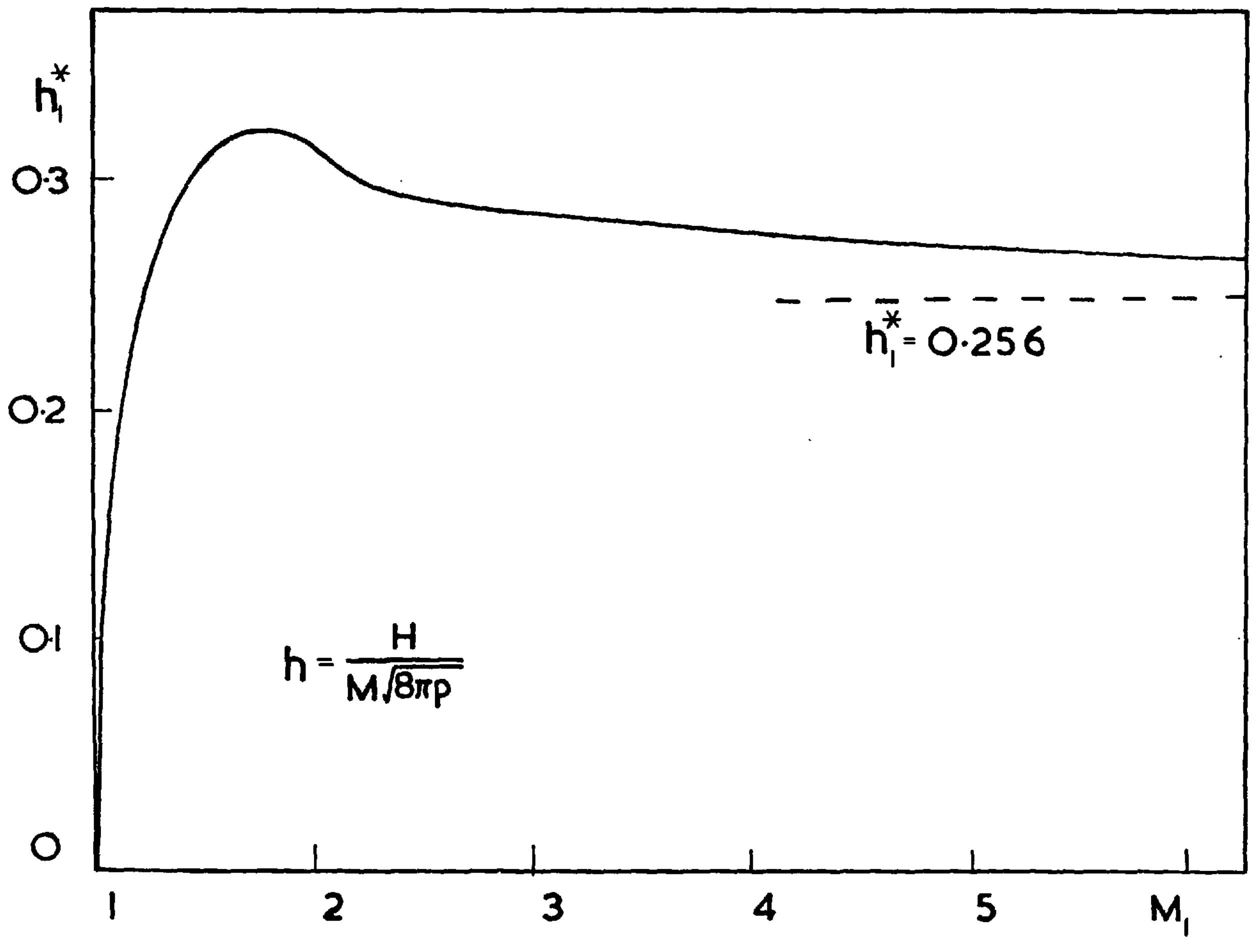

FIG. 3. MINIMUM MAGNETIC FIELD FOR A PURE MAGNETIC SHOCK

For $\gamma = 5/3$ this reduces to

$$20z_{2}^{3} - 12z_{2}^{2} + 15z_{2} - 5 = 0 . \qquad (4.22)$$

the solution of which is

$$z_{2} = 0.375 ,$$

and the corresponding h_1 is

$$h_1^{*} = 0.256 .$$

In terms of the ordinary variables H and M, figure 3 shows that for low Mach numbers, when there is a sharp rise, H is proportional to M^2 but that for larger Mach numbers, when the curve has flattened out to its asymptotic value, H is directly proportional to M.

Equation (4.6) may be given an interpretation in the h - z plane. In figure 2(a) $\frac{1}{4\pi\sigma v_1}\frac{dh}{dx}$ is equal to the area of rectangle OAEF minus the area of rectangle OABC, i.e. it equals the rectangle CBEF. Thus we can see how the quantity $\frac{1}{4\pi\sigma v_1}\frac{dh}{dx}$ varies through the shock by following the rectangle CBEF as E goes from P to Q.

For strong shocks, however, the viscosity cannot be neglected and the equations must be considered in their more general form

$$\frac{dh}{dx} = 4\pi\sigma v_1 f(h, z) , \qquad (4.23)$$

$$\frac{dz}{dx} = \frac{3m}{4\mu z} g(h, z) . \qquad (4.24)$$

where μ and σ are funcrions of τ . These two equations may be combined to give one equation

$$\frac{dh}{dz} = \frac{16\pi\sigma\mu}{3\rho_1} \frac{z f(h,z)}{g(h,z)}, \qquad (4.25)$$

which is more suitable for a discussion in the $h - z$ plane. As we are still assuming that σ is never zero in the steady states (1) and (2) we have

$$f(h, z) = 0 , \qquad (4.26)$$

and

$$g(h, z) = 0 \qquad (4.27)$$

Thus (h_1 , z_1) and (h_2 , z_2) are singular points in the $h - z$ plane and, by linearizing the equations in the neighbourhood of these two points, it will be possible to decide whether they are nodes or saddle points.

We have

$$\frac{\partial f}{\partial h} = z , \qquad \frac{\partial f}{\partial z} = h , \qquad (4.28)$$

$$\frac{\partial}{\partial z}\left(g/z\right) = \tfrac{1}{2}(\gamma+1) - \frac{1}{z^2}\left[\tfrac{1}{2}(\gamma-1) + \gamma\Theta_1 - 2(\gamma-1)h_1(h-h_1)\right] = \ell , \qquad (4.29)$$

$$\frac{\partial}{\partial h}\left(g/z\right) = 2\gamma h - \frac{2}{z}(\gamma-1)h_1 = m , \qquad (4.30)$$

and thus, if we let Δh and Δz be small variations in h and z near to either of the two singular points, equations (4.25) may be written

$$\frac{d(\Delta h)}{d(\Delta z)} = \frac{a\Delta z + b\Delta h}{\ell\Delta z + m\Delta z} , \qquad (4.31)$$

where $$a = \frac{16\pi\sigma\mu}{3\rho_1} h \quad , \tag{4.32}$$

$$b = \frac{16\pi\sigma\mu}{3\rho_1} z \quad , \tag{4.33}$$

and a , b , ℓ and m are evaluated at the singular point. Moving the origin to the singular point, we can write h and z for Δh and Δz respectively, whence equation (4.31) becomes

$$\frac{dh}{dz} = \frac{az + bh}{\ell z + mh} \tag{4.34}$$

This is a well known equation whose solution, found by writing $h/z = v$, is

$$(h - \alpha z)^{\mu}(h - \beta z)^{\nu} = k_1 , \tag{4.35}$$

where k_1 is a constant of integration, and α and β are roots of the equation

$$m v^2 - (b - \ell)v - a = 0 , \tag{4.36}$$

$$\mu = \frac{\ell + m\alpha}{m(\alpha - \beta)} \quad \text{and} \quad \nu = \frac{\ell + m\beta}{m(\alpha - \beta)} . \tag{4.37}$$

When μ and ν are both positive equation (4.35) represents a family of curves having asymptotes $h = \alpha z$ and $h = \beta z$ in common. The asymptotes themselves are integral curves, but apart from them, no integral curves pass through the origin, which is called a saddle point. When μ and ν are of opposite signs, the equation of the integral curves may be written

$$h - \alpha z = k_2 (h - \beta z)^{\rho'} \qquad (4.38)$$

where $k_2 = (1/k_1)^{\frac{1}{\mu}}$ and $\rho' = -\mu/\nu$. Since ρ' is positive, every integral curve passes through the origin which is called a node.

To determine whether the singular points are nodes or saddle points it is thus necessary to consider the sign of $\mu\nu$ at the singularities. It may be shown that $\mu\nu$ has the same sign as the determinant

$$D = \begin{vmatrix} \ell & m \\ a & b \end{vmatrix} , \qquad (4.39)$$

which in our case may be written

$$D = \frac{16\pi\mu\sigma}{3\rho_1}\left\{\frac{1}{2}(\gamma+1)z - \frac{1}{z}\left[\frac{1}{2}(\gamma-1) + \gamma\theta_1 - 2(\gamma-1)h_1 \times (zh - h_1) - 2\gamma h^2\right\}\right. . \qquad (4.40)$$

At the singular points we have the equations (4.26) and (4.27) and thus this relation may be written

$$D = \frac{16\pi\mu\sigma}{3\rho_1}\left\{(\gamma+1)z - \gamma(1+\theta_1) - \left[(2-\gamma)h^2 + \gamma h_1^2\right]\right\} \qquad (4.41)$$

We, therefore, see that at (h_1, z_1) D is > 0 , provided $h_1^2 < \frac{1}{2}$ and that at (h_2, z_2) D is < 0 . An example where $h_1^2 > \frac{1}{2}$ corresponds to $\left(\frac{v_1}{b_1}\right)^2 < 1$ where b is the Alfvén velocity. Such an example would not really represent a shock wave and is, therefore, not relevant for this discussion. Thus (h_1, z_1) is a saddle point and (h_2, z_2) a node, and as a consequence there will be only one integral curve of equation (4.25) which will connect the points (1) and (2). In other words the shock transition is unique.

A paper by G. S. S. Ludford[21] considers the existence of shock transitions for an oblique shock. Whereas for a plane shock there is always a unique transition from the one steady state to the other, for an oblique shock this is not always true and there may be many, or even no solutions joining two steady states which are solutions of the shock conservation equations.

Throughout the wave h must increase and, therefore,

$$f(h, z) > 0 \tag{4.42}$$

Similarly, through the wave z must decrease and thus

$$g(h, z) < 0 \tag{4.43}$$

As a consequence of (4.42) and (4.43) the integral curves representing a shock transition must lie within the region enclosed by the two curves $f(h, z) = 0$ and $g(h, z) = 0$. It is interesting to note that, provided we are dealing with strong enough shocks for θ_1 to be neglected, the final state (h_2, z_2) and the position of the curves $f(h, z) = 0$ and $g(h, z) = 0$ in the $h - z$ plane depend only on the value of h_1.

Marshall has constructed the shock profiles for shock waves, in which viscosity is not neglected, for various limit cases. He assumes that the shock wave is advancing into an ionized gas, and has, therefore, taken

$$\frac{\mu}{\mu_1} = \tau^{\frac{5}{2}} \quad \text{and} \quad \frac{\sigma}{\sigma_1} = \tau^{3/2} \quad . \qquad (4.44)$$

In figure 4 profiles similar to those obtained by Marshall, for a large initial electrical conductivity σ_1, are shown for comparison with those obtained later. The shock is moving to the left and it can be seen that there is a sharp shock preceded by a wide region in which all the variables change slowly.

5. Shock wave advanging into a cold gas

When there is a cold gas ahead of the shock front the basic differential equations must be considered in the form

$$\frac{dh}{dx} = 4\pi\sigma v_1 f(h, z, c) \quad , \qquad (5.1)$$

$$\frac{dz}{dx} = \frac{3m}{4\mu z} g(h, z, c) \quad . \qquad (5.2)$$

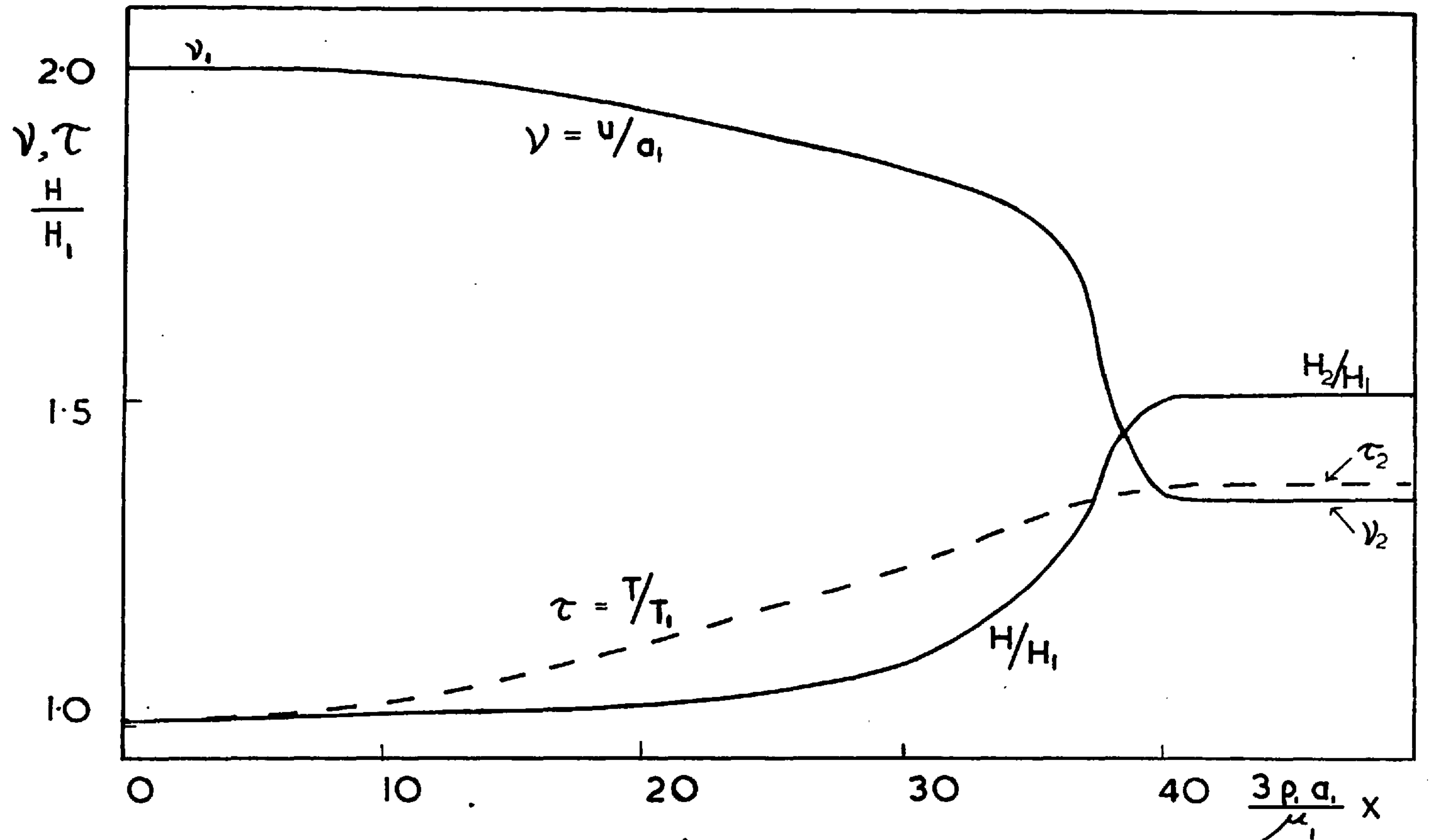

FIG. 4. SHOCK PROFILES (FOR A WAVE ADVANCING INTO A GAS WITH FINITE CONDUCTIVITY)

In the initial stages of the shock front the electrical conductivity will be zero, as the gas will not yet be ionized, but as ionization occurs the conductivity will rise, though its magnitude will not be very great until quite a high degree of ionization has been attained. At this stage there will be a sharp rise in the conductivity and when the gas is fully ionized σ will be proportional to $T^{3/2}$ as described in chapter V. For the work in this section, however, we shall assume that below a certain temperature T' the conductivity is zero, and above this temperature it has the value attributed to a fully ionized gas, transverse to a strong magnetic field. We shall take $\mu \propto T^{\frac{1}{2}}$ for $T < T_0$ and $\mu \propto T^{\frac{5}{2}}$ for $T > T_0$, T_0 being the temperature at which the two curves cross.

In addition to the changes in viscosity there will be corresponding changes in the adiabatic exponent γ and in the equation of state due to ionization. These effects, although important for the detailed structure of the shock front, have been neglected in the interests of simplicity. It is assumed that γ takes the value 5/3, its value for a monatomic gas, throughout the whole shock wave. In fact, before ionization sets in its value will be closer to 7/5, if the shock wave is propagating into hydrogen. This approximation only affects that part of the shock front where the field and the density are changing rapidly, and the effect of such an approximation would be too small to alter the final results as shown in the curves of figures 8, 9 and 10.

The constant C in equations (5.1) and (5.2) is determined by the boundary conditions which are: $h = h_1$ and $z = 1$ at $x = -\infty$ and (ii) that at $x = +\infty$ both h and z converge to a finite limit. Once C is determined the final state (h_2, z_2) can be found, and is given by the intersection in the $h - z$ plane of $g(h, z, c) = 0$ and the hyperbola $z h = c$. Analytically the final state is given by $h_2 = C/z_2$, where z_2 is the real root of the cubic

$$\frac{\gamma - 1}{2} z^3 - \gamma(1 + \theta_1 + h_1^2) z^2 + \left(\gamma\theta_1 + \frac{\gamma - 1}{2} + 2(\gamma - 1)C h_1\right) z$$
$$(2 - \gamma) C^2 = 0 \qquad (5.3)$$

Before carrying out a detailed analysis of the equations it is interesting to consider the integral curves qualitatively in the $h - z$ plane again. In the initial stages of the wave h will be constant and the solution will follow the line $h = h_1$ to a point B in figure 6 where $\tau = \tau'$. For the solution to represent an infinite wave it is necessary for h to increase and z to decrease monatomically, and thus we must have $f(h, z, c) > 0$ and $g(h, z, c) < 0$ throughout the wave. In other words the solution must lie in the region enclosed by the two curves $f(h, z, c) = 0$, $g(h, z, c) = 0$ and the straight line OA, $h = h_1$.

Although the solution must lie inside the enclosed region it must not extend to the right of CD for, as before, it is not possible for $\frac{dh}{dz}$ to be positive at any stage, if the solution is to represent an infinite wave. This region will not exist at all if the initial magnetic field h_1 is less than a certain value. However, this critical value is not found as easily as when the conductivity was everywhere non zero. From the condition that $\left(\frac{dh}{dz}\right)_2 = 0$ and $zh = C$ we have that

$$(\gamma - 1) = \gamma(1 + \theta_1 + h_1^{*2}) - C^2/z^2 \qquad (5.4)$$

Theoretically this equation could be combined with equation (5.3) to give h_1^* as a function of C and the Mach number M $\left(\theta_1 = \frac{1}{\gamma M^2}\right)$. For a given h_1, there is a unique value of C which must be chosen in such a way that there is a solution to the equation (5.1) and (5.2) which satisfies all the boundary conditions. This, as will be seen in the next section, is quite a complicated matter and thus the determination of h_1^*, as a function of M would involve a lengthy interative procedure.

Near the final state, for strong shocks, we have σ large and thus from equation (5.1) $f(h, z, c) \simeq 0$, i.e. the solution will approach (h_2, z_2) very close to the hyperbola $zh = C$. Thus a solution which wanted to cross CD does not seem likely to represent a physical case and would occur only for very weak shocks.

6. Procedure for the numerical integration

The two non-linear simultaneous differential equations have been integrated numerically by a step-by-step procedure using London University's Ferranti Mercury computer. This integration, however, is not straightforward because of the rapid changes in the order of magnitude of the coefficients of $f(h, z, c)$ and $g(h, z, c)$ in equations (5.1) and (5.2), and because the partial derivatives of $4\pi\sigma v_1\, f(h, z, c)$ and $\frac{3m}{4\mu z}\, g(h, z, c)$ with respect to h and z are very large. As a result a very small step length must be taken for the integration.

The method used for the numerical integration is the Runge Kutta method. Consider the differential equations

$$\frac{dy_1}{dx} = f_1(x, y_1, y_2), \qquad (6.1)$$

$$\frac{dy_2}{dx} = f_2(x, y_1, y_2). \qquad (6.2)$$

Assuming that the conditions at $x = x_0$ are known, i.e.

$$\left.\begin{array}{l} y_1 = y_{10} \\ y_2 = y_{20} \end{array}\right\} \text{at } x = x_0, \qquad (6.3)$$

then the increments Δy_1 and Δy_2 for advancing the dependent variables are given by

$$\Delta y_1 = \frac{1}{6}\delta(k_1 + 2k_2 + 2k_3 + k_4), \qquad (6.4)$$

$$\Delta y_2 = \frac{1}{6}\delta(\ell_1 + 2\ell_2 + 2\ell_3 + \ell_4), \qquad (6.5)$$

where

$$\begin{aligned} k_1 &= f_1(x_0\; y_{10}\; y_{20}), \\ \ell_1 &= f_2(x_0\; y_{10}\; y_{20}), \end{aligned} \qquad (6.6)$$

$$\begin{aligned} k_2 &= f_1(x_0 + \tfrac{1}{2}\delta,\; y_{10} + \tfrac{1}{2}k_1,\; y_{20} + \tfrac{1}{2}\ell_1), \\ \ell_2 &= f_2(x_0 + \tfrac{1}{2}\delta,\; y_{10} + \tfrac{1}{2}k_1,\; y_{20} + \tfrac{1}{2}\ell_1), \end{aligned} \qquad (6.7)$$

$$\begin{aligned} k_3 &= f_1(x_0 + \tfrac{1}{2}\delta,\; y_{10} + \tfrac{1}{2}k_2,\; y_{20} + \tfrac{1}{2}\ell_2), \\ \ell_3 &= f_2(x_0 + \tfrac{1}{2}\delta,\; y_{10} + \tfrac{1}{2}k_2,\; y_{20} + \tfrac{1}{2}\ell_2), \end{aligned} \qquad (6.8)$$

$$\begin{aligned} k_4 &= f_1(x_0 + \delta,\; y_{10} + k_3,\; y_{20} + \ell_3), \\ \ell_4 &= f_2(x_0 + \delta,\; y_{10} + k_3,\; y_{20} + \ell_3) \end{aligned} \qquad (6.9)$$

δ being the increment in the independent variable x. This integrating procedure has an accuracy of the order δ^5.

Advantages of the method are that no special techniques are required to start the solution and that the step length δ may be altered at any stage in the integration. A disadvantage of the Runge Kutta method is that there is no check on the accuracy of the solution obtained. However, the repetitive nature of the method makes it very amenable for use with a digital computer, and this disadvantage may be overcome in the following way. After integrating over a step length δ the integration may be repeated by integrating twice, over the same total change δ in the independent variable but with a step length $\delta/2$. If the two values at the end of the step length δ differ by more than a predetermined accurary then the step length may again be halved, and this process repeated until the required accuracy has been obtained.

This checking system, although giving an accurate solution, will naturally increase the amount of computation to be done. It is clearly more efficient, with respect to computer time, to subdivide the interval δ only once or twice to obtain the required degree of accuracy. Thus the initial interval must be chosen with some care. The correct interval δ to use for the integration is

$$\delta = \frac{\Delta}{\mathrm{Max}\left(\frac{\partial f_1}{\partial y_1}, \frac{\partial f_1}{\partial y_2}, \frac{\partial f_2}{\partial y_1}, \frac{\partial f_2}{\partial y_2}\right)}, \qquad (6.10)$$

where Δ depends on the accuracy required and may be taken as 0.1 for an accuracy of about 10^{-5} and Max $\left(\frac{\partial f_1}{\partial y_1}, \frac{\partial f_1}{\partial y_2}\right.$

$\left.\frac{\partial f_1}{\partial y_2}, \frac{\partial f_2}{\partial y_2}\right)$ denotes the maximum of the partial derivatives $\frac{\partial f_1}{\partial y_1}, \frac{\partial f_2}{\partial y_2}, \frac{\partial f_1}{\partial y_1}, \frac{\partial f_2}{\partial y_1}$. For the equations in which we are interested estimates of these derivatives may be made and an approximate value of δ chosen.

If the step length is not chosen to be of the correct order of magnitude then another difficulty may arise. It may happen that, because of a bad choice of step length, such large errors appear in the evaluation of k_2, k_3, k_4, ℓ_2, ℓ_3 and ℓ_4 that numbers larger than the computer can handle arise. Should this happen, then the computer would stop calculating and the stage of halving the interval would never be reached.

7. Numerical integration of the equations.

In the initial stages of the wave h will remain constant until the temperature reaches τ', when the electrical conductivity becomes finite. The value of z at this stage is easily found from the formula

$$\tau' = \frac{\gamma(\gamma-1)}{2} M^2 (1 - z')^2 \qquad (7.1)$$

i.e.

$$z' = 1 - \frac{1}{M}\sqrt{\frac{2\tau'}{\gamma(\gamma-1)}} \qquad (7.2)$$

As a result of the discontinuity in σ there arises a discontinuity also in $\frac{dh}{dx}$, and this implies the existence of a current sheet.

Let x' be the value of x when $z = z'$ then, for a given value of the constant c the equations may be integrated from (h_1, z', x') towards $x = +\infty$. However, c must be chosen such that as $x \rightarrow +\infty$

$$f(h, z, c) \longrightarrow 0, \tag{7.3}$$

and

$$g(h, z, c) \longrightarrow 0. \tag{7.4}$$

Because $(zh - c) \geqslant 0$, c must lie within the range $0 \leqslant C \leqslant z' h_1$. Choosing a value of c in this range the equations may be integrated from (h_1, z'), but if c is chosen too big the solution will cross the curve $f(h, z, c) = 0$; on the other hand if it is chosen too small then the solution will cross the curve $g(h, z, c) = 0$. This is illustrated in figure 5. Thus, by a continuous process of trial and error, a series of upper and lower bounds c_1^r and c_2^r may be determined which converge to

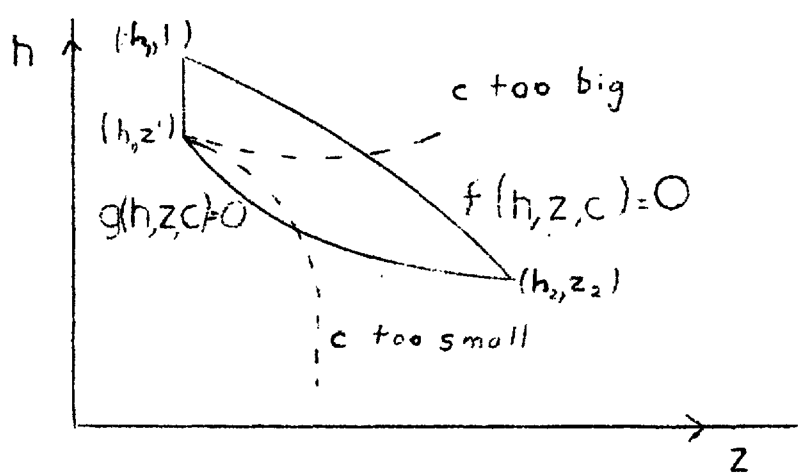

Figure 5

the value c, i.e.

$$C_1^{\tau} < C < C_2^{\tau} , \tag{7.5}$$

and

$$(C_2^{\tau} - C_1^{\tau}) \longrightarrow 0 \quad , \text{as } \tau \rightarrow \infty \tag{7.6}$$

By such a process c may be determined quite accurately. The integral curves, however, are very sensitive to small variations in c and consequently it is not practicable to carry out the integration over the whole range of x in this manner. Once c has been determined, to a fair degree of accuracy, h and z should be calculated and the equations integrated from (h_2 , z_2) to give a value for z'. This value will differ from the initial value of z' only to the extent of an insignificant decimal place.

Near the final state (h_2 , z_2), σ is large because τ is large and thus, since $\frac{dh}{dx}$ is small, it follows from equation (5.1) that f(h, z, c) $\triangleq$ 0, i.e. the solution is very close to the hyperbola $zh = c$. We therefore see that, in this neighbourhood, the two simultaneous differential equations reduce to just one. Using the fact that f(h, z, c) = 0, h may be eliminated from equations (5.16) and (5.17) to give the single differential equation for z and the equation for τ (z, c). We have

$$\frac{dz}{dx} = -\frac{3}{4}\frac{m}{\mu z}(1 - z)\left[\frac{\gamma+1}{2}z - \frac{\gamma-1}{2} - \frac{c - h_1 z}{z(1 - z)}\left\{2\gamma h_1 + (2 - \gamma)c\right\}\right], \tag{7.7}$$

$$\tau = \frac{1}{2}\frac{(\gamma - 1)}{\theta_1}\left[(1 - z)^2 - \frac{2}{z}\left(c - h_1 z\right)\right]. \quad (7.8)$$

This method is only suitable when f(h, z, c) is very small: when f(h, z, c) differs appreciably from zero it is necessary to continue the solution by the step-by-step process using equations (5.1) and (5.2). The manner in which f(h, z, c) varies as we move along the hyperbola from (h_1, z') may be found by combining equations (5.1) and (5.2) and approximating to $\frac{dh}{dx}$ by its value on the hyperbola. Combining equations (5.1) and (5.2) gives

$$\frac{dh}{dz} = \frac{4\pi\sigma v_1 \; f(h, z, c)}{\frac{3m}{4\mu z} \; g(h, z, c)} \; ; \quad (7.9)$$

the approximate value of $\frac{dh}{dz}$ is $-\left(c/z^2\right)$ and thus equation (7.8) may be expressed as

$$f(h, z, c) = \frac{\frac{3m}{4\mu z} \, g(h, z, c)}{4\pi\sigma v_1}\left(-\frac{c}{z^2}\right). \quad (7.10)$$

It should be noted, however, that the values of h and z used to continue the solution, once f(h, z, c) differs appreciably from zero, should be values corrected in the following way. Given z at any point the equation z h = c leads to an approximate h, equation (7.9) will then give a very good approximation to f(h, z, c) and the corrected value of h, from the definition of f(h, z, c), is given by

$$h = \frac{c + f(h, z, c)}{z} \tag{7.11}$$

The manner in which the solution approaches (h_2, z_2), as x tends to infinity, can be found by linearizing the equations in the neighbourhood of (h_2, z_2).

We let
$$h = h_2 + \Delta h ,$$
$$z = z_2 + \Delta z , \tag{7.12}$$
$$\alpha = \frac{1}{4\pi\sigma\nu_1} , \tag{7.13}$$
$$\beta = \frac{4\mu_1}{3m} \tag{7.14}$$

Substitution of (7.12) into equations (5.1) and (5.2) yields

$$\frac{d\Delta h}{dx} = h_2 \Delta z + z_2 \Delta h, \tag{7.15}$$

$$\frac{d\Delta}{dx} = \left\{ \frac{\gamma+1}{2} - \frac{1}{z_2^2}\left[\tfrac{1}{2}(\gamma-1) - \gamma\theta_1\right] + \frac{2c}{z_2}(h_2 - h_1)(\gamma-1)\right\}\Delta z$$

$$+ 2h_2 \Delta h \tag{7.16}$$

Let
$$\Delta z = A_1 \exp\left\{\frac{1}{\beta}\tau_2^{-\frac{5}{2}}\lambda x\right\}, \tag{7.17}$$

and
$$\Delta h = A_2 \exp\left\{\frac{1}{\beta}\tau_2^{-\frac{5}{2}}\lambda x\right\}, \tag{7.18}$$

Substituting these into equations (7.15) and (7.16), and taking the determinant of the coefficients yields the following equation for λ

$$\bar{\sigma}\lambda^2 - (\bar{\sigma}\bar{\nu} + z_2)\lambda + (z_2\bar{\nu} - 2h_2^2) = 0, \tag{7.19}$$

where $$\bar{\sigma} = \frac{\alpha}{\beta\, \tau_2^{\,4}} , \tag{7.20}$$

and $$\bar{\nu} = \frac{\gamma - 1}{2} - \frac{1}{2}\left[\frac{1}{2}(\gamma - 1) - \gamma\theta_1 - \frac{2(\gamma-1)}{\tau_2^{\,2}}\, c(h_2 - h_1) \right] \tag{7.21}$$

The ratio $\frac{A_2}{A_1}$ may also be found from these equations. For $h_1 = 0.256$ and $M = 212$, c has the value 0.195 and λ then has the value -2.5.

8. Results

A numerical example is now given to show just how the theories of the preceding sections work. Hydrogen gas is considered, and we shall take

$$\begin{aligned} h_1 &= 0.256 \\ \rho_1 &= 1.12.10^{-7}\,\text{gm/cm}^3 \\ \text{and} \quad M &= 212 \end{aligned} \tag{8.1}$$

This value of ρ_1 corresponds to an initial pressure of about 1 m.m. of mercury for an initial temperature of 300^0K. The actual value of the magnetic field H_1 corresponding to $h_1 = 0.256$ is $H_1 = 1.31.10^4$ gauss. To carry out the numerical integration a value for τ', the temperature at which the conductivity becomes finite, must be taken and for purposes of illustration this has been taken as 250. Taking different values of τ' does not affect the numerical results obtained appreciably, as was found by repeating the calculations for different values of τ' .

The value of $\tau' = 250$ leads to a value of z'

$$z' = 0.89994 \, , \qquad (8.2)$$

and thus the initial limits on c are

$$0 < c < 0.2304 \, . \qquad (8.3)$$

Starting with $c = 0.19$ and a step length of 0.0002 in x the equations may be integrated from $(h_1, z', 0)$ and after about 12 integrations we may take

$$c = 0.19535 \, , \qquad (8.4)$$

as being correct to 5 decimal places. For this value of c the final steady state conditions may be obtained and are

$$h_2 = 0.59223 \, , \qquad (8.5)$$

$$z_2 = 0.32985 \qquad (8.6)$$

Starting from these values of h_2 and z_2 the integration has been carried out and the results are shown in table 2. Only x and z are shown because h and z are coupled directly through the relation

$$z h = c \, . \qquad (8.7)$$

At $x = 1.26$ the function $f(h, z, c)$ has the value $1.99 . 10^{-5}$ and thus at this stage, the integration may be continued by using equations (5.1) and (5.2). The corrected value of h which must be used to start this integration is given by

$$h = \frac{0.19535 + 0.0000199}{0.369502} \, ,$$

$$= 0.5287384 \, . \qquad (8.8)$$

An interval of 0.0002 in x was used, though where h and z change rapidly a smaller interval was used. The results are shown in table 3, though it was arranged that the computer did not necessarily print out the new values of the variables at the end of each interval. As may be seen, any modification to the value of z' in this case is insignificant. These results are shown in the $h - z$ plane in figure 7.

An immediate consequence of a transverse magnetic field is the reduction of the final steady state temperature of the gas behind the shock front and thus, in the absence of a magnetic field, a weaker shock will reach the same final temperature. If the suffix n is used to denote the non-magnetic case and m the magnetic case, the two Mach numbers are given by

$$\tau_n = \frac{\gamma(\gamma-1)}{2} M_n^2 (1 - z_n)^2 , \qquad (8.9)$$

$$\tau_m = \frac{\gamma(\gamma-1)}{2} M_m^2 (1 - z_m)^2 \left[1 - \frac{2}{z_m} \left(\frac{c - h_1 z_m}{1 - z_m} \right)^2 \right] . \qquad (8.10)$$

Thus, if $\tau_n = \tau_m$

$$M_n = \frac{1 - z_m}{1 - z_n} \sqrt{1 - \frac{2}{z_m} \left(\frac{c - h_1 z_m}{1 - z_m} \right)^2} \; M_m . \qquad (8.11)$$

In this formula $z_n = \frac{\gamma - 1}{\gamma + 1}$, assuming that the shock is fairly strong. For the numerical example being considered, M_m = 212, and the corresponding non-magnetic Mach number is M_n = 173.

For comparison, the integration for each example has been carried out for the same case without a magnetic field. To compare shock profiles it is necessary for both waves to have the same final temperature; the integration for the non-magnetic case of the example being considered has, therefore, been carried out with M_n = 173. Table 4 shows the numerical results obtained from this integration and in figure 9 the magnetic and non-magnetic shock profiles are shown together. The shock is moving to the left and the numbers on the curves represent values of the temperature τ.

The solution to the equations has been found for several cases, and the results are shown in table 5, where the third case shown in the one which has just been considered in detail. Once T_1 has been fixed at 300°K, there are only four parameters which may be varied, M_m, τ', ρ_1 and h_1 and of these ρ_1 and h_1 have been kept constant for seven out of the eight examples. As may be seen, taking different values for τ' does not appreciably affect the numerical results obtained. The second and third examples are illustrated in the $h - z$ plane in figures 6 and 7; the shock profiles for these two examples, together with the seventh are illustrated in figures 8 to 10. All the shocks are moving to the left and again numbers on the curves represent values of the temperature τ .

Consider first figures 6 and 7 showing h as a function of z. It can be seen that the solutions follow $f(h, z, c) = 0$ for all but a small region near the initial state and that the stronger the shock, the smaller is this region. For given τ' the distance AB is inversely proportional to the Mach number of the shock and thus, for very weak shocks, this distance will be quite large. In fact, for shocks of Mach number less than $\sqrt{\frac{(\gamma+1)^2}{2\gamma(\gamma-1)}\tau'}$ all the compression arises from the viscous forces and the magnetic field remains constant throughout the motion.

From equation (2.17) we have

$$\frac{d\tau}{dx} = \frac{1}{2}\gamma(\gamma-1)M^2\left\{\left[-2(1-z)-2(\theta_1+h_1^2-h^2)\right]\frac{dz}{dx} + \frac{1}{4\pi\sigma\nu_1}\left(\frac{dh}{dx}\right)^2\right\}. \tag{8.12}$$

The first term in this equation corresponds to adiabatic and viscous heating, whilst the second corresponds to Joule heating by the electric currents. Numerical investigation shows that the second term is relatively larger near the front of the wave, where the conductivity is not yet too large. Hence it is in this region that Joule heating is most important.

Comparing the wave profiles given in figures 8, 9 and 10 with the example of Marshall's curves shown in figure 4, the main difference is seen to be the sharp change in the initial stages of the wave, which replaces Marshall's extended region. As can be seen for the profiles of figures 8, 9 and 10 there is not much difference between the magnetic and non-magnetic cases. For the relatively weak shock the width of the shock front is slightly less in the magnetic case and the rise in temperature of the gas is slightly quicker. This tendency is visible but hardly significant in the other examples. In all cases the temperature rises to about a quarter of its final steady state value in the region where the density rises rapidly.

TABLE 2

Integration of equations (5.7) & (5.8).

x	z	τ	
2.000	0.330000	9.352, 3	
1.980	0.330183	9.345, 3	
1.700	0.335032	9.25, 3	
1.560	0.340372	9.15, 3	
1.460	0.346482	9.02, 3	
1.400	0.351520	8.92, 3	
1.340	0.357960	8.79, 3	
1.300	0.363240	8.68, 3	
1.260	0.369502	8.55, 3	f = 1.99, −5
1.220	0.376961	8.40, 3	
1.180	0.385902	8.21, 3	
1.160	0.391043	8.10, 3	
1.140	0.396711	7.98, 3	
1.120	0.402980	7.85, 3	
1.100	0.409941	7.70, 3	
1.080	0.417709	7.53, 3	
1.060	0.426430	7.34, 3	f = 5.0, −5
1.040	0.436295	7.13, 3	
1.020	0.447563	6.89, 3	
1.000	0.460597	6.61, 3	
0.080	0.475935	6.29, 3	
0.060	0.494428	5.90, 3	
0.040	0.517553	5.43, 3	
0.030	0.531670	5.15, 3	
0.020	0.548283	4.82, 3	
0.010	0.568492	4.43, 3	f = 2.98, −4
0.005	0.580535	4.21, 3	
0.000	0.594419	3.95, 3	

$h_1 = 0.256$ $c = 0.19535$
$M = 212$ $\tau' = 250$
$\rho_1 = 1.123, -7$ $\tau = T/T_1$
$u_1 = 3.06, 7$ $h = c/z$

m, n represents the number $m.10^n$

TABLE 3

Integration of equations (5.I) & (5.2).

$c = 0.19535$ $h_1 = 0.25600$ $z_1 = 0.89994$
$\tau' = 250$ $h_2 = 0.59223$ $z_2 = 0.32985$

m, n represents the number $m.10^{n}$

x	h	z	τ	(zh−c)
1.26000	0.52874	0.36950	8550	1.99, −5
1.25500	0.52751	0.37036	8537	2.03, −5
1.23500	0.52238	0.37400	8461	2.20, −5
1.21375	0.51653	0.37824	8373	2.41, −5
1.19375	0.51063	0.38262	8280	2.62, −5
1.17562	0.50491	0.38696	8189	2.83, −5
1.15875	0.49925	0.39135	8096	3.06, −5
1.14297	0.49365	0.39579	8001	3.29, −5
1.12820	0.48812	0.40028	7906	3.53, −5
1.11320	0.48220	0.40520	7801	3.80, −5
1.09820	0.47595	0.41053	7687	4.10, −5
1.08320	0.46934	0.41632	7563	4.45, −5
1.06820	0.46234	0.42263	7427	4.84, −5
1.05320	0.45493	0.42952	7280	5.29, −5
1.04320	0.44973	0.43449	7173	5.64, −5
1.03320	0.44431	0.43980	7059	6.02, −5
1.02320	0.43866	0.44548	6938	6.46, −5
1.01320	0.43274	0.45158	6808	6.95, −5
1.00320	0.42654	0.45816	6668	7.53, −5
0.99320	0.42003	0.46528	6517	8.19, −5
0.98320	0.41317	0.47302	6353	8.98, −5
0.97320	0.40592	0.48150	6175	9.93, −5
0.96320	0.39821	0.49085	5980	1.11, −4
0.95320	0.38998	0.50125	5765	1.26, −4
0.94820	0.38563	0.50692	5648	1.35, −4
0.94320	0.38111	0.51296	5525	1.45, −4

TABLE 4

Integration for the non-magnetic case.

x	z	τ	
0.8740	0.999	1.000	
0.8750	0.836	4.490,	2
0.8760	0.740	1.122,	3
0.8770	0.705	1.451,	3
0.8790	0.663	1.884,	3
0.8830	0.616	2.446,	3
0.8870	0.586	2.846,	3
0.8950	0.545	3.436,	3
0.9030	0.517	3.882,	3
0.9110	0.495	4.246,	3
0.9270	0.461	4.827,	3
0.9430	0.436	5.286,	3
0.9590	0.416	5.666,	3
0.9750	0.400	5.991,	3
1.0070	0.374	6.522,	3
1.0390	0.354	6.944,	3
1.0710	0.338	7.288,	3
1.1030	0.325	7.574,	3
1.1350	0.314	7.815,	3
1.1670	0.306	8.019,	3
1.2310	0.292	8.345,	3
1.2950	0.281	8.588,	3
1.3590	0.274	8.770,	3
1.4870	0.264	9.013,	3
1.6150	0.258	9.153,	3
1.8710	0.253	9.284,	3
2.3830	0.250	9.345,	3
3.4070	0.250	9.353,	3

$M = 173$
$\rho_1 = 1.123, \ -7$
$u_1 = 2.495, \ 7$

m, n represents the number $m.10^n$

TABLE 5

Results for the Structure

of the Shock Front

	M_m	τ'	ρ_1 (gm/cm^3)	h_1	c	Width of shock front (cms)	τ_2	h_2	z_2	z'	M_n	H_1 (Gauss)
1	40	100	$1.12.10^{-7}$	0.256	0.06478	0.007	$5.60.10^3$	0.2587	0.2504	0.6646	39.97	$2.48.10^3$
2	80	100	$1.12.10^{-7}$	0.256	0.09366	0.028	$1.91.10^3$	0.3541	0.2645	0.8323	76.85	$4.96.10^3$
3	212	250	$1.12.10^{-7}$	0.0256	0.19539	0.87	$9.35.10^3$	0.5922	0.3299	0.8994	173	$1.31.10^4$
4	212	50	$1.12.10^{-7}$	0.256	0.19561	0.90	$9.38.10^3$	0.5965	0.3280	0.9553	173	$1.31.10^4$
5	212	100	10^{-8}	0.256	0.21464	12.6	$8.45.10^3$	0.6274	0.3421	0.9367	165.5	$3.93.10^3$
6	212	100	$1.12.10^{-7}$	0.100	0.057235	3.2	$1.35.10^4$	0.2222	0.2576	0.9367	207.7	$5.14.10^3$
7	550	250	$1.12.10^{-7}$	0.256	0.236611(5)	40.5	$4.94.10^4$	0.6583	0.3594	0.9614	397.6	$1.82.10^4$
8	700	100	$1.12.10^{-7}$	0.256	0.243695	974	$7.61.10^4$	0.6673	0.3652	0.9810	494.0	$1.29.10^4$

$T_1 = 300^\circ K$

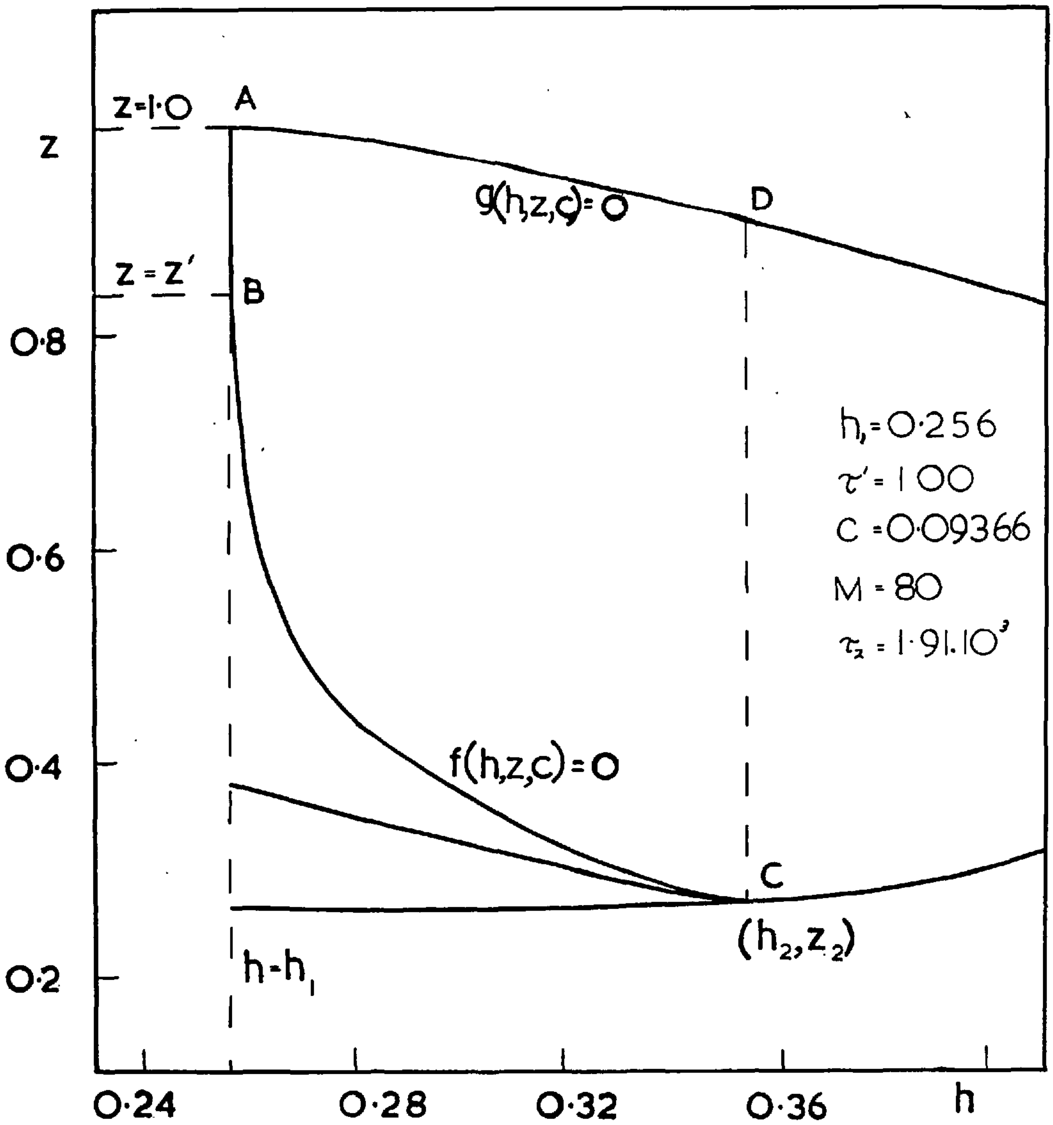

FIG. 6. h-z CURVE (FOR A WAVE ADVANCING INTO A COLD GAS)

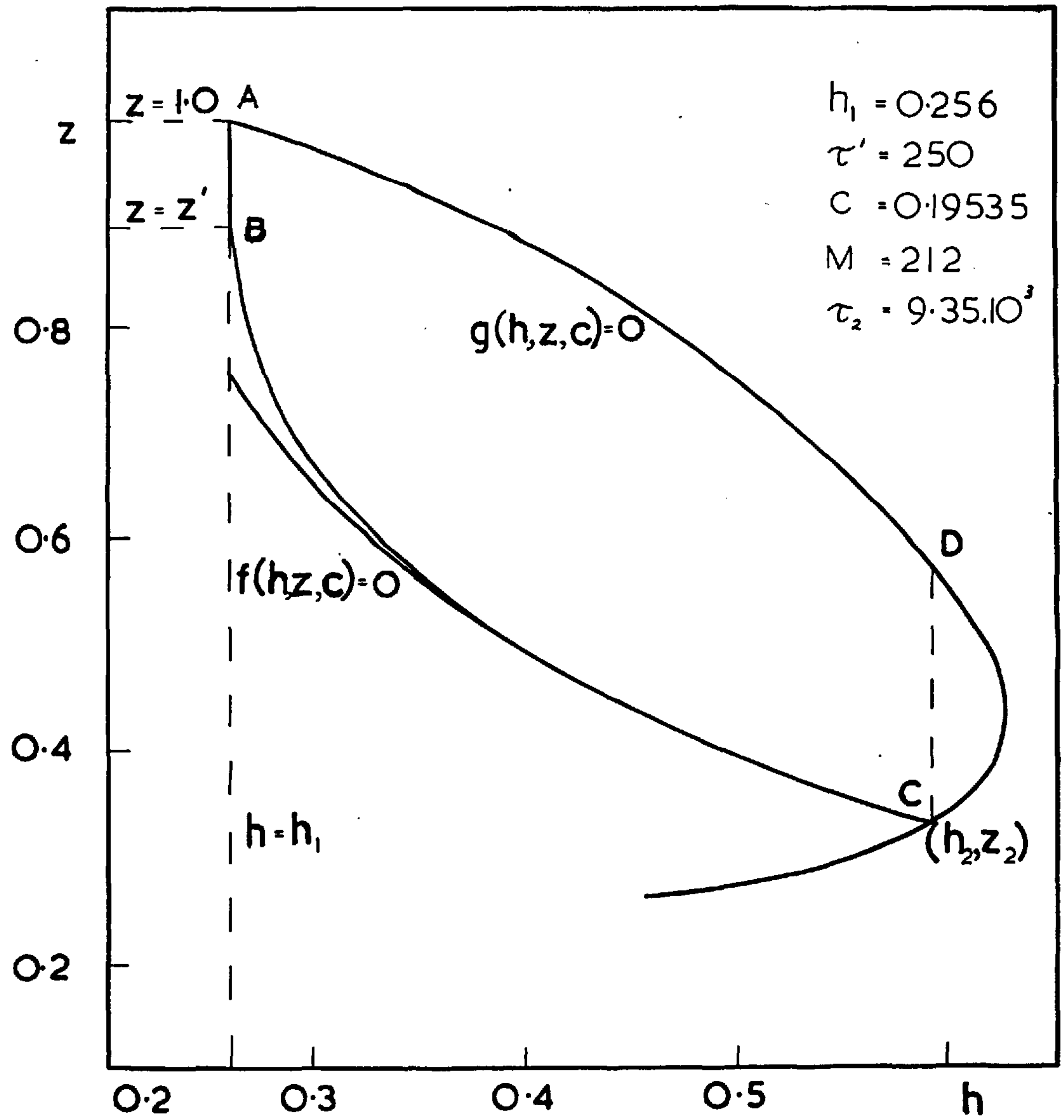

FIG. 7. h-z CURVE (FOR A WAVE ADVANCING INTO A COLD GAS)

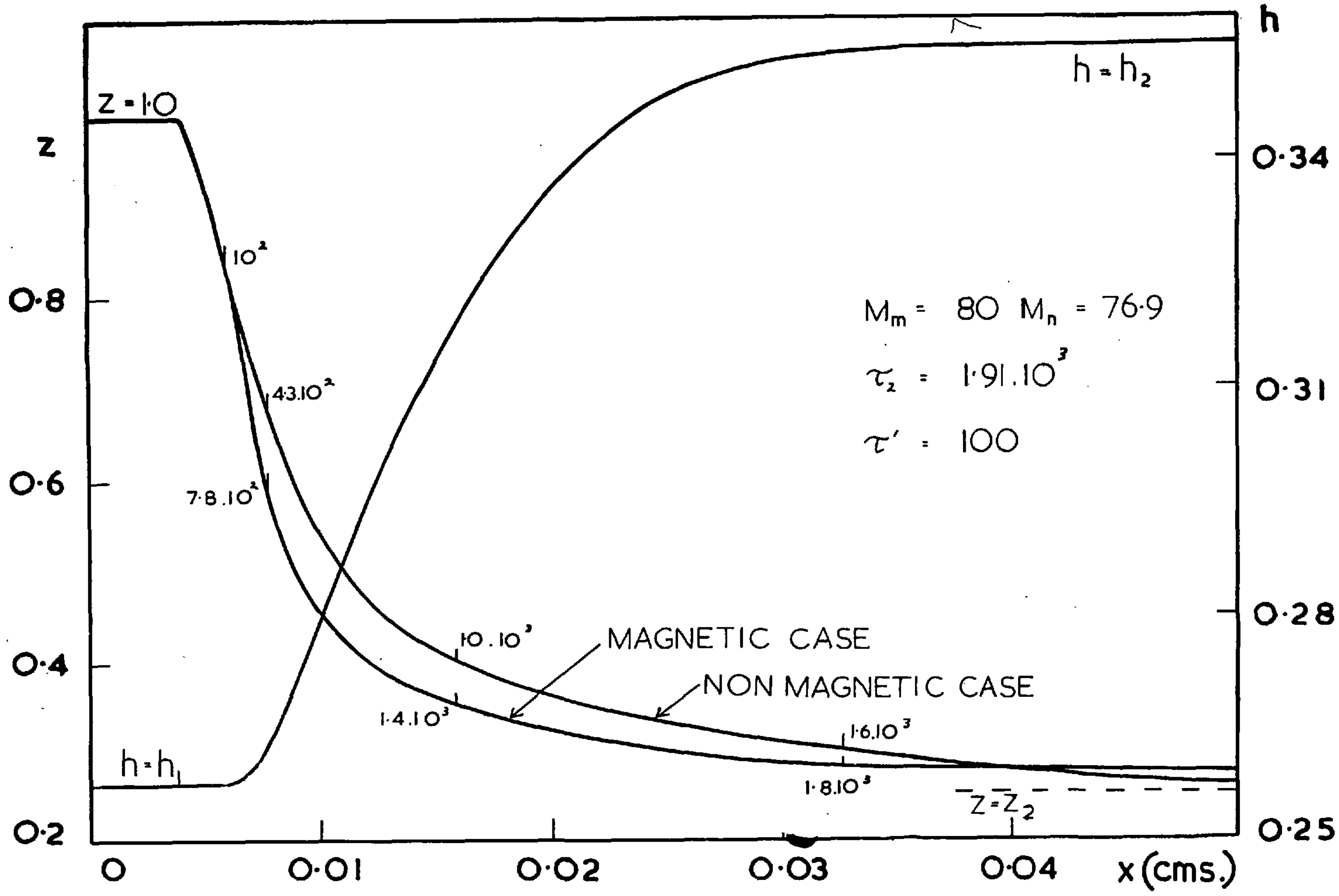

FIG. 8. SHOCK PROFILES (MAGNETIC & NON MAGNETIC CASES)

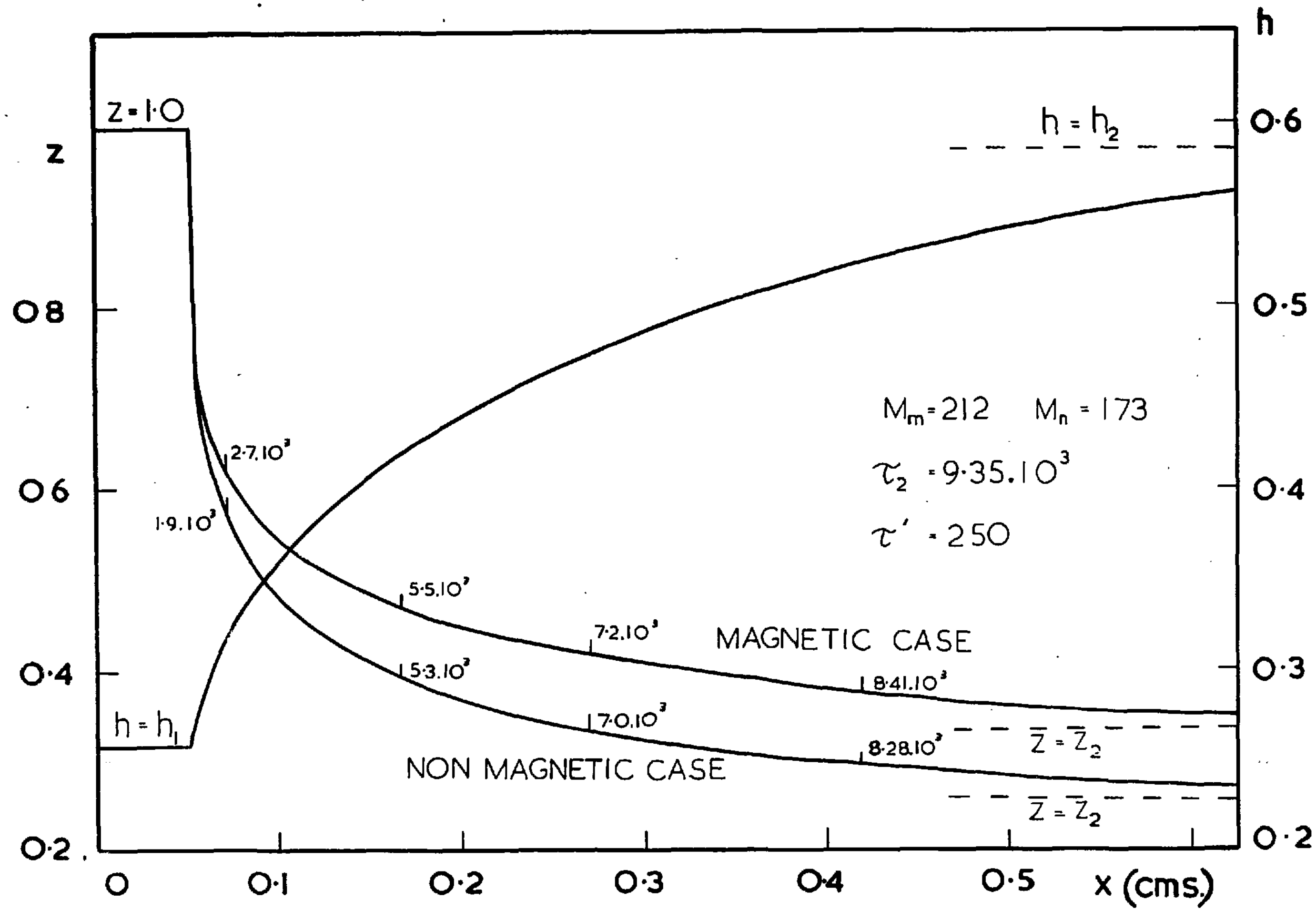

FIG. 9. SHOCK PROFILES (MAGNETIC & NON-MAGNETIC CASES)

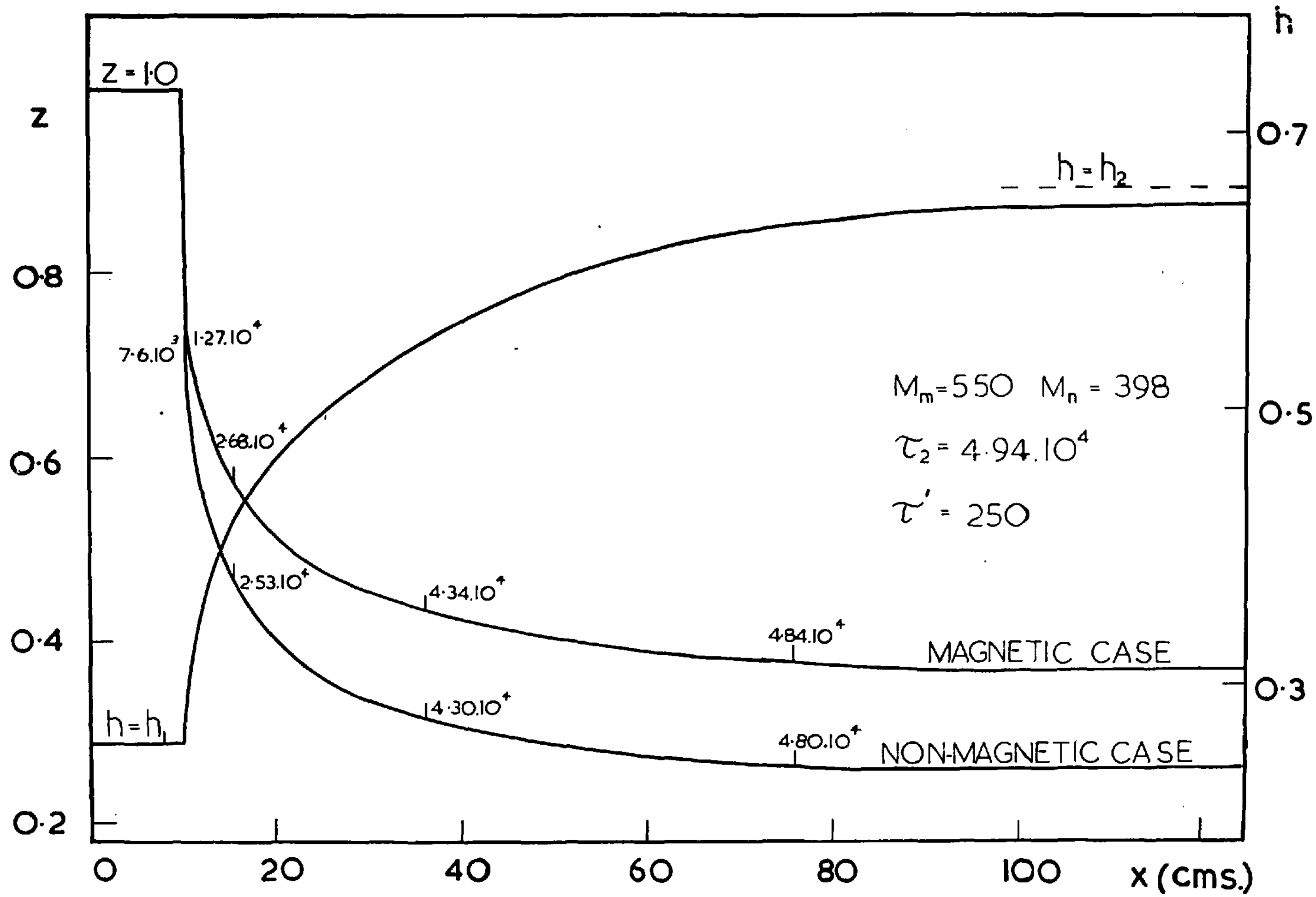

FIG. 10. SHOCK PROFILES (MAGNETIC & NON-MAGNETIC CASES)

REFERENCES

Chapter I

1. Elmore, W.C., Little, E.M. & Quinn, W.E. (1958), Phys. Rev. Letters, 1, 32.
2. Kolb, A.C. (1957), Phys. Rev., 107, 345.
3. Kolb, A.C. (1958), Phys. Rev., 112, 291.
4. Patrick, R.M. (1959), Phys. of Fluids, 2, 589.
5. Wright, J.K. & Black, E.M. (1959), Jour. Fluid Mechs., 6. 289.

Chapter II

6. Cowling, T.G. (1957), Magnetohydrodynamics, Interscience. New York.
7. DeHoffman, F. & Teller, E. (1950), Phys. Rev., 80, 692.
8. Landau, L.D. & Liftshitz, E.M. (1960), Electrodynamics of Continuous Media, Pergamon: London.
9. Spitzer, L. (1956), Physics of Fully Ionized Gases, Interscience: New York.

Chapters III and IV

10. Courant, R. & Friedrichs, K.O. (1956), Supersonic Flow and Shock Waves, Interscience: New York.
11. Mitchner, M. (1959), Phys. of Fluids, 2, 62.

Chapter V

12. Chapman, S. & Cowling, T.G. (1939), The Mathematical Theory of Non-Uniform Gases, Cambridge University Press.

13. Chapman, S. (1954), Astrophys. Jour. 120, 151.

14. Cohen, R., Spitzer, L. & Routley, P. (1950), Phys. Rev., 80, 230.

15. Kennard, E.H. (1938), Kinetic Theory of Gases, McGraw Hill: New York.

16. Spitzer, L. (1952), Astrophys. Jour. 116, 299.

17. Spitzer, L. & Härm, R. (1953), Phys. Rev., 89, 977.

Chapter VI

18. Burgers, J.M. (1957), Magnetohydrodynamics, edited by R. Landshoff, Stamford University.

19. Gilbarg, D. (1951), Amer.Jour.Maths., 73, 256.

20. Kulikouskii, A.G. & Lyubimov, G.A. (1960), Revs. Mod. Phys., 32, 977.

21. Ludford, G.S.S. (1959), Jour. Fluid Mechs., 5, 387.

22. Marshall, W. (1955), Proc. Roy. Soc. A, 233, 367.

23. Lord Rayleigh (1910), Proc. Roy. Soc. A, 84, 247.